PETROLOGY AND GEOCHEMISTRY OF HOST ROCK AND GOLD MINERALIZATION AT SOUTHERN PART OF ULU SOKOR GOLD DEPOSIT, KELANTAN, MALAYSIA

AHMAD FAUZAN BIN YUSOFF

**FACULTY OF SCIENCE
UNIVERSITI MALAYA
KUALA LUMPUR**

2022

PETROLOGY AND GEOCHEMISTRY OF HOST ROCK AND GOLD MINERALIZATION AT SOUTHERN PART OF ULU SOKOR GOLD DEPOSIT, KELANTAN, MALAYSIA

AHMAD FAUZAN BIN YUSOFF

DISSERTATION SUBMITTED IN FULFILMENT OF THE REQUIREMENTS FOR THE DEGREE OF MASTER OF SCIENCE

FACULTY OF SCIENCE
UNIVERSITI MALAYA
KUALA LUMPUR

2022

UNIVERSITI MALAYA

ORIGINAL LITERARY WORK DECLARATION

Name of Candidate: **AHMAD FAUZAN BIN YUSOFF**

Matric No: **17028465/3**

Name of Degree: **MASTER OF SCIENCE**

Title of Dissertation ("this Work"):

PETROLOGY AND GEOCHEMISTRY OF HOST ROCK AND GOLD MINERALIZATION AT SOUTHERN PART OF ULU SOKOR GOLD DEPOSIT, KELANTAN, MALAYSIA

Field of Study: **GEOLOGY**

I do solemnly and sincerely declare that:

(1) I am the sole author/writer of this Work;
(2) This Work is original;
(3) Any use of any work in which copyright exists was done by way of fair dealing and for permitted purposes and any excerpt or extract from, or reference to or reproduction of any copyright work has been disclosed expressly and sufficiently and the title of the Work and its authorship have been acknowledged in this Work;
(4) I do not have any actual knowledge nor do I ought reasonably to know that the making of this work constitutes an infringement of any copyright work;
(5) I hereby assign all and every rights in the copyright to this Work to the University of Malaya ("UM"), who henceforth shall be owner of the copyright in this Work and that any reproduction or use in any form or by any means whatsoever is prohibited without the written consent of UM having been first had and obtained;
(6) I am fully aware that if in the course of making this Work I have infringed any copyright whether intentionally or otherwise, I may be subject to legal action or any other action as may be determined by UM.

Candidate's Signature Date:18th April 2022

Subscribed and solemnly declared before,

Witness's Signature Date:18th April 2022

Name:

Designation: Supervisor

PETROLOGY AND GEOCHEMISTRY OF HOST ROCK AND GOLD MINERALIZATION AT SOUTHERN PART OF ULU SOKOR GOLD DEPOSIT, KELANTAN, MALAYSIA

ABSTRACT

The petrology and geochemistry of host rock and gold mineralization at southern part of Ulu Sokor gold deposit, Kelantan, Malaysia is poorly understood. This study area is located at the Central Belt of Peninsular Malaysia and hosted as an orogenic gold deposit from previous study. Particular deposits in this study area are New Found and New Discovery loads which located at the southern part of the whole Ulu Sokor gold deposit boundary. Two types of host rocks were identified such as phyllite as a metasedimentary rock unit and rhyolite as a volcanic rock unit. Based on the petrological and geochemical data presented, phyllite have been derived from shale and classified as pelitic and felsic source. It was undergone little heavy mineral fractionation and sediment recycling since these samples slightly enriched with Light Rare Earth Elements (LREEs). Some of these samples studied have elevated K_2O content that indicate K-metasomatism, which reflects secondary addition of potassium. According to the Chemical Index Alteration (CIA) and Index Compositional Variability (ICV) calculation, it shows that the phyllite are intensely weathered with matured sources. The classifications of depositional conditions are plotted as continental island arc and oceanic island arc. Continental island arc and oceanic island arc are dominated by the development of the subduction process, which synchronic with the tectonic evolution of the Bentong-Raub suture zone. The other type of host rock is rhyolite, which is a typical type of rock that exists in the volcanic arc environment based on the relationship between the collision of Sibumasu and East Malaya blocks. The geochemical features including the enrichment in Large Ion Lithophile Elements (LILEs) relative to High Field Strength Elements (HFSEs), and the restricted calc-alkaline to shoshonitic rocks are indicative of volcanic arc type. The trace and major geochemical elements of volcanic rocks support the evidence of volcanic arc setting. Gold mineralization is primarily hosted in structurally controlled quartz vein, which occurs in various degrees of ductile-brittle environment. Based on the field relationships, ore microscopy, and geochemical data analysis, the main gold mineralization type in the southern part of Ulu Sokor gold deposit is gold (Au)-bismuth (Bi). In terms of mineral exploration and gold prospecting, the significant enrichment in this study area is bismuth. However, some other metals can also be considered as a significant value in this area such as Pb, As, Cu and Zn. From the bulk ore chemistry, the geometric mean values of Au and Bi are 1.8972 ppm (n=23) and 96.3 ppm (n=22) respectively.

Keywords: Petrology, Geochemistry, Phyllite, Rhyolite, Bismuthinite

PETROLOGI DAN GEOKIMIA BATUAN INANG DAN MINERALISASI EMAS DI BAHAGIAN SELATAN MENDAPAN EMAS ULU SOKOR, KELANTAN, MALAYSIA

ABSTRAK

Petrologi dan geokimia batuan inang dan mineralisasi emas di bahagian selatan mendapan emas Ulu Sokor, Kelantan, Malaysia adalah kurang difahami. Kawasan kajian ini terletak di Jalur Tengah Semenanjung Malaysia dan dikelaskan sebagai mendapan emas orogenik dari kajian sebelumnya. Mendapan kawasan kajian ini adalah New Found dan New Discovery yang terletak di bahagian selatan keseluruhan batas mendapan emas Ulu Sokor. Dua jenis batuan inang dikenal pasti seperti phyllite sebagai unit batuan metasedimen dan rhyolite sebagai unit batuan vulkanik. Berdasarkan data petrologi dan geokimia, phyllite berasal dari serpih dan diklasifikasikan sebagai sumber pelitik dan felsik. Ia mengalami sedikit pecahan mineral berat dan kitar semula sedimen kerana sampel ini diperkayakan sedikit dengan Light Rare Earth Elements (LREEs). Sebilangan sampel yang dikaji mempunyai K_2O tinggi, di mana ia menunjukkan K-metasomatisma yang mencerminkan penambahan kalium sekunder. Menurut pengiraan Chemical Index Alteration (CIA) dan Index Compositional Variability (ICV), ini menunjukkan bahawa phyllite mengalami hakisan yang kuat dengan sumber yang matang. Klasifikasi keadaan mendapan digambarkan sebagai busur pulau benua dan busur pulau laut. Busur pulau benua dan busur pulau laut didominasi oleh pengembangan proses subduksi, yang selaras dengan evolusi tektonik zon jalur Bentong-Raub. Seterusnya adalah rhyolite, mempunyai jenis persekitaran lengkungan gunung berapi, berdasarkan hubungan dengan perlanggaran blok Sibumasu dan Tanah Melayu Timur. Ciri-ciri geokimia termasuk pengayaan dalam Large Ion Lithophile Elements (LILEs) berbanding dengan High Field Strength Elements (HFSEs) dan tertumpu pada batuan calc-alkaline ke batuan shoshonitic, menunjukkan jenis busur

gunung berapi. Jejak dan unsur utama geokimia batuan vulkanik menyokong pengaturan arka gunung berapi. Emas terutamanya bermineralisasi dalam kawalan urat kuarza secara struktural yang berlaku dalam pelbagai tahap persekitaran rapuh mulur. Berdasarkan hubungan lapangan, mikroskop bijih dan analisis data geokimia, jenis utama mineralisasi emas di bahagian selatan mendapan emas Ulu Sokor adalah emas (Au)-bismut (Bi). Dari segi penerokaan mineral dan pencarian emas, pengayaan yang signifikan di kawasan kajian ini adalah Bi. Walaubagaimanapun, beberapa logam lain juga dapat dipertimbangkan sebagai nilai yang signifikan di kawasan ini seperti Pb, As, Cu dan Zn. Daripada kimia bijih pukal, nilai minimum geometri Au dan Bi ialah 1.8972 ppm Au (n = 23) dan 96.3 ppm Bi (n = 22).

Kata Kunci: Petrologi, Geokimia, Phyllite, Rhyolite, Bismuthinite

ACKNOWLEDGEMENTS

In the name of Allah, The Most Gracious and The Most Merciful. I have successfully completed my thesis as a requirement of my academic qualification in Master's Degree in Science (Research Work). I accept full responsibility for all information written in this study. I am indebted to both of my supervisor and assistant supervisor, Dr. Jasmi Hafiz Abdul Aziz and Dr. Muhammad Hatta Roselee for the provision of boundless guidance towards the end of this research, and for providing me valuable opportunities to develop my technical competencies throughout this journey as a postgraduate student. I would also like to thank my peers who have helped me develop a better understanding on geological concepts and techniques used for this research.

Among these are Nur Nadwa Syahirah Ai Zamruddin, Siti Nadzirah Nazri, Muhammad Nadzmi Abdul Ghofur, Muhammad Amiruddin Amran, Nur Amalina Ahmad Thana'ani, and Nur Fatehah Norran. Furthermore, I would like to express my gratitude to Management of CNMC Goldmine Holdings for funding my research and for supporting my field work. It has been a privilege to be able to conduct my research study with the financial support from the management. Lastly, I would like to give my deepest appreciation to my supporting parents, Sulaimah Supian and Yusoff Desa, my beloved wife, Nur Azreeny Huzaimah Tahir, and my loving daughter, Aara Auliya for their continued support in all my endeavours. They are the driving forces of my motivation to continue pursuing for matters that are close to my heart.

TABLE OF CONTENTS

LIST OF FIGURES

LIST OF TABLES

LIST OF SYMBOLS AND ABBREVIATIONS

For examples:

ACM	:	Active Continental Margin
CIA	:	Chemical Index Alteration
CIA	:	Continental Island Arc
GPS	:	Global Positioning System
HFSEs	:	High Field Strength Elements
HREEs	:	High Rare Earth Elements
ICPMS	:	Inductively Coupled Plasma-Mass-Spectrometry
ICV	:	Index Compositional Variability
LECO	:	Carbon and Sulphur determination
LILEs	:	Large Ion Lithophile Elements
LOI	:	Loss of Ignition
LREEs	:	Light Rare Earth Elements
MORB	:	Mid Oceanic Ridge Basalt
OIA	:	Oceanic Island Arc
PAAS	:	Post-Archean Australian Shale
PM	:	Passive Margin
REEs	:	Rare Earth Elements
TAS	:	Total Alkali Silica
UCC	:	Upper Continental Crust
WGS84	:	World Geodetic System 84
XRF	:	X-Ray Fluorescence

CHAPTER 1: INTRODUCTION

1.1 Overview

In the early 15th century, Southeast Asia Peninsular was known as Aurea Chersonesus or Golden Peninsula. This first world map was led by Claudius Ptolemy in the early of the 2nd century. However, it was revised by Muhammad Ibn Musa al-Khwarizmi in the early 9th century in terms of city coordinates and other geographical features. Peninsular Malaysia was established as an important gold producer in the past before the discovery of enormous goldfield such as in the Witwatersrand Basin, Johannesburg, South Africa. The long history of minor scale gold mining activities was done in the Central Belt of Peninsular Malaysia such as in Kelantan and Pahang states.

The deposition of gold in Central Belt was controlled by the regional Bentong-Raub suture zone which was formed due to the process of amalgamation from the Sibumasu Block and the East Malaya Block in Late Triassic to Early Jurassic. The main gold deposits producer which was located in the region of Central Belt are Ulu Sokor, Kelantan and Selinsing, Pahang (Figure 1.1). Both of these gold deposits are currently active with fine gold production. During first half of the year 2020 in Ulu Sokor and Selinsing, the gold produced are 6222 k ounces (Optiro, 2020) and 17360 k ounces (Snowden, 2019), respectively. In terms of mineral resources which are reported inclusive of reserves, the Ulu Sokor area was estimated to have 13,220 k tonnes with grade at 1.7 g/t of gold (Optiro, 2020), while Selinsing was estimated to have 18,378 k tonnes with 1.7 g/t of gold (Snowden, 2019). The development of gold mineralization in Peninsular Malaysia is significant to the hydrothermal fluid activity, especially in Kelantan and Pahang.

The project area is situated at the North of Kelantan state which lies on the Central Belt of Peninsular Malaysia. The latest study on the Ulu Sokor gold deposits is from Bin Li and others with their title “Geology and fluid characteristics of the Ulu Sokor gold deposit, Kelantan, Malaysia: Implication for ore genesis and the classification of the deposit”. According to their studies, the mechanism for gold deposition in this study area is fluid immiscibility and consistent classified as an orogenic gold deposit (Li et al., 2015). Ulu Sokor gold deposit was chosen due to lacking on determine the petrogenesis and gold mineralization enrichment pattern in relative to other trace elements. This study was based on the new data of microscopic and geochemical analysis to reveal the objectives.

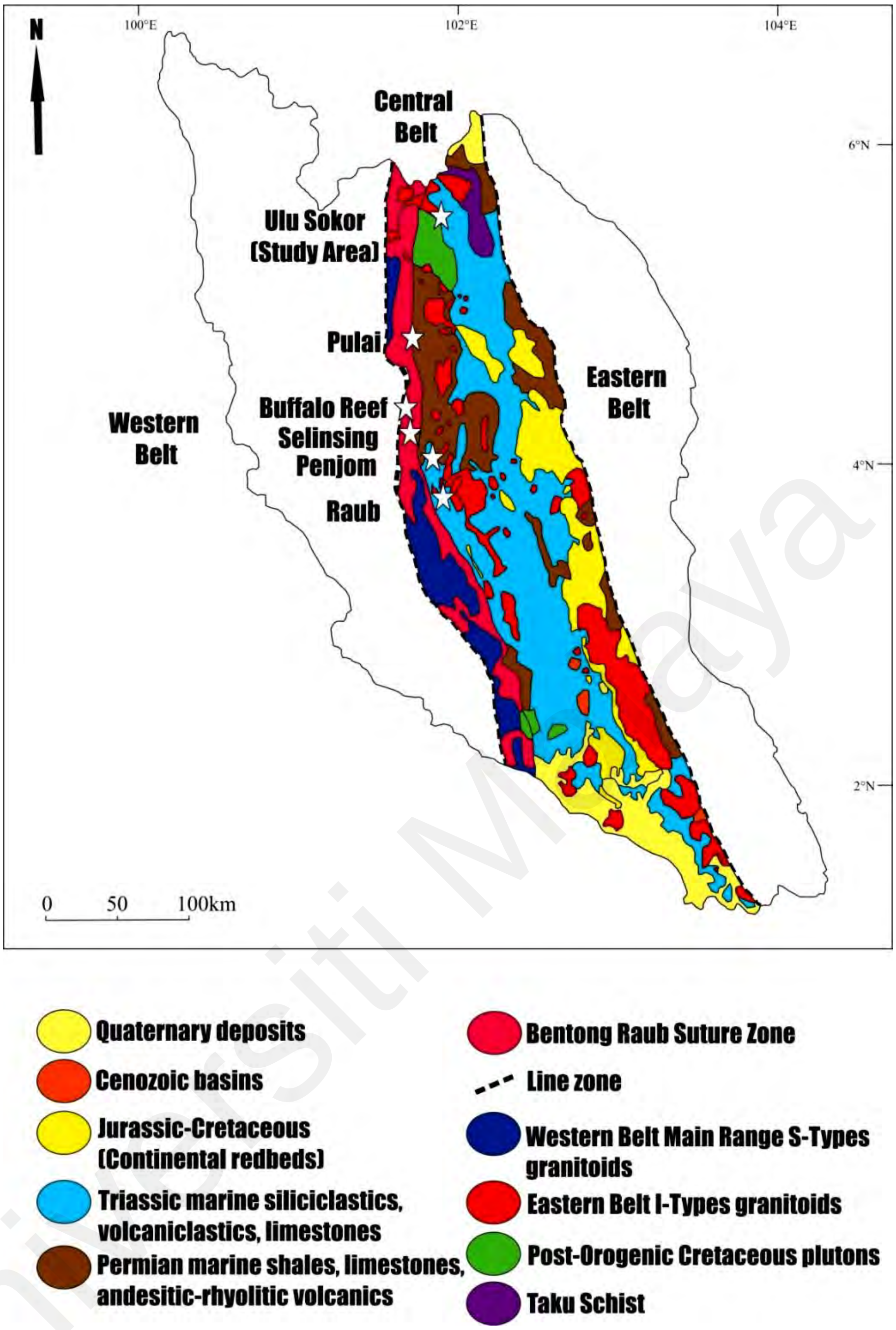

Figure 1.1: Map of Central Belt of Peninsular Malaysia showing the location of study area and other major occurrence of gold deposits. Note the white star symbol in the map represent the major gold deposit. After (Tate et al., 2009).

1.2 Research questions

a) What is the general geology of this gold deposit?

b) What is the prospect of gold mineralization in this gold deposit in terms of distribution and relationship in various mineral assemblages?

1.3 Objectives

a) To determine the petrology and geochemistry of the host rock and their relations to the enrichment of gold and other metals.

b) To establish the paragenetic sequence and the significant element that contributed to the mineralization of gold within the various mineral assemblages.

1.4 Geography

1.4.1 Location

The Ulu Sokor gold deposit is located at the North of Kelantan state, which is approximately 80.0 km southwest of the township of Kota Bharu. This study area can be accessed via paved road from Kota Bharu to Kampong Bukit, followed by an unpaved road from the Kampong Bukit to the Ulu Sokor gold deposit. It takes about 18.0 km to reach the site.

1.4.2 Topography

The topographic features in Kelantan are categorized into five units based on the mean elevation which are low laying, rolling, undulating, hilly to mountainous. Basically, the Ulu Sokor gold deposit had topographic features from undulating to hilly with mean elevation between 31.0 to 300.0 m above sea level. The deposit area is bounded to the west by Stong Igneous Complex, to the north by Kemahang Granite and to the east by Boundary Range Granite. Most of these intrusions have mean elevation more than 301.0 m above sea level.

1.4.3 Climate

The Ulu Sokor gold deposit is situated at the East Coast of Peninsular Malaysia with a tropical rainforest climate. The rainfall in Kelantan state is governed by two types of monsoons which are southwest monsoon and northeast monsoon. Both of these monsoons occur from February until October and from November until March, respectively. Southwest monsoon commonly has less rainfall which reflects hot and dry conditions. Meanwhile, northeast monsoon brings heavy rainfall, thus this area has cold and high soil moisture.

CHAPTER 2: LITERATURE REVIEWS

2.1 Tectonic setting of Peninsular Malaysia

Peninsular Malaysia is a part of Southeast Asia in the continental crust of Sundaland (Metcalfe, 2013a). In general, Peninsular Malaysia comprises of two tectonic blocks which are Sibumasu Block to the West and East Malaya Block to the East. Sibumasu Block was derived from the northwest of Australian Gondwana by late Early Permian, while East Malaya Block was derived from Gondwana margin by Early Devonian (Metcalfe, 2013a). It was assembled by Late Triassic and delineated by one major suture line called as Bentong-Raub suture zone (Metcalfe, 2013b) (Figure 2.1).

Several studies on the stratigraphy, structural, magmatism, geophysical signatures, and geological evolution in Peninsular Malaysia are characterized into three significant belts which are Western, Central and Eastern Belts (Metcalfe, 2013b). Western Belt lies within Sibumasu Block, while Central and Eastern Belts are joined as East Malaya Block. However, based on studies on the mineralization in Peninsular Malaysia, it is also classified into three distinct belts which are Western Tin Belt, Central Gold Belt and Eastern Tin Belt (Yeap, 1993) (Figure 2.2). The formation of Bentong-Raub suture zone is related with the subduction of the Palaeo-Tethys Ocean beneath the East Malaya Block and it was believed that it was initiated during Carboniferous period. However, it was completely closed by Late Triassic to Early Jurassic period (Metcalfe, 2000).

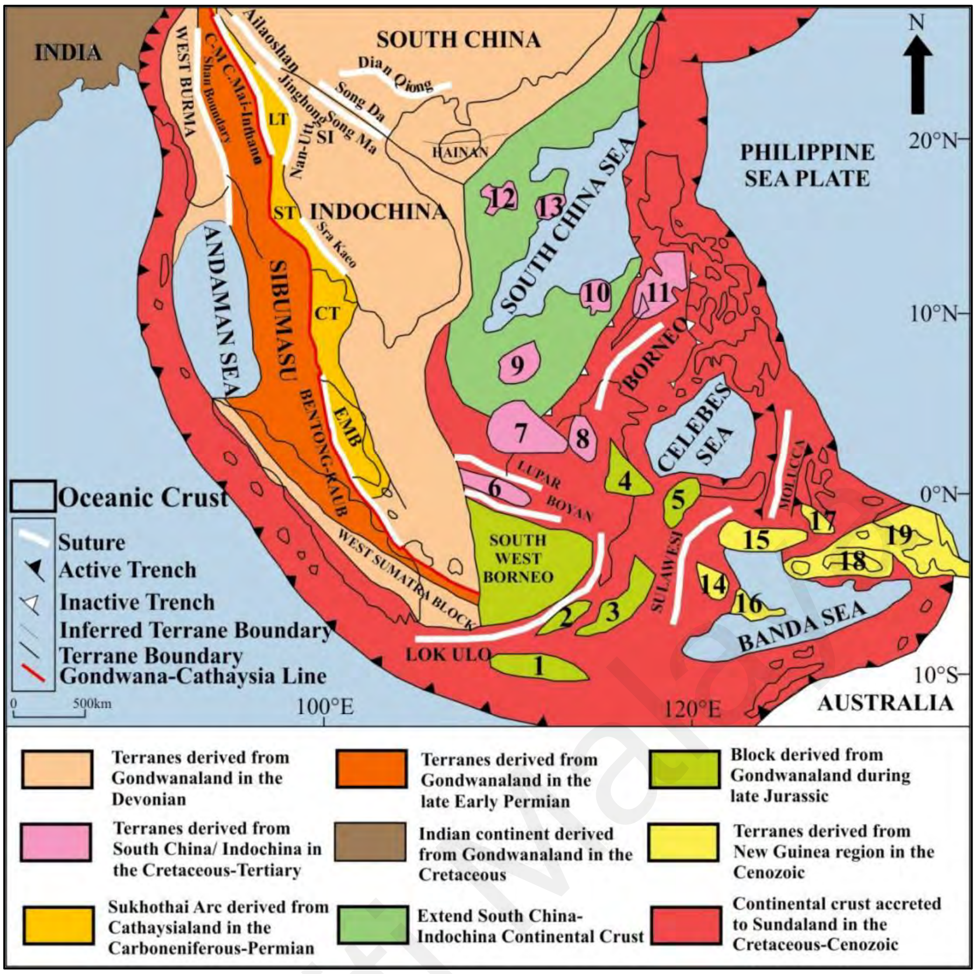

Figure 2.1: The regional map of South East Asia. After (Metcalfe, 2011).

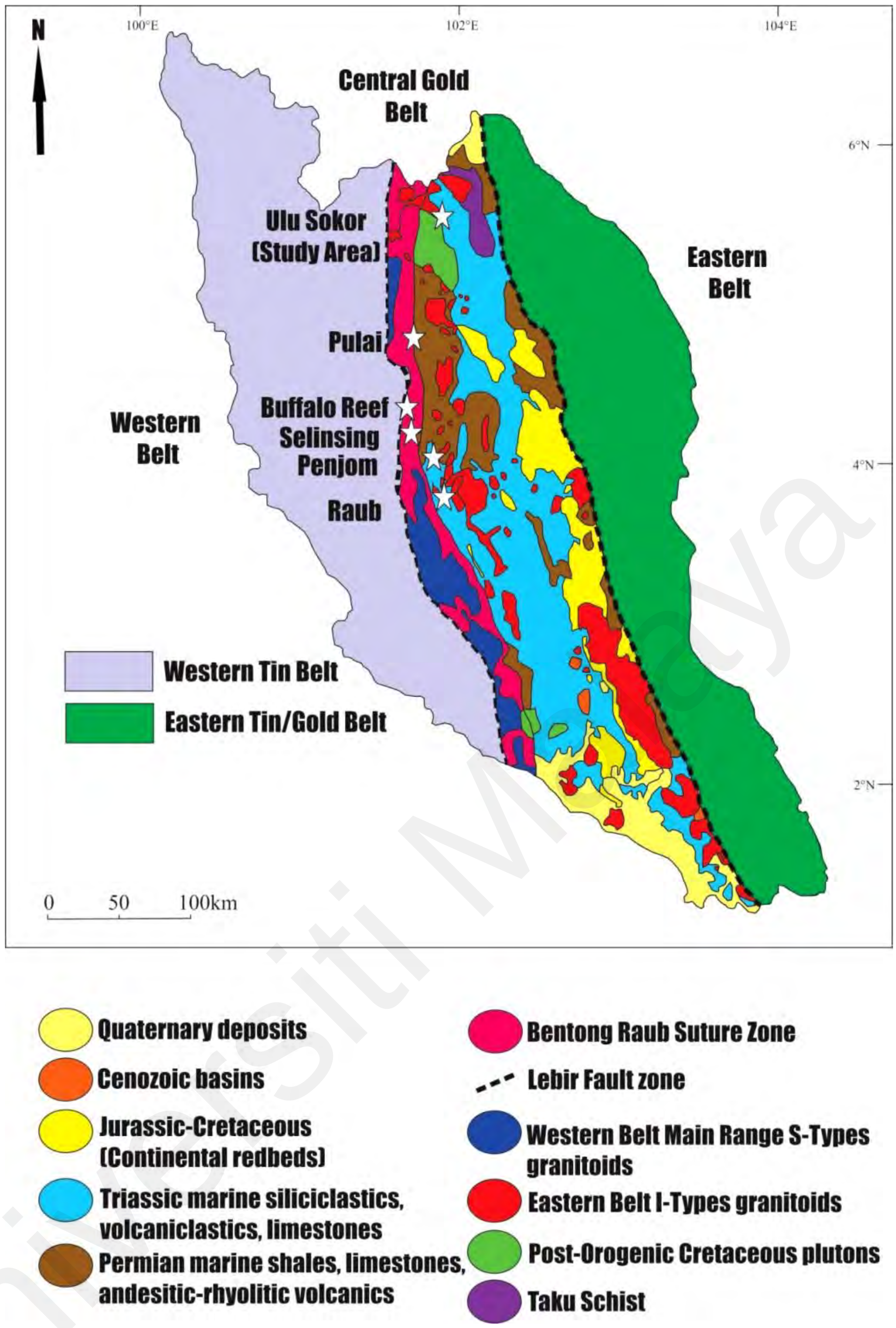

Figure 2.2: The major mineralization belt of Peninsular Malaysia. Note the white star symbol in the map represent the major gold deposit. After (Yeap, 2000; Tate et al., 2009).

2.1.1 Western Belt

The stratigraphic sequences in Western Belt comprise of several units. The sequences are from Early Paleozoic continental margin sequences, Late Paleozoic to Triassic platform carbonates, Triassic deep basinal clastic sequences and Jurassic to Cretaceous continental deposits along the north to southward of this belt (Makoundi et al., 2014; Li et al., 2015). The Quaternary deposits are widespread from the coastline to the mountain ridge of main range S-Type granitoids which are the dominant magmatic rocks in the Western Belt at Late Triassic to Early Jurassic (Tate et al., 2009; Metcalfe, 2013b). However, a small part at the further northwest of this belt has an I-Type granitoid (Figure 2.3).

To the north of the Western Belt, the region has Early Paleozoic rocks namely Cambrian Baling Group which contain sandstone and metasandstone interbedded with siltstone. Further north, there is Silurian-Devonian Sungai-Patani Formation which contains black-shale sequences. Towards southwest, the Terolak Formation comprising of schist, phyllite, slate and limestone which were dated from the Ordovician period. The Late Paleozoic-Triassic platform carbonates comprise of Semanggol Formation which is in the Permian-Triassic aged bedded chert, conglomerate and turbidite sandstone (Makoundi et al., 2014). Jurassic-Cretaceous continental deposit represents the Saiong Formation which is the sequence of polimict conglomerate to conglomeratic redbeds, red sandstone, shale and mudstone (Rahman, 2019).

The volcanic rocks in the Western Belt are volumetrically small and only occur in several formations, namely Jerai Formation, Baling Group (Lawin Tuffs) and in the Dinding schist. It was dated ranging from Late Cambrian-Ordovician to Early Silurian (Metcalfe, 2013b). These felsic volcanics are likely related to the intracratonic rifting on the Gondwana margin (Metcalfe, 2013a). According to the volumetrically small feature, it was suggested maybe the remnants of large volumes of main range felsic volcanics are now eroded away (Metcalfe, 2013b).

2.1.2 Central Belt

In general, Central Belt is deposited in a forearc portion of the palaeo-arc basin (Richardson, 1939; Gobbett & Hutchison, 1973; Tan, 1984; Leman, 1994; Metcalfe, 2002; Makoundi et al., 2014). This belt consists of deep to shallow marine clastic sediments and limestone with predominantly abundannce of intermediate to felsic volcanic and volcaniclastic rocks (Figure 2.3). It has undergone low grade metamorphism and it was mainly formed during Permo-Triassic activities.

The prolonged exposure during Upper Cretaceous and Paleocene resulted in the eroded post-Triassic successions in Peninsular Malaysia (Clements et al., 2011; Li et al., 2015). The magmatism in the Central Belt is characterized by dominantly I-Type granitoids, calc-alkaline granitoids and alkaline series of intrusive bodies ranging from monzonite (163 Ma), gabbro-diorite (157 Ma) to quartz syenite (127 Ma) (Bignell & Snelling, 1977; Hutchison, 1977; Shuib & Ghani, 2003; Searle et al., 2012; Yong et al., 2004; Li et al., 2015).

Volcanics and volcaniclastic are common and significant in the East Malaya Block. Thick piles of volcaniclastics reworked tuffs and agglomerates of Permo-Triassic age occur in the Central Belt of Peninsular Malaysia (Metcalfe et al., 1982; Metcalfe & Chakraborty, 1996; Metcalfe, 2013b), together with products of the Sukhothai arc which is intermediate to felsic volcanics and they were generally younger in age, mainly formed in the Middle Triassic age and considered products of subduction related I-Type granitoids (Ghani, 2009).

2.1.3 Eastern Belt

The Eastern Belt lies within the eastern part of East Malaya Block which consists of exposed strata of poly-deformed Carboniferous continental margin siliciclastics and carbonates, Permian shallow-marine carbonates and clastics that were unconfomably overlain by Jurassic-Cretaceous continental deposits (Metcalfe, 2013b; Makoundi et al., 2014; Li et al., 2015). This belt has a major fault, namely Lebir Fault Zone due to the highly deformed formation and it exhibits several phases of folding and refolded folds according to expression of orogenic deformation related to the closure of the back arc basin which are located in the offshore region of eastern Peninsular Malaysia (Metcalfe,. 2013b) (Figure 2.3).

The granitoids in this belt include a wide range of compositions, including biotite granite, hornblend-biotite granite/granodiorite, K-feldspar megacrystic granodiorite/granite and tonalite (Metcalfe, 2013b; Makoundi et al., 2014; Li et al., 2015). These granitoids are subduction related, calc-alkaline and have U-Pb zircon ages that range from early Middle Permian to early Late Triassic (Searle et al., 2012; Li et al., 2015) and it was classified to I-Type granitoids. According to the subduction related feature, these granitoids were generated by the subduction of the Palaeo-Tethys beneath Indochina-East Malaya and it was related to the Sukhothai arc (Sone & Metcalfe, 2008; Li et al., 2015).

Volcanic products in the Eastern Belt of Peninsular Malaysia are represented predominantly by rhyolitic and andesitic pyroclastics, tuff, agglomerate and minor lava flows of the Pahang volcanic series (Ghani, 2009; Metcalfe, 2013b). The change in geochemistry of volcanics in the East Malaya block from intermediate (andesitic) in the Permian to felsic (rhyolitic) in the middle Late Triassic indicates a major change in Sukhothai arc products which were the results from the collision of Sibumasu Block and East Malaya Block in the Early Triassic and the subduction stopped by Middle Triassic period (Metcalfe, 2013b).

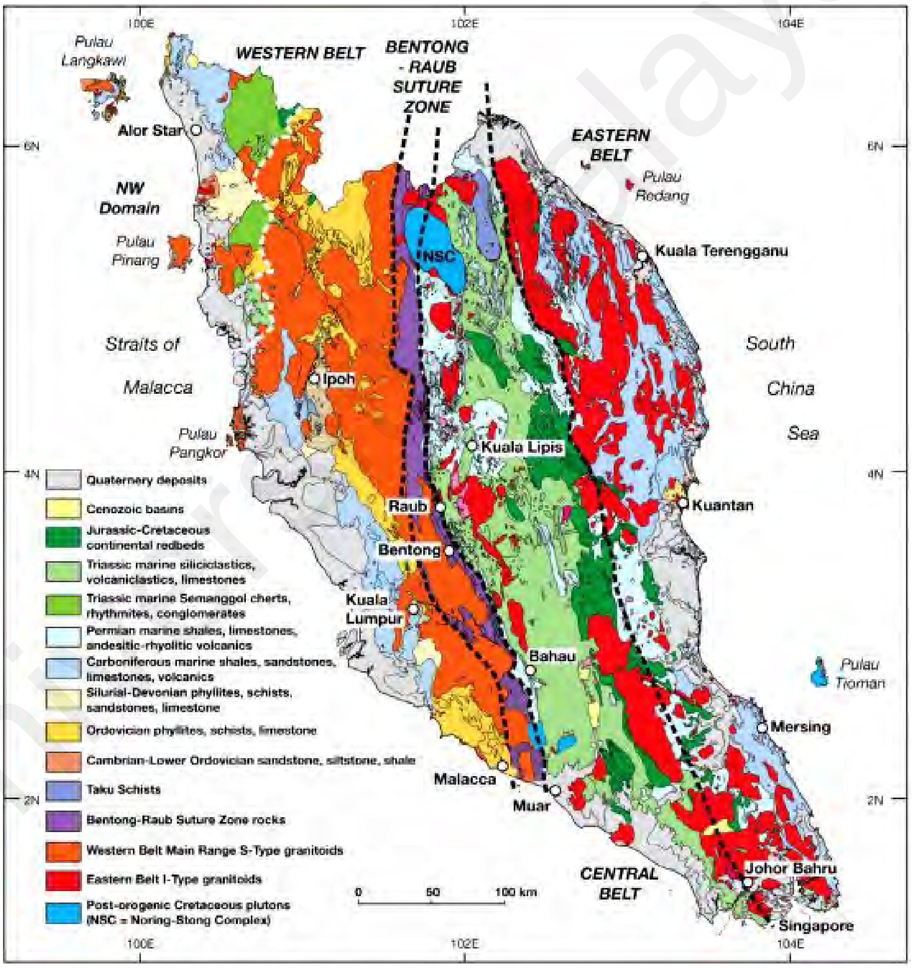

Figure 2.3: The geological map of Peninsular Malaysia. After (Tate et al., 2009).

2.2 Bentong -Raub suture zone

The Bentong-Raub suture zone is a major suture line between Sibumasu Block and East Malaya Block of Peninsular Malaysia (Figure 2.4). It is the remnant of subduction of the Palaeo-Tethys Ocean beneath the East Malaya Block which was dated back from the Carboniferous period (Metcalfe, 2000). The evidence of widespread volcanics materials in continental margin and the Carboniferous sediments in the East Malaya Block represent the eastern part of the Peninsular Malaysia (Metcalfe, 2000). The continuation of northward subduction of Palaeo-Tethys Ocean in Permian to Triassic period resulted in formation of I-type granitoids and intermediate to acidic volcanics of the East Malaya Block.

During late Early Permian period, the Cimmerian continental strip was separated from the Gondwana margin. The Cimmerian continental strip consisted of several unit blocks which were the western Cimmerian continent, Qiangtang and Sibumasu. The strip was rapidly drifted northwards and a part of it, which was the Sibumasu Block was subducted beneath East Malaya Block during Permian to Triassic period (Metcalfe, 2000). The consequences of this process constructed an accretionary complexity of off-scraped oceanic sediments and me´lange (Metcalfe, 2000). Prolonged time of accretionary complex process was developed in the outer part of arc which represents shallow marine limestone. However, some of it was incorporated as clasts into me´lange (Metcalfe, 2000).

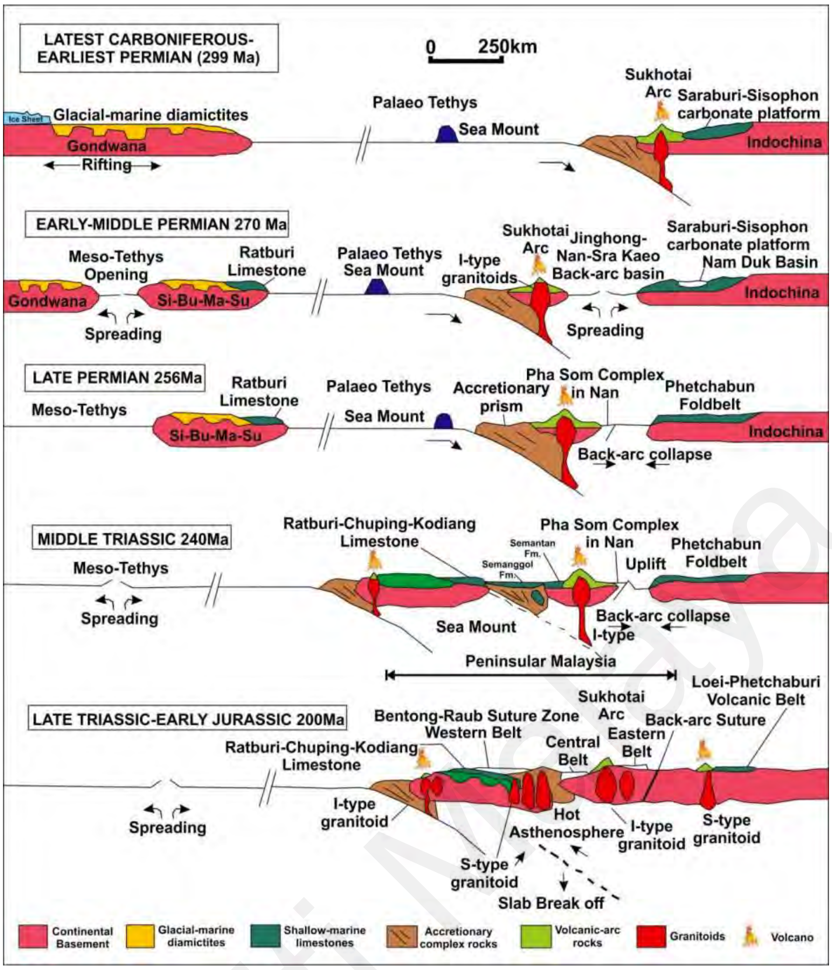

Figure 2.4: The conceptual of formation Bentong-Raub suture zone by the subduction of Palaeo-Tethys ocean and and collision of Sibumasu block and East Malaya block. After (Ueno & Hisada, 1999; Metcalfe, 2002; Sone & Metcalfe, 2008; Searle et al., 2012).

2.3 Local geology

The Kelantan state is bounded approximately by the latitudes of 5°30'25"-5°10'00" and longitudes of 101°55'30"-102°60'00". The total area occupied is approximately 15,000 km^2 (Figure 2.5). The general geology of the Kelantan state consists of three significant types of rocks which are sedimentary, metasedimentary and granitic intrusion rocks (Goh et al., 2006). Permo-Triassic sedimentary and metasedimentary rocks are mainly deposited in the center of Kelantan which comprise of siltstone, shale, slate, phyllite, sandstone and limestone. The Main Range Granite and Boundary Range Granite are the two main granitic rocks that bordered both Permo-Triassic sedimentary and metasedimentary rocks to the west and east respectively. Both these intrusions are related to the subduction during Late Triassic to Early Jurassic events (Goh et al., 2006).

There are some windows of granitic intrusion which are Senting Granite, Stong Igneous Complex and Kemahang Granite within the central part of this state. These belts of granite and country rocks have a north-south trending and it is believed that it is a continuation of the regional geology from north Pahang northwards to the south Thailand (Goh et al., 2006). To the east part of this state, the Boundary Range Granite is overlain by the Quaternary sediments such as coastal alluvial flats of Sungai Kelantan.

The metasedimentary rocks are deposited as a north-south trending which are bordered to the foothills of the Main Range Granite, and they are classified as the oldest rocks in this Kelantan state. It is approximately located at the southwest Kelantan as a Lower Paleozoic sequence. They are mainly meta-pelite with less volcanic fragments and minor arenaceous and calcareous intercalations. On the other hand, amphibolite and serpentinite have been recorded as rare occurrences (MacDonald, 1967; Goh et al., 2006).

To the east of Kelantan, Permian volcanic-sedimentary rocks occur widespread and they are overlying unconformably. Triassic rocks which are mainly argillo-arenaceous sediments with intercalated volcanic, and limestone are distributed within the central-south of Kelantan. In addition, several Permian rocks are exposed through this veneer of Triassic sediments (MacDonald, 1967; Goh et al., 2006). The youngest rock in this state is Jurassic-Cretaceous which overlies the Boundary Range Granite and Triassic sediments. They are deposited between the boundary of Kelantan, Terengganu and Pahang states. This sequence consists of a conglomerate overlain by sandstone with sporadic volcanic intercalations (Rishworth, 1974; Goh et al., 2006).

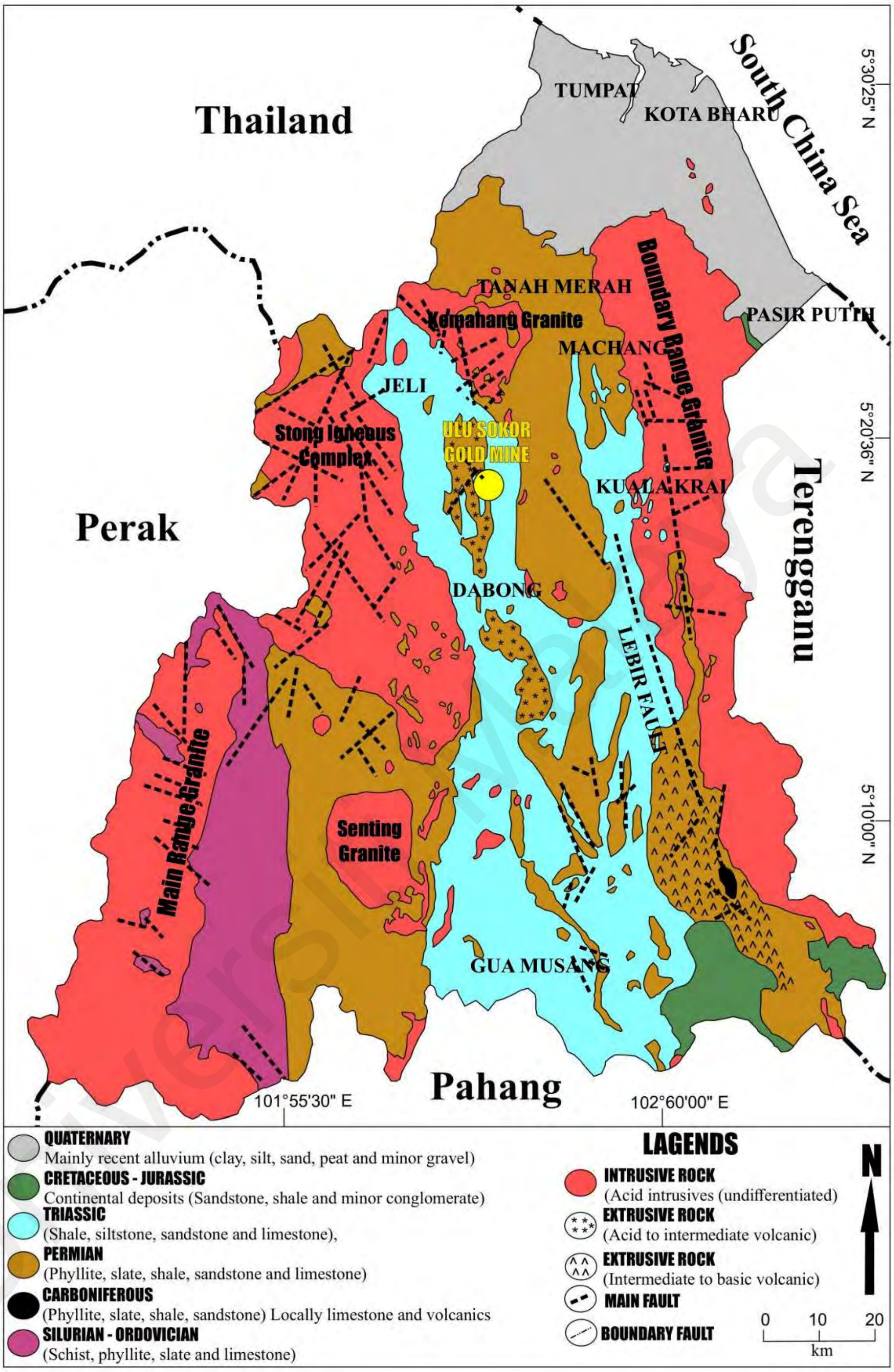

Figure 2.5: The geological map of Kelantan, Peninsular Malaysia. After (Teoh et al., 1987).

2.4 Central Belt of gold deposit in Peninsular Malaysia

The contribution of extensive tectonic deformation, metamorphism, magmatism and fluid flow in Peninsular Malaysia play a role in driving the formation of mineralization deposit (Ariffin, 2012). The deposition of mineralization in Peninsular Malaysia is widespread such as base metal and precious metal. According to this study, the gold mineralization deposits are largely found in Central Belt of Peninsular Malaysia. It is mined from quartz lode and stockwork deposits which is mostly associated with the accretionary prism due to the formation of Bentong-Raub suture zone (Ariffin, 2012).

The Central Belt of gold mineralization in Peninsular Malaysia is generally developed in the area of low grade metamorphic rock. It took place in the area of metasedimentary and volcanic rocks terrain which was formed during the collision of Sibumasu Block and East Malaya Block. This area was associated by the widespread of deformation system such as brittle, ductile, and shearing system zone (Ariffin, 2012). Consequences of the metamorphism and magmatic process in this area created a suitable environment for trap and source of gold mineralization (Ariffin, 2012).

According to the Wan Hassan & Purwanto (2002), the type of deposits of primary gold mineralization in Central Belt of Peninsular Malaysia can be divided into three; which are quartz vein, massive sulphide and skarn. However, the most prominent type of gold mineralization in this belt is quartz veins. It was developed in two styles which are gold with sulphide minerals and gold with base metal and carbonate minerals. In terms of the properties of fluid inclusion, structural control and geological setting, these characteristics are consistent with the orogenic gold deposit classification (Groves et al., 1998).

2.5 History and geology of Ulu Sokor gold deposit

According to Crawford (1970), discovery of precious mineral especially gold in Ulu Kelantan was founded by Robert William Duff in 1894. He was the Superintendent of Police in 1892 for the Pahang government. In 1896, he was appointed as Chief Police Officer in Pahang state. However, he resigned his appointment as Chief Police Officer Pahang in 1900 and returned to Kelantan. Mining activity was started on 10th October 1900 when His Highness Sultan Muhammad IV, Raja of Kelantan affixed an agreement to Robert William Duff personally for the rights to develop two very large areas in north and east of the Kelantan state based on the Lebir river. This agreement took place for a period of forty years.

Three years later from the date of agreement, Robert William Duff founded a company with the name Duff Development Company. He engaged with the mining engineers to prospect for minerals. Four dredges were installed on the Galas river and they recovered a considerable quantity of gold. During this time, the company's concession covered 2500 square miles or 1.6 million acres of Kelantan territory. However, the concession was reduced to 32000 acres by a new agreement which was signed on the 15th July 1912. It was after the Deed of Cancellation was signed in which the Duff Development Company surrendered its concession, granted for previous agreement.

Several companies such as Eastern Mining and Metals Company took over this area from 1966 to 1970, Asia Mining Sdn. Bhd. from 1989 to 1991, TRA Mining (Malaysia) Sdn. Bhd. from 1997 to 1998 and the latest is CNMC Goldmine Holding Limited from 2007 until now. In 2016, this company was granted with a mining license (ML 10/2016) which they have the right to access Sokor Block or Ulu Sokor covering approximately 10 km^2 (Figure 2.6). The license is currently extended until the 31st of December 2034. This area is covered by deposits from Rixen, Ketubong, New Found, New Discovery, Manson's Lode, Among River and Tiger River. However, this research only focuses on New Found and New Discovery deposit areas which are located at the southern part of Ulu Sokor.

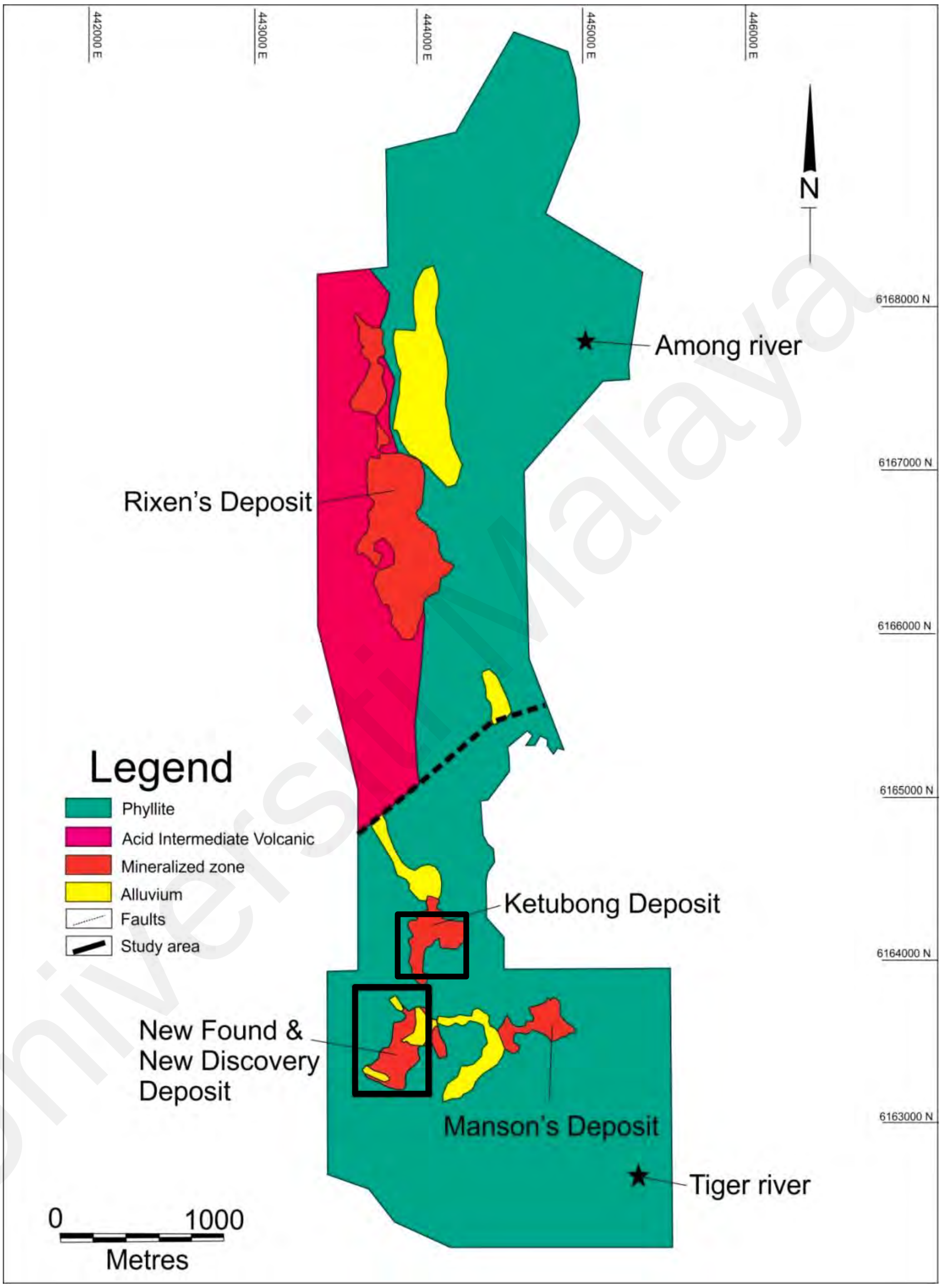

Figure 2.6: The geological and deposit map of Ulu Sokor gold mine, Peninsular Malaysia.

Ulu Sokor area is primarily underlain by a Permian lithologies (Figure 2.5) such as phyllite, tuffaceous phyllite, carbonaceous phyllite, slate, shale and limestone with widespread of volcanics. However, phyllite covers most of the mining area and is interbedded mainly with rhyolite, slate, shale and less commonly with Permian limestone (Li et al., 2015). The Triassic lithology (Figure 2.5) mainly consist of interbedded sandstone, siltstone and shale with lesser amounts of volcaniclastics (Ariffin, 2012). According to these lithologies present, it shows that overall mining area is undergone low grade metamorphism.

The lithologies in this area are highly folded and observed various dip angles due to geological structure. According to the Li et al. (2015), the main structural feature in the Ulu Sokor area is a series of major N/S-striking folds and faults and ENE–SWW and NW–SE oriented faults. The Permian–Triassic E/W regional compression activity and normal faults that formed in the Central Belt was contributed for the N/S-striking folds and faults in the Permian metasedimentary rocks (Li et al., 2011; Li et al., 2015). In addition, Li et al. (2011) and Li et al. (2015) indicate the formation of ENE- and NW-trending faults in the Pre cambrian metasedimentary rocks and Triassic sedimentary rocks most probably appear due to Late Triassic–Jurassic compressional tectonics activity.

These two sets of folds and faults may correspond to two episodes of folding and uplift that occurred in Peninsular Malaysia. The major N–S trending faults are interpreted as the oldest structures and are related to oblique amalgamation of Sibumasu Block and the East Malaya Block during the Permian–Triassic, and the ENE- and NW-trending faults are interpreted to be Late Triassic to Jurassic in age (Metcalfe, 2013b).

CHAPTER 3: RESEARCH METODOLOGY

3.1 Overview

All rock samples have been collected based on the lithology and by the author personally at the Ulu Sokor gold deposit. The area is actively mined by CNMC Goldmine Holdings Limited. There are three types of rock which have been selected: metasedimentary rock, volcanic rock and ore rock. This study involves fieldwork and laboratory works including sample preparation for thin section and geochemical analysis.

3.2 Fieldwork

A total of 52 most fresh rock samples were collected from the outcrops of the Ulu Sokor gold deposit. They comprise of host rock and ore rock samples. All sampling points were marked by Global Positioning System (GPS) using coordinate system of World Geodetic System 84 (WGS84) (Figure 3.1). During the fieldwork, several aspects have been taken in order to achieve the objective of this study. It includes documentation and observing the lithology, structural and mineralogy distribution.

3.3 Sample preparation

All the host rock and ore rock samples were prepared for microscopy and geochemistry analysis. Thin sections and polished sections were prepared at the Department of Geology, University of Malaya, Malaysia. However, the pulverized host rock and ore rock samples were analyzed for geochemistry including major oxides, trace elements and Rare Earth Elements (REEs) at ACME Analytical Laboratories, Vancouver, Canada.

3.4 Microscopy analyses

Microscopy studies were performed by using transmitted light microscope (Carl Zeiss Axioplan) with 5× to 40 × magnification powers. This microscope is used to study in a more detailed manner about the petrographic aspect of the host rock. However, reflected light microscope (Olympus DSX510) with resolution up to 0.01nm and 13× to 30× magnification powers is used to study more about the gold mineralization in ore rock samples. Both of microscopic studies (Figure 3.2) were done at Department of Geology in University of Malaya, Malaysia and Crest Nanosolution Sdn Bhd, Malaysia respectively.

3.5 Whole rock geochemistry analyses

Pulverized rock from host rock and ore rock samples had undergone geochemical analysis in order to determine the characteristics of the distribution pattern of various mineral assemblages. Lithium Borate dioxide fusion on 12 grams sample pulp followed by X-ray fluorescence spectrometry (XRF) analysis was carried out for major oxides. Loss of Ignition (LOI) was measured after ignition to 1000°C. Carbon and sulphur determination (LECO) analysis on 2 grams sample powder was used for total carbon and sulphur. The value of LOI (in weight %) can be determined by using the formula, LOI = 100% × ((a - b)/ (a - c)). “a” is the weight of the crucible with sample before sintering, “b” is the weight of the crucible with sample after sintering and “c” is the weight of the empty crucible.

Trace and REEs were determined by Inductively Coupled Plasma Mass Spectrometry (ICPMS) using Lithium metaborate/ tetraborate fusion and nitric acid digestion of a 0.2 grams sample. In addition, a separate 0.5 grams split was digested in Aqua Regia and analysed by ICPMS in determining the precious and base metal elements. The detection limits for major oxides, total carbon and total sulfur range from 0.01% to 0.1%, However, detection limits for trace and REEs range from 0.0005 ppm to 1 ppm. The geochemical analysis was performed at ACME Analytical Laboratories, Vancouver, Canada.

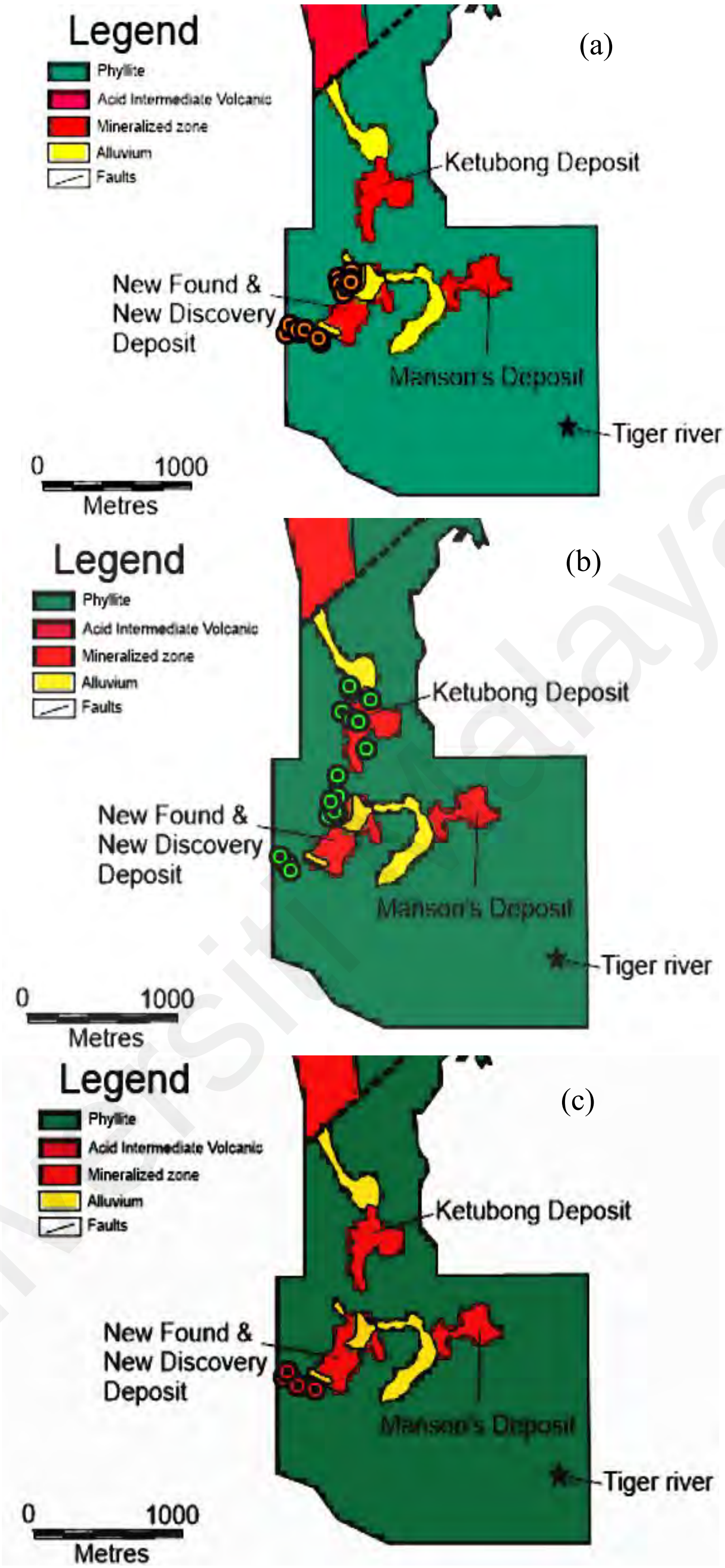

Figure 3.1: The locations of (a) Ore rocks (b) Rhyolite (c) Phyllite. The samples are collected for whole rock major and trace element geochemistry analysis.

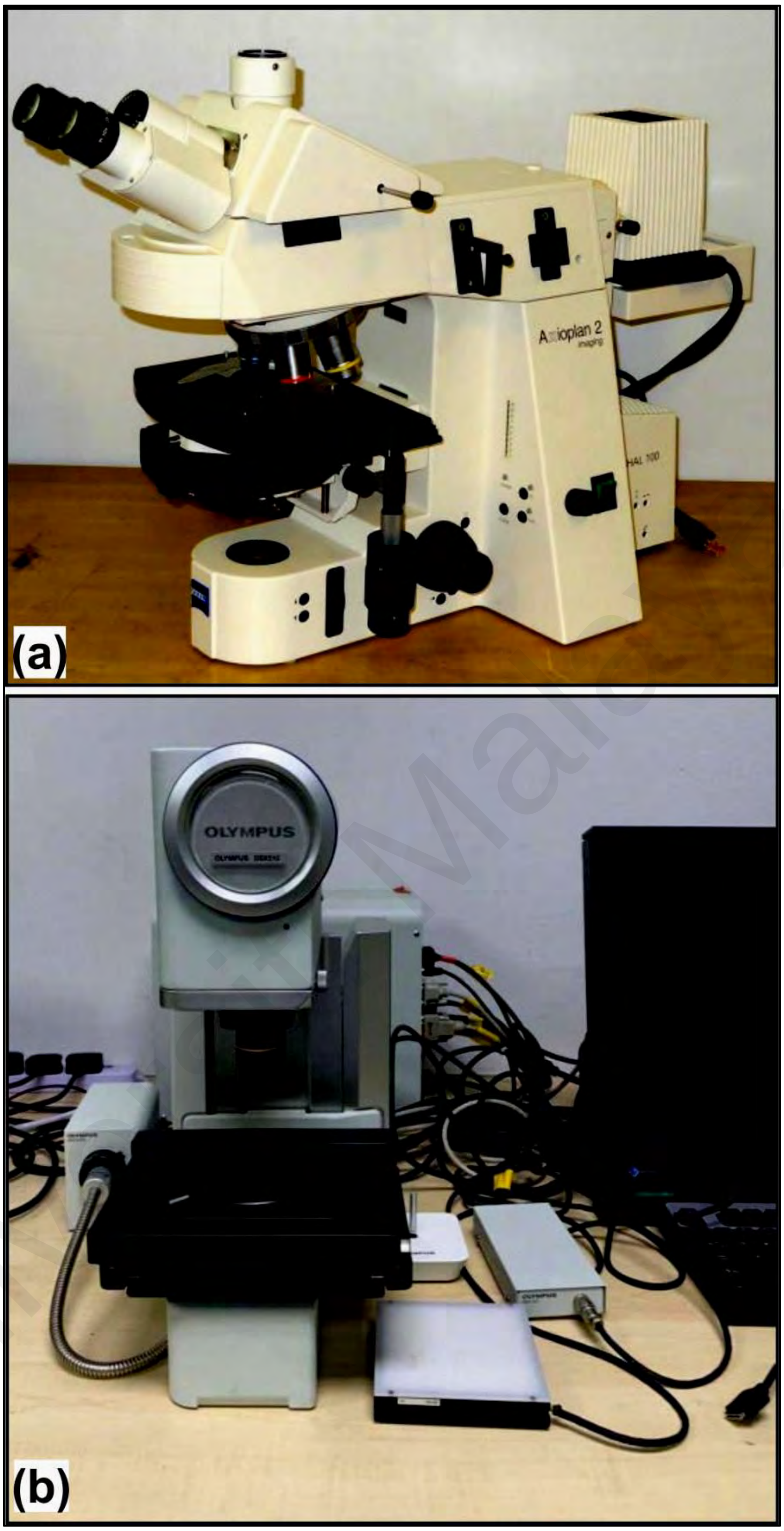

Figure 3.2: (a) Microscope used for the petrography analysis. Transmitted light microscope (Carl Zeiss Axioplan) with 5× to 40× magnification powers. (b) Microscope used for the mineralization analysis. Reflected light microscope Olympus DSX510 with resolution up to 0.01nm and magnification power 13× to 30×.

CHAPTER 4: RESULTS AND DISCUSSIONS

4.1 Overview

This chapter will describe results and discussion from petrographic observations (microscopically) and geochemical analysis of sedimentary, volcanic and ore rocks from Ulu Sokor gold deposit. The sedimentary and volcanic rocks in this particular deposit is dominantly occurred as phyllite and rhyolite, respectively. The ore rock which is mineralized with gold is dominantly associated with bismuth.

4.2 Petrography of phyllite

On the hand specimen scale, phyllite shows moderate foliation texture and is generally fine grained. The colour varies from grey to brown where the latter is in weathered condition. When observed on microscopic scale (Figure 4.1), phyllite is mostly composed of quartz, feldspar and subordinate micas which have been fully or partially altered to chlorite. The size of the mineral is generally less than 0.2mm in diameter. Quartz shows wavy extinction and mostly it is formed as anhedral crystal in shape. K- feldspar generally shows sharp extinction with some exhibit simple twinning. Mica which consists of both biotite and muscovite is formed as platy shaped mineral. Biotite has strong pleochroism which varies from light brown to dark brown while muscovite does not show any pleochroism characteristics. Some of the biotite has been partly or fully altered to chlorite. Foliation texture is quite significant where the minerals are aligned in preferred orientation. Phyllite can be sub-divided into chlorite-rich phyllite and mica-rich phyllite. The presence of deformed quartz grain and fine grain pyrite mineralization is commonly observed in chlorite-rich phyllite compared to mica-rich phyllite.

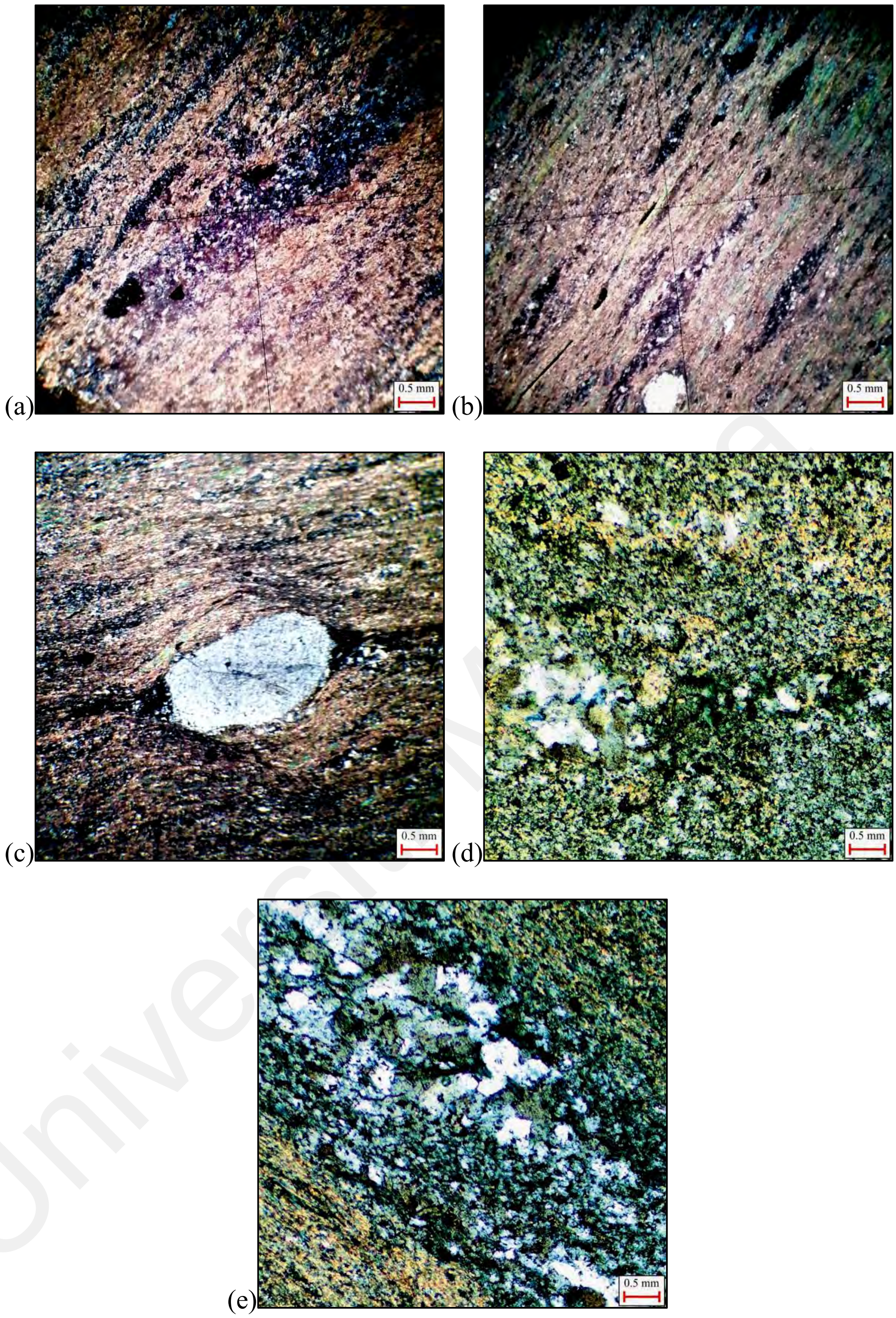

Figure 4.1: Photomicrograph of transmitted light (crossed nicols) for southern part of Ulu Sokor gold deposit (a) to (c) mica-rich phyllite and (d) to (e) chlorite-rich phyllite.

4.3 Petrography of rhyolite

The main type of igneous rock in this study area is dominated by rhyolite (Figure 4.2). When it is observed from hand specimen, rhyolite shows strong porphyritic texture with very less common aphanitic texture. The phenocryst generally comprises of plagioclase, K-feldspar, quartz with minor biotite. The phenocryst also reflects the composition of the groundmass or matrix.

Most of the samples has been undergone some of hydrothermal alteration and metamorphism. Some of the alteration is sericite and chlorite which has been altered from feldspar and biotite, respectively. The groundmass or matrix is formed as microcrystalline to cryptocrystalline of quartzo-feldsphatic compositions. Plagioclase is formed as lath in shape or prismatic crystals while K- feldspar is formed as euhedral to subhedral crystal in shape. Quartz often shows anhedral in shape. Like K-feldspar and plagioclase, quartz is also formed both as individual phenocryst and as interstitial within groundmass. Biotite is the only ferromagnesian mineral which is strongly pleochroic from light brown to dark brown sometimes replaced by chlorite.

Embayed structure of quartz and K-feldspar is the most common feature in rhyolite. There are also some of foliated structures which show rhyolite that has undergone metamorphism with some evidence of alteration of biotite to chlorite. Apatite is formed as individual prismatic crystals. Opaque mineral is formed as individual mineral and clots.

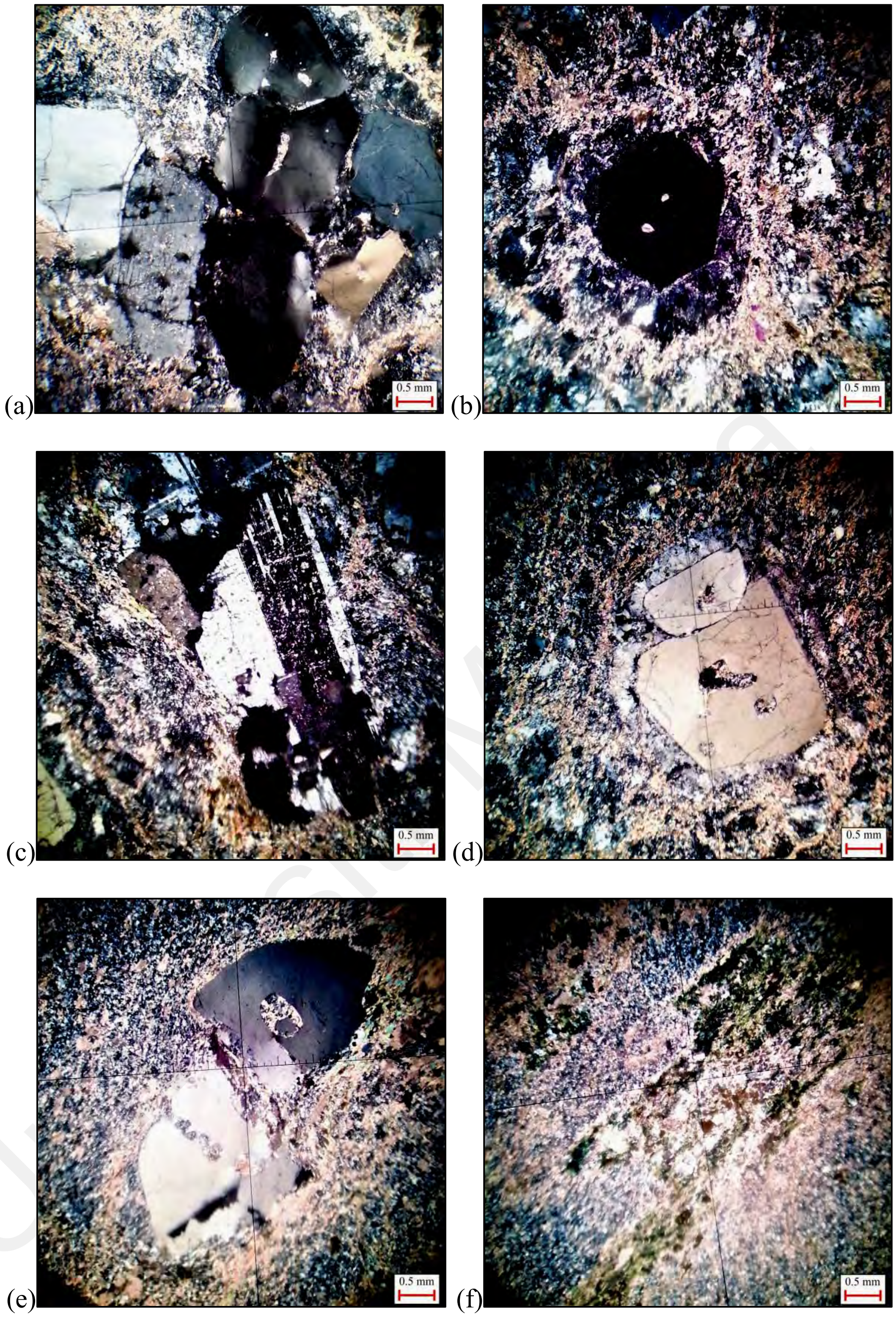

Figure 4.2: (a) to (e) Photomicrograph of transmitted light (crossed nicols) for southern part of Ulu Sokor gold deposit rhyolite.

4.4 Petrography of ore rock

The hydrothermal mineral assemblage consists of quartz and minor calcite gangue with the ore assemblage of bismuthinite (Bi_2S_3), galena (PbS), arsenopyrite (FeAsS), pyrite (FeS_2), chalcopyrite ($CuFeS_2$), sphalerite (ZnS) and gold (Au) in descending ordered of abundance as shown in (Figures 4.3, 4.4, 4.5, 4.6, 4.7 and 4.8).

4.4.1 Native gold

Gold dominantly occurs as inclusion with bismuthinite. It is also associated with fractures together with sulphide minerals such as galena, arsenopyrite, chalcopyrite, sphalerite and pyrite in descending order of abundance. However, gold is also observed as inclusion with bismuthinite along the quartz veins. In term of grain size occurrences, the gold is normally observed as fine grains with size ranging from 10 µm to 20 µm.

4.4.2 Pyrite

In terms of gold mineralization, pyrite is not closely related because according to the microscopy studied, most of the pyrite grain is formed individually. It seems to be formed at the early and late stage based on the anhedral to euhedral shape. In the samples which have gold mineralization, pyrite is not common.

4.4.3 Arsenopyrite

Arsenopyrite seems to be formed later than pyrite and it occurs as fine to coarse grains or aggregates with various sizes ranging from 100 µm to 500 µm. The shape is predominantly formed as euhedral to subhedral with some are fractured or brecciated. Bismuthinite bearing gold is the most dominant association which is formed as interstitial spaces in the arsenopyrite aggregates.

4.4.4 Sphalerite

Sphalerite is formed earlier than chalcopyrite and galena. It occurs as fine to coarse grains or aggregates with size ranging from 50μm to 100μm. However, it is also can observed as fracture infilling and interstitial spaces in arsenopyrite, chalcopyrite and galena. Some are partially rimmed on the galena and they occur as chalcopyrite disease.

4.4.5 Chalcopyrite

Chalcopyrite is formed later than sphalerite. It is formed as a fine grain and it infills the interstitial spaces and fractures within sulphide and quartz veins. Some of the chalcopyrite occurs in the form of disease in the sphalerite. It is also observed in the form of replacing and corroding by sphalerite. It can be closely linked with bismuthinite bearing gold association because it occurs as an inclusion in this aggregate.

4.4.6 Galena

Galena is formed later than chalcopyrite and sphalerite. The shape and distribution occurrences are as coarse grains or aggregates and fracture infillings within sulphide and quartz veins. The size observed varies from 100 μm to 500 μm. Galena is often seen closely related or associated with bismuthinite bearing gold. Some of it can be observed as inclusions in the galena. There is also observed bismuth-gold infilling the cracks and fractures of galena.

4.4.7 Bismuthinite

Bismuthinite is always dominantly associated with gold, and it is closely contact with the sulphide minerals such as galena, arsenopyrite, chalcopyrite, sphalerite, and pyrite in descending order of abundance. However, it also can be observed along the quartz vein without any contact with other sulphide minerals. In terms of shape, the bismuth observed is in the form of anhedral with size ranging from 50 μm to 300 μm. It seems to be formed later than other sulphide minerals.

4.4.8 Covellite

Covellite occurs as infilling in fractures present in chalcopyrite (thin veinlets). Its origin is attributed to supergene alteration of chalcopyrite.

The ore minerals of paragenetic sequence in the southern part of Ulu Sokor gold deposit is shown in the table below (Table 4.1).

Table 4.1: The paragenetic sequence of ore mineralization at southern part of Ulu Sokor gold deposit.

	Early	Middle	Late	Secondary
Ductile deformation				
Early quartz	------------------	--		
Early carbonate	------------------	--		
Pyrite	--------------	-----		
Arsenopyrite	-----------	-------		
Brittle deformation				
Late quartz		------------------	--	
Late carbonate		------------------	--	
Sphalerite		------------	---------------	
Chalcopyrite		-----------	--------	
Galena			------------	
Native gold		--	------------------	
Bismuthinite		---------	------------------	
Supergene				
Covellite				------------------

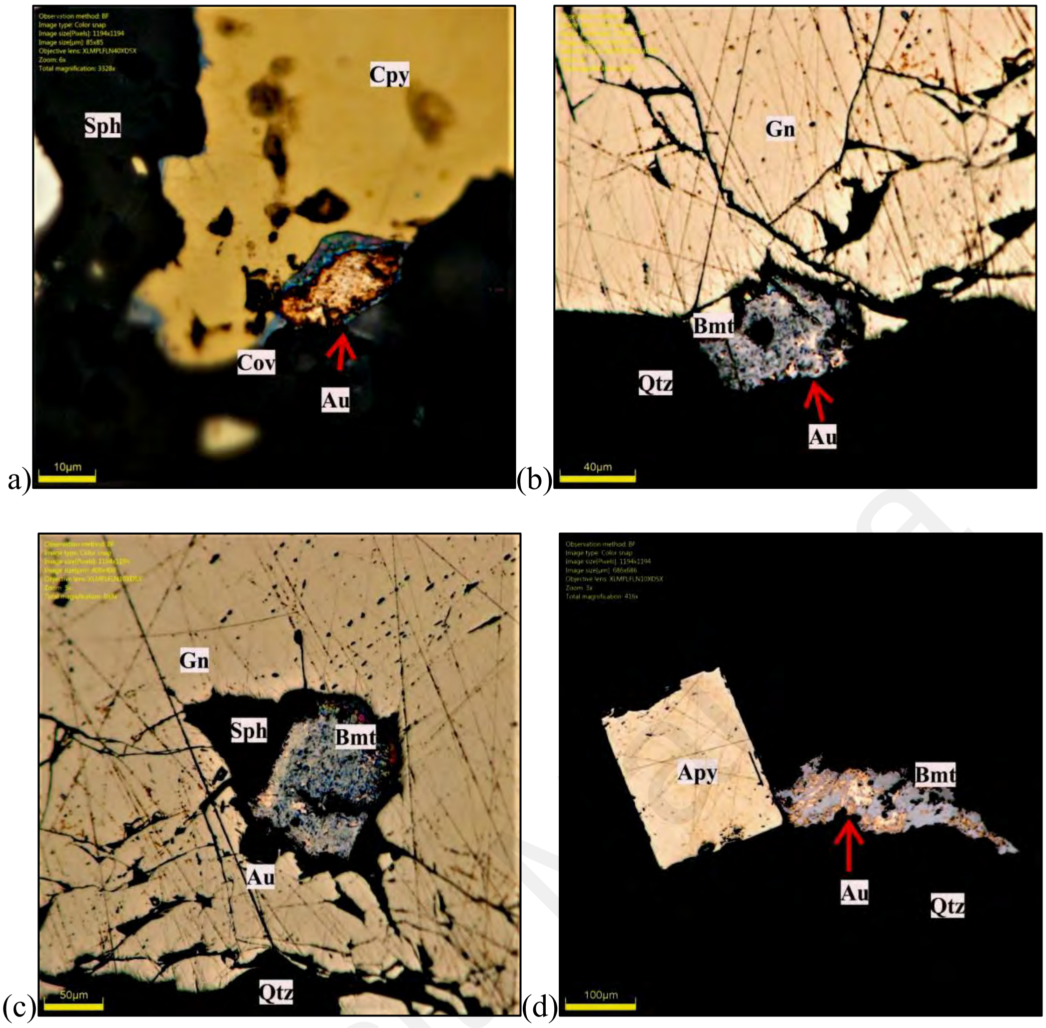

Figure 4.3: Photomicrograph of reflected light (plane light) for ore rock at southern part of Ulu Sokor gold deposit. (a) Anhedral chalcopyrite which associated by gold is enclosed by sphalerite. Covellite is at the boundary of chalcopyrite (b) Gold is closely associated with bismuthinite at the contact of brecciated galena. (c) Fractures in brecciated galena with gold associated bismuthinite infill. (d) Subhedral coarse grained arsenopyrite in quartz vein. Gold associated with bismuthinite in quartz vein.

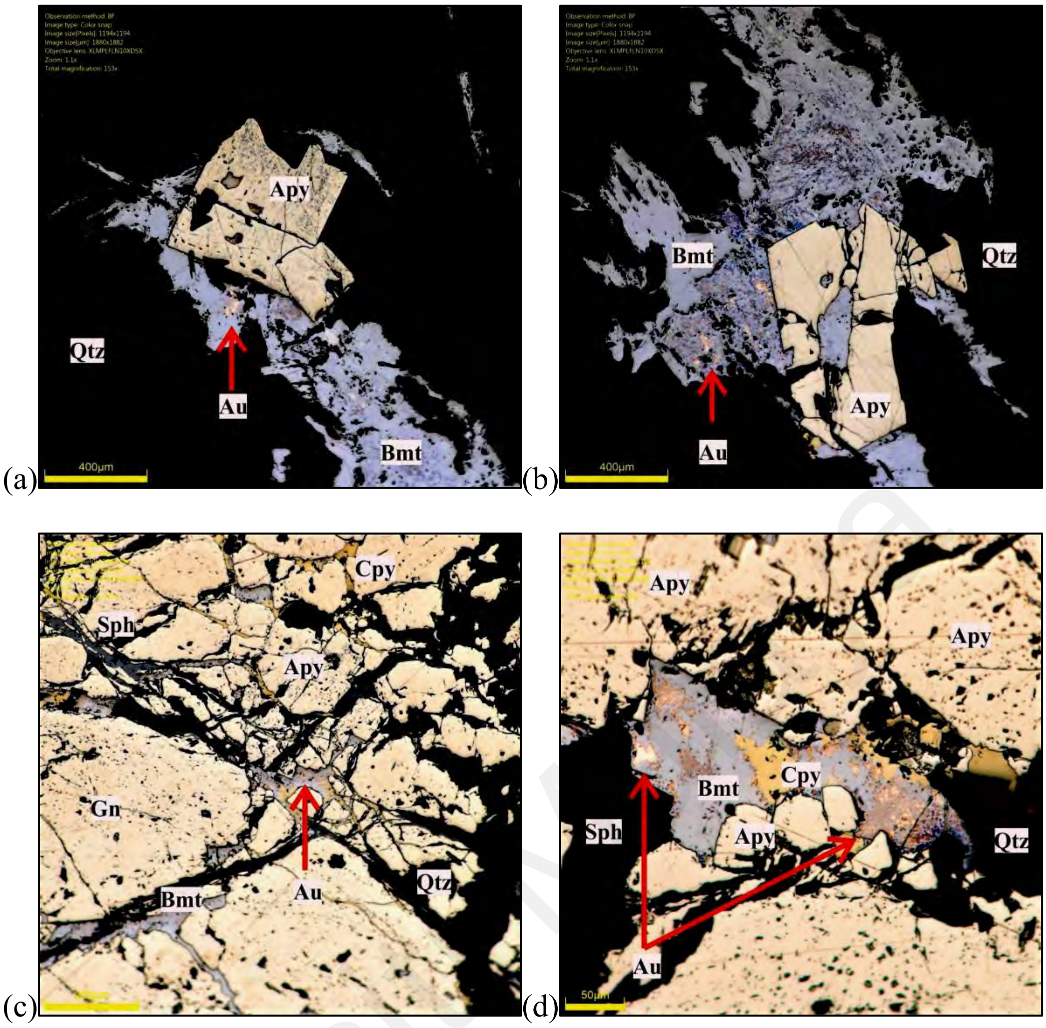

Figure 4.4: Photomicrograph of reflected light (plane light) for ore rock at southern part of Ulu Sokor gold deposit. (a) to (b) Anhedral arsenopyrite with gold associated by bismuthinite in quartz vein. (c) Brecciated of galena and arsenopyrite with infilling of sphalerite and gold associated by bismuthinite. Chalcopyrite also fill in the fractures of arsenopyrite (d) Arsenopyrite is partly enclosed to bismuthinite bearing gold. Bismuthinite bearing gold is enclosed by sphalerite.

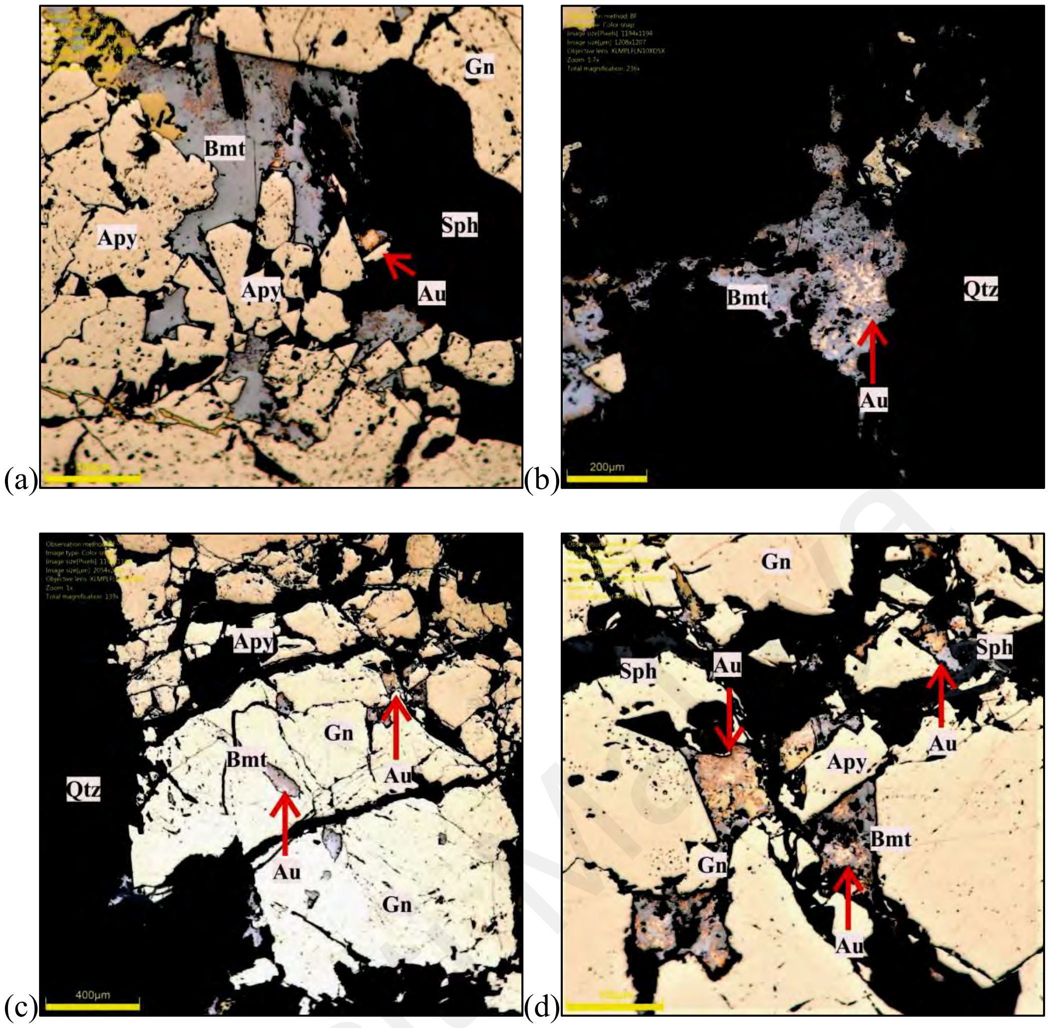

Figure 4.5: Photomicrograph of reflected light (plane light) for ore rock at southern part of Ulu Sokor gold deposit. (a) Subhedral to anhedral grained of arsenopyrite associated with bismuthinite bearing gold. Galena looks like enclosed by sphalerite and chalcopyrite fill in the fractures in between of arsenopyrite grains. (b) Bismuthinite bearing gold in the quartz vein. (c) Bismuthinite bearing gold as a inclusion in galena. Brecciated arsenopyrite is closely related to the galena. (d) Subhedral to anhedral of galena and arsenopyrite grained is associated together by infilling of bismuthinite bearing gold in the fractures. Some galena is enclosed by sphalerite.

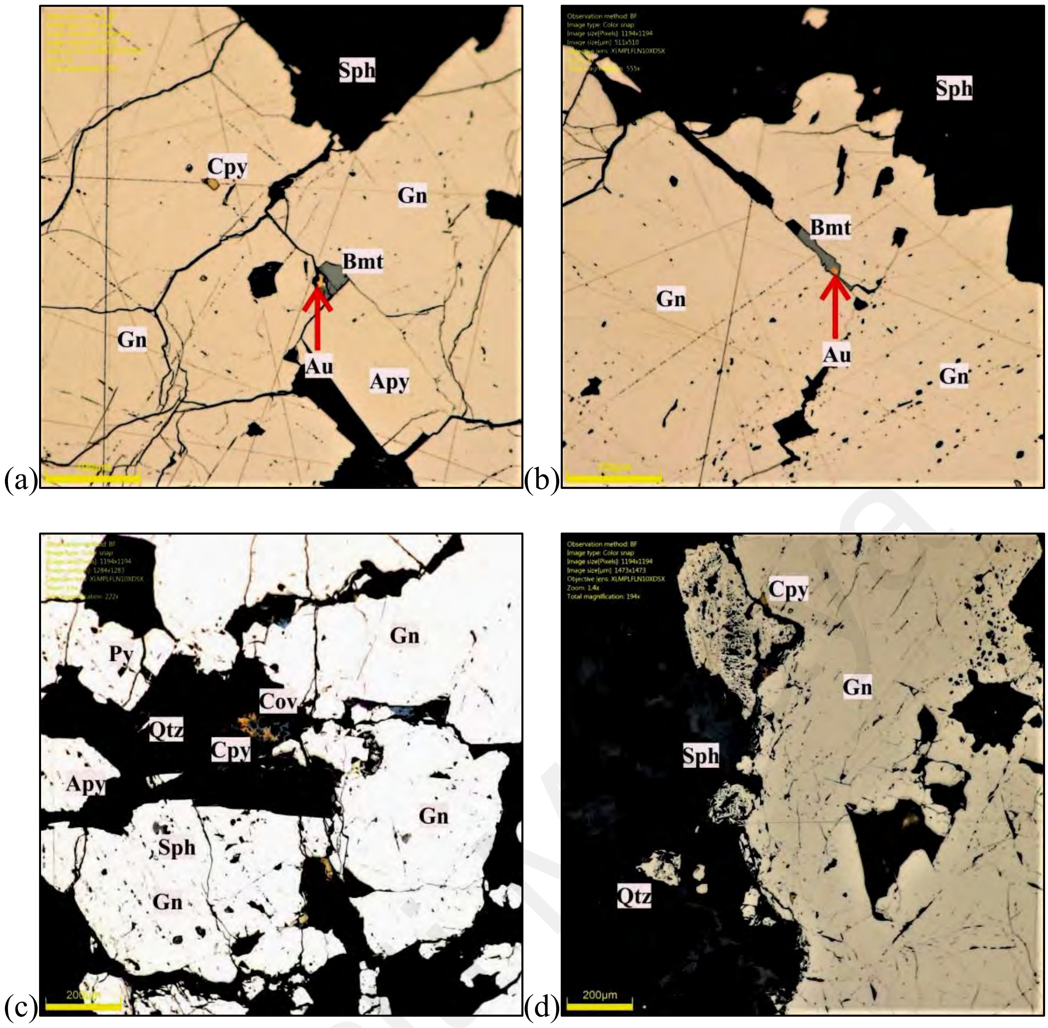

Figure 4.6: Photomicrograph of reflected light (plane light) for ore rock at southern part of Ulu Sokor gold deposit. (a) Large grained of galena and subhedral grained of arsenopyrite infilling by bismuthinite bearing gold in the cavity. (b) Bismuthinite bearing gold veinlet in brecciated galena. Galena seems to enclosed by sphalerite. (c) Chalcopyrite grained is enclosed by covellite. Some galena grained have sphalerite inclusion. (d) Chalcopyrite as a inclusion in the large grained galena.

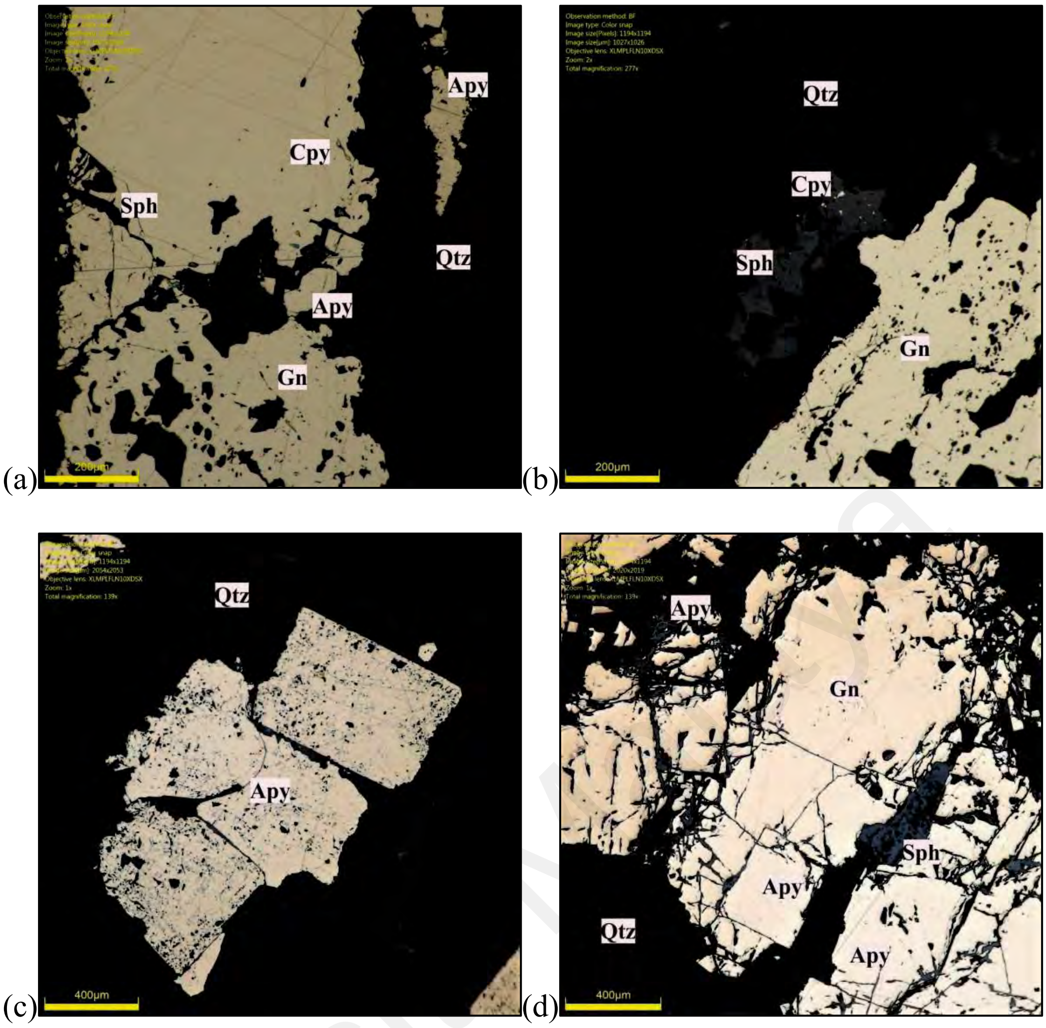

Figure 4.7: Photomicrograph of reflected light (plane light) for ore rock at southern part of Ulu Sokor gold deposit. (a) Subhedral to anhedral arsenopyrite and galena is closely associated with chalcopyrite as a inclusion in the galena. (b) Sphalerite with chalcopyrite disease. (c) Individual subhedral grained of arsenopyrite in quartz vein. (f) Subhedral to anhedral arsenopyrite and galena is closely associated in quartz vein.

(a) 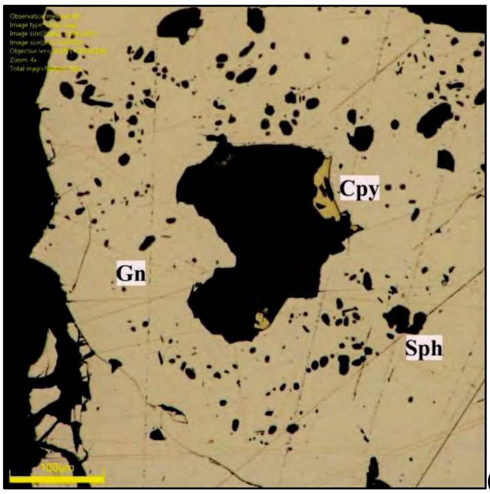

(b) 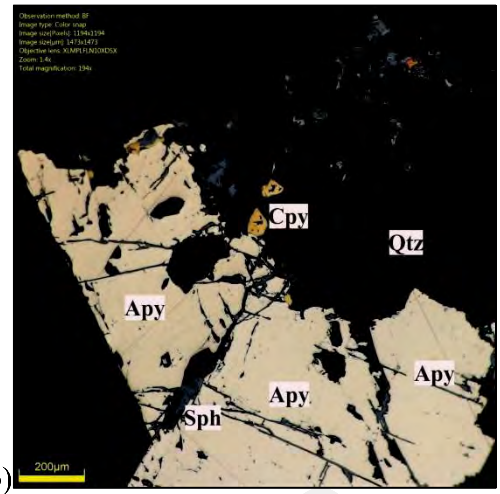

Figure 4.8: Photomicrograph of reflected light (plane light) for ore rock at southern part of Ulu Sokor gold deposit. (a) Sphalerite as a inclusion in galena grained. Chalcopyrite as a infilling in the cavity of galena. (b) Subhedral arsenopyrite with infilling by spahlerite.

4.5 Geochemistry of phyllite

22 representative metasedimentary rock samples were analyzed for major oxides and trace elements, including Rare Earth Elements (REEs) (Tables 4.2, 4.3 and 4.4), respectively. The average samples study with other average chemical composition such as Post-Archean Australian Shale (PAAS), (Taylor & McLennan, 1985; McLennan, 2001) and Upper Continental Crust (UCC) (Rudnick & Gao, 2003) are noted in these tables. The metasedimentary rock is classified as phyllite which mostly covers the whole area of southern part. It shows that the entire area is governed by low grade of metamorphism.

The phyllite show a restricted and wide range for almost all major elements contents (Tables 4.2 and 4.3). Based on PAAS and UCC, it is characterized by low contents of MgO with average of 1.71 wt %, which reflects the evolved nature is from igneous protolith (El-Bialy, 2013). According to the high content of Al_2O_3 with average more than 15 wt %, this also suggests high clay content. The elevated K_2O/Na_2O ratio in some samples from this study area such as SGM1, SGM3, SGM10, SGM12, SGM16, SGM21 and SGM22 most likely reflect secondary addition of potassium (K-metasomatism). Based on geochemical classification diagram from (Herron, 1988), all the metasedimentary rocks are plotted in shale field (Figure 4.9).

According to the UCC-normalized multi-element spider diagram (Rudnick & Gao, 2003) (Figure 4.10), this rock is generally has low concentration of Ba, Nb, Ta, Sr, P, Hf and Zr, which is possibly due to chemical weathering. All phyllite samples are homogeneous showing negative Sr anomalies which indicate dissolution of plagioclase feldspar (Mader & Neubauer, 2004). The Cl chondrite-normalized REEs from (Nakamura, 1974) for this study shows parallel to sub-parallel where the Light Rare Earth Elements (LREEs) are slightly enriched compared to the Heavy Rare Earth Elements (HREEs) values. It shows slight shallow negative Eu anomaly (Figure 4.11).

The average of Eu/ Eu* ratio is 0.70 which is more or less in average with PAAS (0.66) and UCC (0.72) values.

This phyllite is characterized by a moderate degree of REEs fractionation with their average $(La/Yb)_N$ ratio of 5.77. The LREEs and HREEs fractionation can be determined by using the average ratio of $(La/Sm)_N$, 3.25 and $(Gd/Yb)_N$, 1.30 respectively. The average ∑REEs is 129.42 ppm which is low compared to the PAAS (184.77) and UCC (148.14) values. The Cl chondrite-normalized REEs from (Nakamura, 1974) patterns are also plotted based on the average value of these metasedimentary rocks and they are compared to the average PAAS and UCC (Figure 4.12). They are generally parallel to sub-parallel, and the LREEs are slightly depleted relative to PAAS and UCC, while HREEs are slightly enriched relative to PAAS and UCC. However, they are more or less have the same magnitude of Eu anomalies.

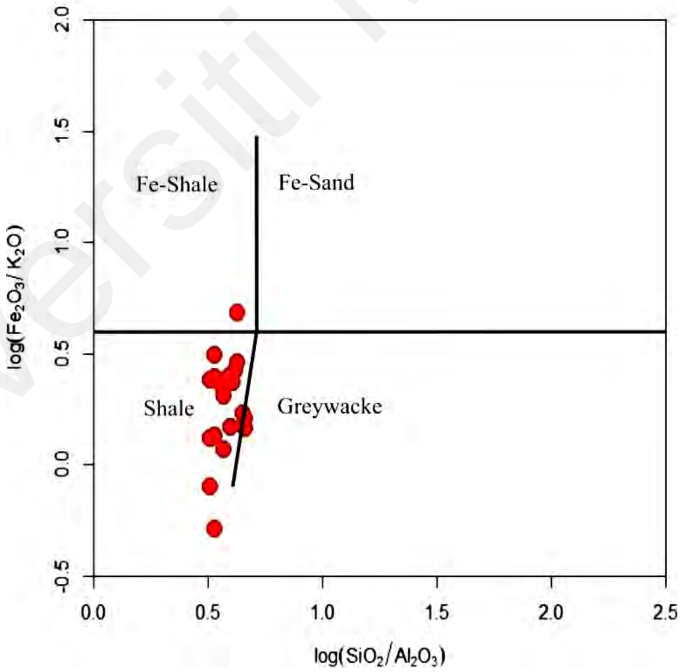

Figure 4.9: The log (SiO_2/ Al_2O_3) versus log (Fe_2O_3/K_2O) diagram for phyllite at southern part of Ulu Sokor gold deposit (Herron, 1988). Red dots indicate sample of phyllite.

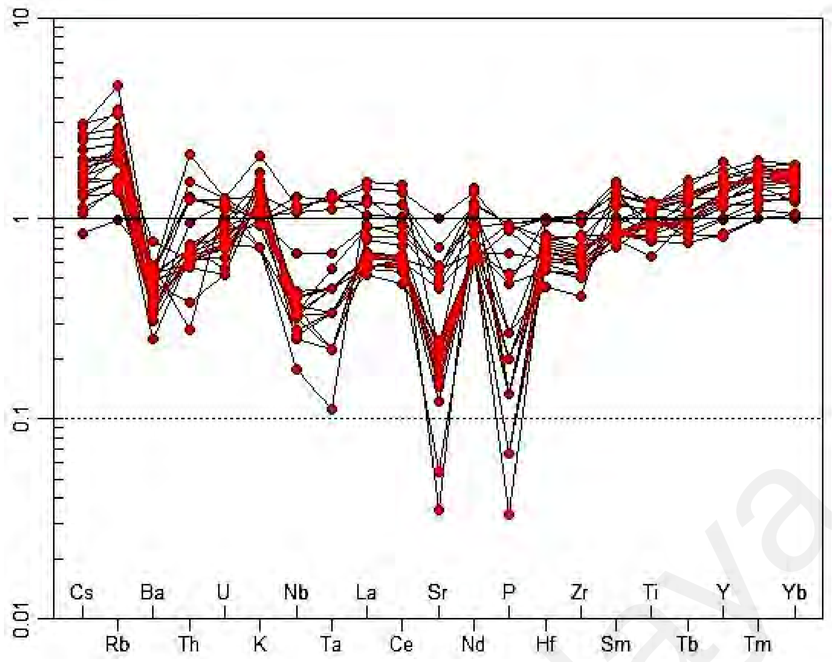

Figure 4.10: The UCC-normalized multi-element spider diagram for phyllite at southern part of Ulu Sokor gold deposit. Normalizing values are from (Rudnick & Gao, 2003). Red dots indicate sample of phyllite.

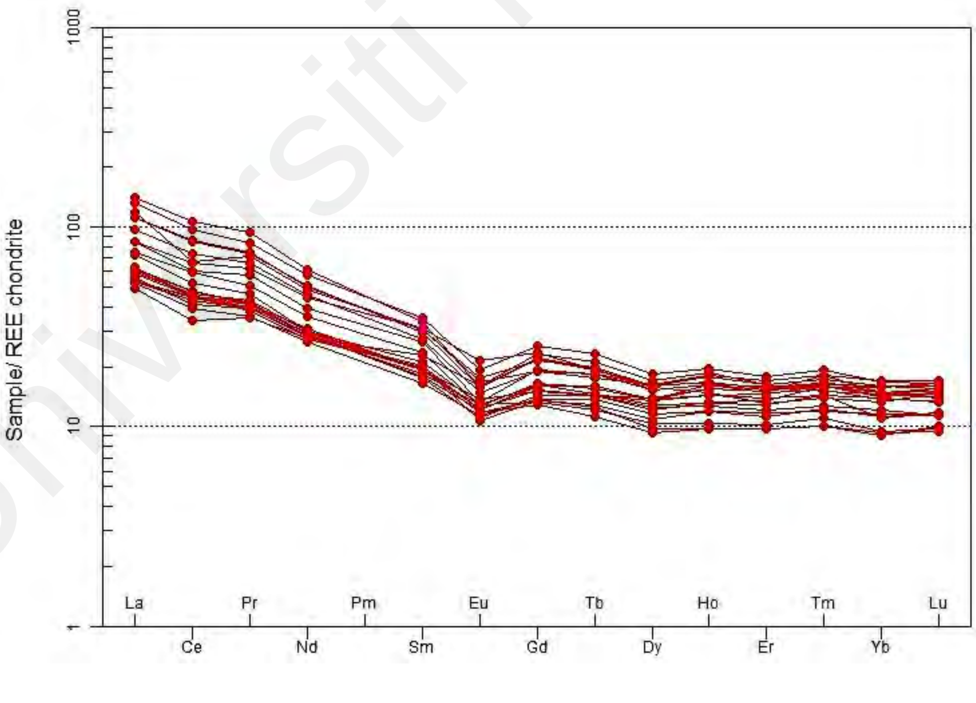

Figure 4.11: The C1 chondrite-normalized rare earth element spider diagram for phyllite at southern part of Ulu Sokor gold deposit. Normalizing values are from (Nakamura, 1974). Red dots indicate sample of phyllite.

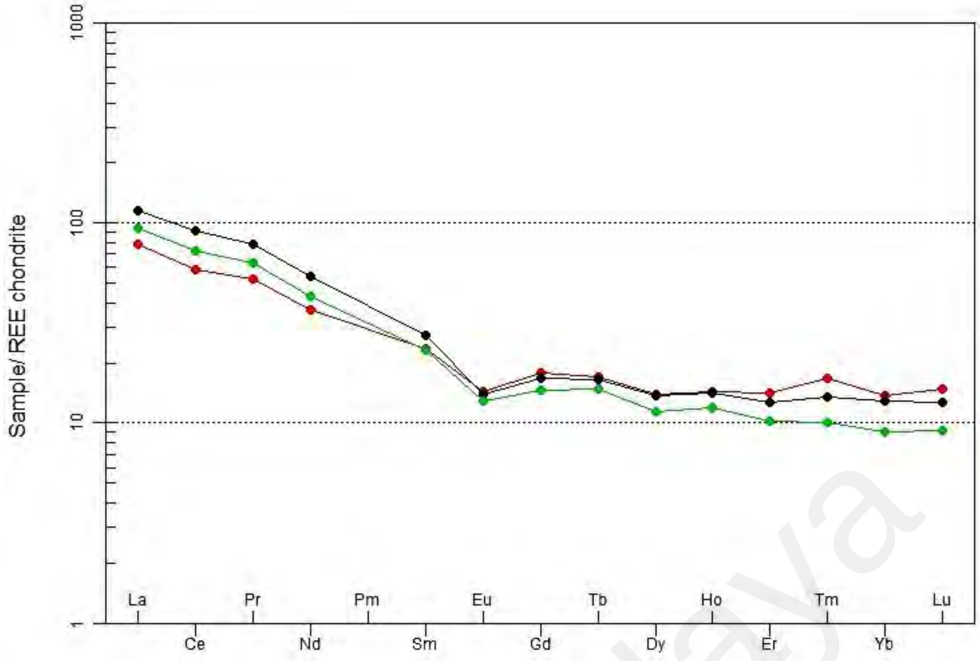

Figure 4.12: The average value of C1 chondrite-normalized REEs spider diagram for phyllite at southern part of Ulu Sokor gold deposit. Normalizing values are from (Nakamura, 1974). Patterns of PAAS and UCC from (Taylor & McLennan, 1985; McLennan, 2001) and (Rudnick & Gao 2003), respectively are constructed for comparison. Black: PAAS, Green: UCC, Red: Average value phyllite.

4.5.1 Sedimentary recycling and sorting

Discrimination plot of Zr/Sc versus Th/Sc from (McLennan et al., 1993), reflects the amount of sedimentary sorting and recycling (Figure 4.13). Zr, Th and Sc are trace elements are categorized as insoluble and they are typically immobile under surface condition which is useful for provenance and recycling evaluation of clastic rocks (El-Bialy, 2013). Sedimentary recycling and chemical differentiation are measured in both Zr/Sc and Th/Sc ratio, respectively. The distribution pattern shown as a positive correlation between Zr/Sc and Th/Sc. The plot pattern followed the magmatic differentiation trend which is slightly toward >10 value ratio of Zr/Sc. It indicates some samples have undergone sediment reworking and sorting.

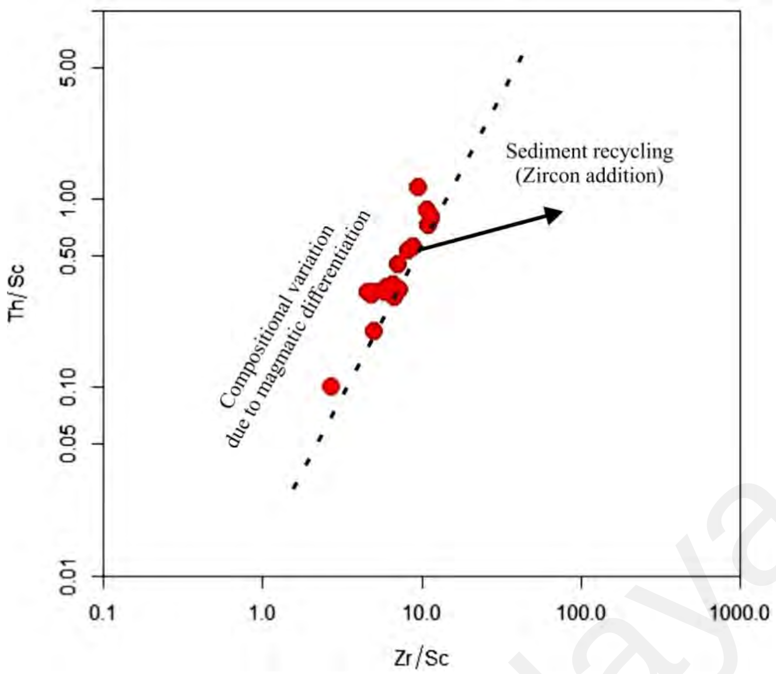

Figure 4.13: Zr/Sc versus Th/Sc diagram for phyllite at southern part of Ulu Sokor gold deposit (McLennan et al., 1993). Red dots indicate sample of phyllite.

Some of the major oxides and trace elements are responsible for the systematic fractionation in sedimentary sorting where these certain elements are preferentially retained in the fine-grained fractionation (Garcia et al., 1994). In order to distinguish the sediments either in psammitic (< 0.33) (metamorphosed medium grain sedimentary rock) or pelitic (> 0.33) (metamorphosed fine-grained sedimentary rock), discrimination ratio of (TiO_2/Zr) × 100 is used which was proposed by Garcia et al. (1994). From this study of phyllite, the average ratio is 0.47.

4.5.2 Degree of weathering

Weathering in the source areas is a process where the chemical composition in the sediment is enriched or depleted. In order to evaluate the weathering conditions, both the degree of weathering and maturity of source rock need to be calculated. The Chemical Index of Alteration ($CIA=Al_2O_3/(Al_2O_3+CaO^*+Na_2O+K_2O)\times100$) and the Index of Compositional Variability ($ICV=(CaO+K_2O+Na_2O+Fe_2O_3+MgO+TiO_2)/Al_2O_3$) are used as proposed by Nesbitt & Young (1982), Cox & Lowe (1995), Cullers & Podkovyrov (2000), and Bhat & Ghosh (2001).

Roddaz et al. (2012) suggested that the CIA values for unaltered plagioclase and K-feldspar are around 50, while those of intensely weathered products such as kaolinite and gibbsite-rich shale are close to 100 (Nesbitt & Young, 1982). The calculated CIA shows that the average is 79.10, implying a more weathered source (Figure 4.14). The intensely weathered source is not due to recent weathering, while it is referred to the chemical weathering effect on the source rock. The ICV values can reveal the maturity of source rocks (Cox & Lowe, 1995; Cullers & Podkovyrov, 2000), where high and low ICV values indicate immature and mature sources, respectively. The calculated ICV shows that the average is 0.78, suggesting mature sources as shown in Figure 4.14.

The ternary diagram Rb/V-Zr/Zn-Eu/Eu* can effectively discriminate the provenance as proposed by Sawant et al. (2017), Xu et al. (2019), as shown in Figure 4.15. The Eu-Eu* and Rb/V ratios represent mafic and felsic end-member provenance, respectively. In general, these samples are plotted in the felsic source field.

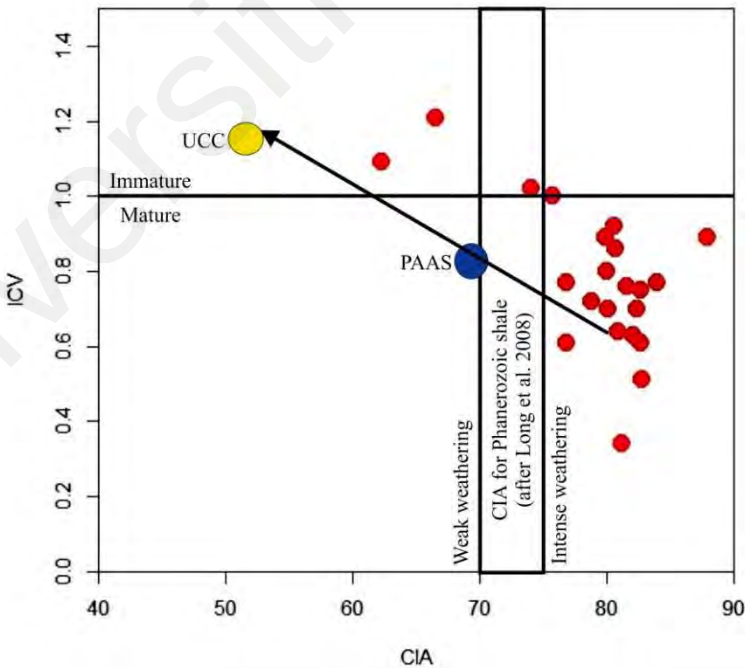

Figure 4.14: Chemical Index of Alteration ($CIA=Al_2O_3/(Al_2O_3+CaO^*+Na_2O+K_2O)\times100$) versus Index of Compositional Variability ($ICV=(CaO+K_2O+Na_2O+Fe_2O_3+MgO+TiO_2)/Al_2O_3$) diagram for phyllite at southern part of Ulu Sokor gold deposit (Cox et al., 1995; Nesbitt & Young, 1984). Red dots indicate sample of phyllite.

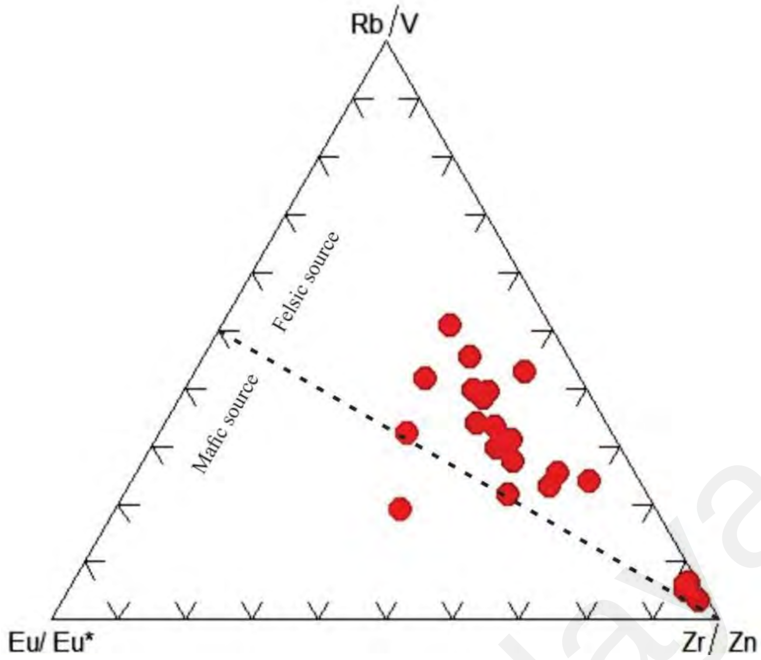

Figure 4.15: Rb/V-Zr/Zn-Eu/Eu* diagram for phyllite at southern part of Ulu Sokor gold deposit (Sawant et al., 2017). Red dots indicate sample of phyllite.

4.5.3 Tectonic setting

Important things that need to be concerned regarding the tectonic setting of the depositional environment are the types of sediment deposition and their geochemical characteristics. Sediments can be transported across any boundaries from the original deposit and it can shows their geochemical characteristic of the deposit, such as major, trace and rare earth elements (Bhatia & Crook, 1986; McLennan, 1989; McLennan et al., 1990).

Based on Bhatia & Crook (1986), the authors used trace elements such as La, Sc, Zr and Th to classify depositional conditions. These are more useful elements because they are immobile or the least mobile in nature. Hence, it is more useful rather than major elements that are mobile in nature. The major distribution plots of these studied samples are in the fields of continental island arc and oceanic island arc for three discriminatory plots, as shown in Figures 4.16, 4.17 and 4.18, which were suggested by Bhatia & Crook (1986).

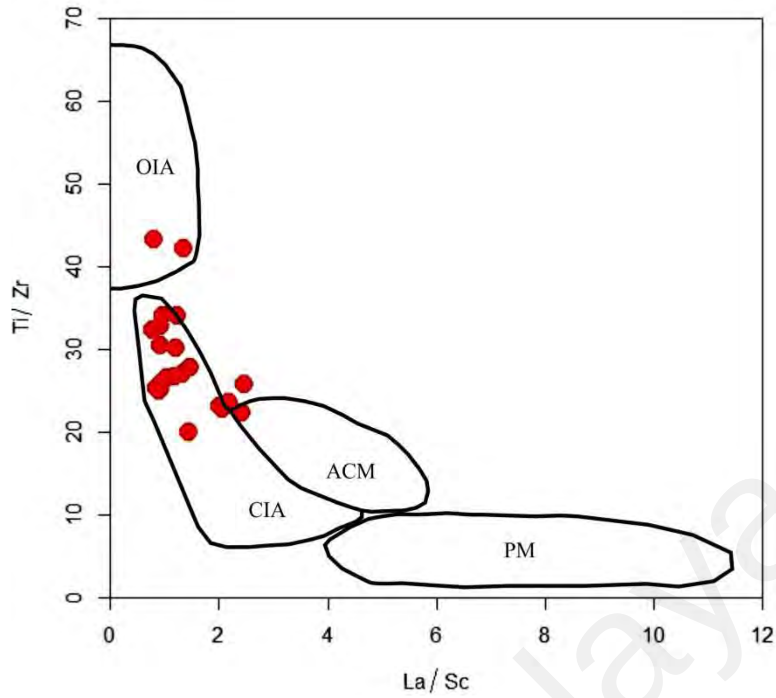

Figure 4.16: La/Sc versus Ti/Zr diagram for phyllite at southern part of Ulu Sokor gold deposit (Bhatia & Crook, 1986). Oceanic Island Arc (OIA), Continental Island Arc (CIA), Active Continental Margin (ACM) and Passive Margin (PM). Red dots indicate sample of phyllite.

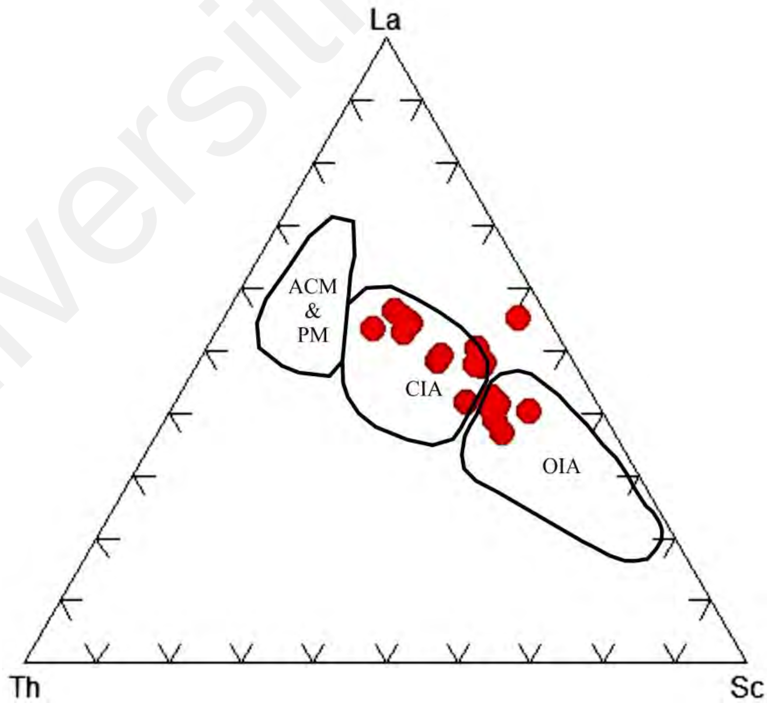

Figure 4.17: Th-La-Sc diagram for phyllite at southern part of Ulu Sokor gold deposit (Bhatia & Crook, 1986). Oceanic Island Arc (OIA), Continental Island Arc (CIA), Active Continental Margin (ACM) and Passive Margin (PM). Red dots indicate sample of phyllite.

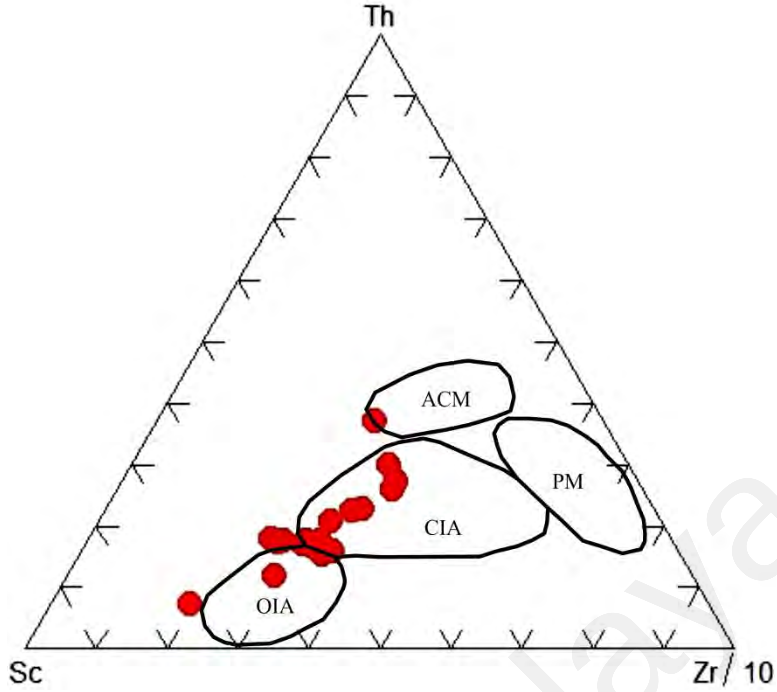

Figure 4.18: Sc-Th-Zr/10 diagram for phyllite at southern part of Ulu Sokor gold deposit (Bhatia & Crook, 1986). (Bhatia & Crook, 1986). Oceanic Island Arc (OIA), Continental Island Arc (CIA), Active Continental Margin (ACM) and Passive Margin (PM). Red dots indicate sample of phyllite.

Continental island arc and oceanic island arc are dominated by the development of the subduction process during that time. This process is synchronized with the tectonic evolution of Bentong-Raub suture zone which represents Sibumasu and East Malaya blocks continental margin (Metcalfe, 2013b). Metcalfe (2013b) proposed that the subduction occurs approximately in Early to Middle Permian period (270 Ma). The geochemical characteristics of these studied samples, including the slight negative Eu anomaly, enriched patterns of LREEs and weak fractionation of HREEs, support the tectonic setting of the depositional environment from the subduction field.

Table 4.2: Major oxides, Loss of Ignition (LOI) and total composition for phyllite at southern part of Ulu Sokor gold deposit. Post-Archean Australian Shale (PAAS), (Taylor & McLennan, 1985; McLennan, 2001) and Upper Continental Crust (UCC) (Rudnick & Gao, 2003). Note that d.l. is detection limit.

Element	**SiO_2**	**Al_2O_3**	**Fe_2O_3**	**MgO**	**CaO**	**Na_2O**	**K_2O**	**TiO_2**	**P_2O_5**	**MnO**	**LOI**	**Sum**
Unit	%	%	%	%	%	%	%	%	%	%	%	%
d.l.	0.01	0.01	0.04	0.01	0.01	0.01	0.01	0.01	0.01	0.01	0.1	0.01
Sample												
SGM1	64.72	15.30	9.58	1.31	0.01	0.09	2.01	0.55	0.04	0.12	6.1	99.86
SGM2	62.50	18.53	6.95	2.50	0.32	1.48	2.85	0.75	0.14	0.08	3.7	99.82
SGM3	62.77	19.61	4.52	0.73	0.02	0.14	5.75	0.78	0.02	<0.01	5.4	99.83
SGM4	59.82	17.76	8.42	2.95	0.44	1.14	2.70	0.72	0.14	0.14	5.5	99.81
SGM5	67.87	17.04	4.59	1.95	0.06	0.53	3.13	0.49	0.03	0.18	4.0	99.86
SGM6	67.71	19.98	1.44	0.14	1.03	0.76	2.84	0.64	0.01	0.02	5.3	99.90
SGM7	67.48	18.04	4.71	0.11	1.03	0.73	1.99	0.59	0.02	0.02	5.2	99.90
SGM8	67.06	17.21	6.23	0.18	0.27	0.79	2.54	0.55	0.03	0.02	5.0	99.88
SGM9	64.99	17.64	6.93	1.99	0.11	0.39	3.19	0.58	0.01	0.07	3.9	99.88
SGM10	63.17	16.95	7.49	2.41	0.04	0.32	3.70	0.58	<0.01	0.06	5.1	99.85
SGM11	67.87	15.84	5.77	2.87	0.19	0.83	2.02	0.51	0.07	0.06	3.8	99.86
Average	64.51	17.21	6.28	1.71	0.58	0.74	3.27	0.63	0.07	0.07	-	99.86
PAAS	62.8	18.9	6.5	2.2	1.3	1.2	3.7	1	0.16	0.11	-	97.87
UCC	66.6	15.4	5.04	2.48	3.59	3.27	2.8	0.64	0.15	0.1	-	100.05

Table 4.2, continued.

Element	SiO_2	Al_2O_3	Fe_2O_3	MgO	CaO	Na_2O	K_2O	TiO_2	P_2O_5	MnO	LOI	Sum
Unit	%	%	%	%	%	%	%	%	%	%	%	%
d.l.	0.01	0.01	0.04	0.01	0.01	0.01	0.01	0.01	0.01	0.01	0.1	0.01
Sample												
SGM12	68.95	14.93	5.14	0.97	0.24	0.31	3.16	0.64	0.01	0.02	5.5	99.89
SGM13	63.58	18.22	6.79	2.10	0.31	1.00	2.82	0.76	0.14	0.08	4.0	99.84
SGM14	62.98	19.35	6.54	2.09	0.39	1.01	2.75	0.72	0.13	0.09	3.7	99.81
SGM15	61.31	17.17	8.49	1.84	0.17	0.53	3.61	0.70	0.07	0.07	5.8	99.79
SGM16	62.63	18.48	5.83	2.08	1.02	0.25	4.31	0.66	0.04	0.09	4.4	99.86
SGM17	66.47	14.94	6.88	2.61	0.25	0.53	4.02	0.62	0.13	0.08	3.3	99.87
SGM18	63.94	15.41	8.25	1.57	0.38	1.90	3.12	0.53	0.10	0.04	4.5	99.79
SGM19	64.77	14.24	5.45	1.07	3.47	1.41	3.75	0.41	0.08	0.06	5.2	99.90
SGM20	61.01	14.99	7.47	2.38	2.78	1.59	3.17	0.72	0.14	0.13	5.5	99.86
SGM21	65.40	17.51	4.48	1.87	0.05	0.32	3.77	0.72	0.01	0.03	5.7	99.88
SGM22	62.19	19.38	6.15	1.99	0.23	0.28	4.71	0.62	0.02	0.05	4.2	99.88
Average	64.51	17.21	6.28	1.71	0.58	0.74	3.27	0.63	0.07	0.07	-	99.86
PAAS	62.8	18.9	6.5	2.2	1.3	1.2	3.7	1	0.16	0.11	-	97.87
UCC	66.6	15.4	5.04	2.48	3.59	3.27	2.8	0.64	0.15	0.1	-	100.05

Table 4.3: Trace element composition for phyllite at southern part of Ulu Sokor gold deposit. Post-Archean Australian Shale (PAAS), (Taylor & McLennan, 1985; McLennan, 2001) and Upper Continental Crust (UCC) (Rudnick & Gao, 2003). Note that d.l. is detection limit.

Element	Cs	Rb	Ba	Th	U	Nb	Ta	Sr	Hf	Zr	Y	Sc	Zn	V
Unit	ppm	ppm	ppm	ppm	ppm	ppm	ppm	ppm	ppm	ppm	ppm	ppm	ppm	ppm
d.l.	0.1	0.1	1	0.2	0.1	0.1	0.1	0.5	0.1	0.1	0.1	1	1	8
Sample														
SGM1	4.1	79.8	367	2.9	3.3	2.1	0.1	11.1	2.4	78.1	26.1	29	89	205
SGM2	5.2	119.3	279	13.2	3.0	12.8	1.0	178.8	5.3	198.0	31.6	18	133	110
SGM3	13.9	379.1	346	21.9	3.4	13.7	1.1	70.6	5.1	181.8	30.9	19	4	119
SGM4	6.6	126.0	211	10.0	3.2	8.0	0.6	185.4	4.2	155.0	30.7	19	215	202
SGM5	10.8	192.6	334	6.2	2.0	3.0	0.2	67.7	2.9	97.6	17.7	20	44	129
SGM6	8.1	188.6	214	6.9	1.9	4.3	0.2	176.1	4.4	152.9	28.3	21	3	105
SGM7	6.2	130.1	156	6.8	2.0	4.0	0.5	181.7	3.9	131.3	33.7	21	5	93
SGM8	7.6	185.5	192	6.8	2.4	3.8	0.2	153.0	3.8	123.8	28.4	21	4	90
SGM9	5.5	111.6	288	7.1	2.1	3.9	0.4	74.6	4.3	137.3	27.8	21	64	105
SGM10	12.2	284.6	304	6.0	1.4	3.9	0.3	64.4	4.1	135.1	24.9	20	73	104
SGM11	6.3	110.5	216	7.0	2.7	3.1	0.3	141.6	2.9	100.6	16.9	22	50	147
Average	8.8	175.8	286	8.7	2.4	6.3	0.5	109.5	4.0	137.7	27.4	20	65	117
PAAS	15	160	650	14.6	3.1	19	1.28	200	5	210	27	16	-	150
UCC	4.9	82	628	10.5	2.7	12	0.9	320	5.3	193	21	14	67	97

Table 4.3, continued.

Element Unit	Cs ppm	Rb ppm	Ba ppm	Th ppm	U ppm	Nb ppm	Ta ppm	Sr ppm	Hf ppm	Zr ppm	Y ppm	Sc ppm	Zn ppm	V ppm
d.l.	0.1	0.1	1	0.2	0.1	0.1	0.1	0.5	0.1	0.1	0.1	1	1	8
Sample														
SGM12	14.4	272.0	262	6.0	2.4	3.9	0.3	39.2	3.4	112.5	20.5	17	15	105
SGM13	7.4	127.5	333	13.4	3.0	15.3	1.1	227.1	5.2	193.5	33.3	17	99	115
SGM14	7.8	124.9	323	15.9	3.4	13.7	1.1	317.5	5.3	193.6	36.1	18	198	109
SGM15	9.7	168.8	349	12.9	3.3	12.9	1.2	162.4	5.2	181.4	30.9	16	99	110
SGM16	7.8	156.1	325	7.4	2.6	4.4	0.3	56.4	4.1	158.9	25.0	23	48	130
SGM17	9.2	179.5	480	6.5	1.7	4.8	0.4	17.4	3.2	113.6	24.1	19	59	102
SGM18	8.8	163.0	227	7.6	2.2	4.9	0.4	51.2	3.3	119.8	23.9	17	61	73
SGM19	11.9	212.9	221	7.8	2.5	4.0	0.4	46.1	3.6	123.0	25.8	14	27	54
SGM20	9.3	161.3	236	6.5	1.9	5.2	0.4	50.6	3.8	127.0	25.8	20	59	87
SGM21	12.8	230.9	301	4.0	1.4	3.3	0.3	78.1	3.1	99.9	40.4	20	26	149
SGM22	7.1	162.1	334	7.4	1.5	4.0	0.4	56.8	3.6	115.2	20.9	23	52	125
Average	8.8	175.8	286	8.7	2.4	6.3	0.5	109.5	4.0	137.7	27.4	20	65	117
PAAS	15	160	650	14.6	3.1	19	1.28	200	5	210	27	16	-	150
UCC	4.9	82	628	10.5	2.7	12	0.9	320	5.3	193	21	14	67	97

Table 4.4: Rare earth elements (REEs) composition for phyllite at southern part of Ulu Sokor gold deposit. Post-Archean Australian Shale (PAAS), (Taylor & McLennan, 1985; McLennan, 2001) and Upper Continental Crust (UCC) (Rudnick & Gao, 2003). Note that d.l. is detection limit.

Element	La	Ce	Pr	Nd	Sm	Eu	Gd	Tb	Dy	Ho	Er	Tm	Yb	Lu
Unit	ppm	ppm	ppm	ppm	ppm	ppm	ppm	ppm	ppm	ppm	ppm	ppm	ppm	ppm
d.l.	0.1	0.1	0.02	0.3	0.05	0.02	0.05	0.01	0.05	0.02	0.03	0.01	0.05	0.01
Sample														
SGM1	39.2	58.2	8.01	30.5	6.35	1.64	6.45	0.90	5.38	1.03	2.93	0.42	2.91	0.50
SGM2	37.2	73.1	8.25	32.3	6.07	1.21	5.98	0.90	5.49	1.18	3.47	0.47	3.46	0.56
SGM3	46.9	92.9	10.55	38.6	6.80	1.21	6.09	0.92	5.26	1.13	3.58	0.49	3.50	0.53
SGM4	28.1	51.9	6.43	24.8	5.37	1.03	5.28	0.86	5.28	1.13	3.35	0.46	3.02	0.46
SGM5	24.0	45.5	5.18	19.0	3.93	0.91	3.57	0.53	3.18	0.68	2.21	0.30	2.05	0.32
SGM6	19.3	39.1	4.61	18.4	3.58	0.85	3.97	0.68	4.76	1.09	3.41	0.54	3.25	0.53
SGM7	28.0	57.7	7.00	27.8	6.33	1.30	5.24	0.83	5.57	1.27	3.83	0.54	3.72	0.58
SGM8	24.9	51.2	5.73	22.5	4.75	0.98	4.54	0.73	4.67	1.09	3.41	0.50	3.28	0.47
SGM9	17.8	38.1	4.42	17.9	4.07	0.93	4.41	0.75	4.72	1.13	3.44	0.48	3.18	0.50
SGM10	18.4	35.3	4.42	18.1	3.94	1.05	4.17	0.68	4.18	0.93	3.06	0.48	3.14	0.48
SGM11	20.2	38.8	4.46	18.6	3.91	0.91	3.76	0.59	3.36	0.68	2.19	0.30	2.00	0.34
Average	25.8	50.3	5.90	23.2	4.8	1.1	4.9	0.8	4.8	1.0	3.2	0.5	3.0	0.5
PAAS	38.2	79.6	8.83	33.9	5.55	1.08	4.66	0.774	4.68	0.991	2.85	0.405	2.82	0.433
UCC	31	63	7.1	27	4.7	1	4	0.7	3.9	0.83	2.3	0.3	2	0.31

Table 4.4, continued.

Element	La	Ce	Pr	Nd	Sm	Eu	Gd	Tb	Dy	Ho	Er	Tm	Yb	Lu
Unit	ppm	ppm	ppm	ppm	ppm	ppm	ppm	ppm	ppm	ppm	ppm	ppm	ppm	ppm
d.l.	0.1	0.1	0.02	0.3	0.05	0.02	0.05	0.01	0.05	0.02	0.03	0.01	0.05	0.01
Sample														
SGM12	21.0	38.9	4.73	17.9	3.74	0.99	3.67	0.57	3.56	0.73	2.30	0.33	2.09	0.33
SGM13	37.1	74.0	8.41	31.7	6.21	1.35	5.88	0.93	5.47	1.24	3.67	0.52	3.52	0.54
SGM14	43.6	84.4	9.41	36.5	7.12	1.48	7.01	1.09	6.35	1.37	4.04	0.58	3.70	0.56
SGM15	32.3	64.3	7.42	28.7	5.61	1.14	5.22	0.86	5.57	1.15	3.54	0.48	3.25	0.51
SGM16	20.5	41.3	4.63	19.7	3.90	0.95	4.19	0.68	4.60	1.01	3.27	0.48	3.11	0.50
SGM17	17.3	34.0	4.02	16.7	3.37	0.88	3.77	0.64	4.00	0.83	2.63	0.36	2.55	0.39
SGM18	17.5	37.0	4.40	18.0	3.96	0.95	4.21	0.67	4.31	0.89	2.71	0.38	2.68	0.39
SGM19	20.3	41.2	4.65	18.4	3.64	0.93	4.48	0.69	4.45	0.92	2.91	0.43	2.43	0.40
SGM20	19.5	40.3	4.81	19.1	4.27	1.00	4.47	0.75	4.69	1.00	3.13	0.43	3.06	0.45
SGM21	16.2	29.7	3.96	17.7	4.64	1.23	6.37	1.00	5.85	1.30	3.63	0.45	3.19	0.48
SGM22	17.6	38.9	4.28	17.4	4.03	0.82	3.72	0.61	3.74	0.83	2.54	0.37	2.46	0.40
Average	25.8	50.3	5.90	23.2	4.8	1.1	4.9	0.8	4.8	1.0	3.2	0.5	3.0	0.5
PAAS	38.2	79.6	8.83	33.9	5.55	1.08	4.66	0.774	4.68	0.991	2.85	0.405	2.82	0.433
UCC	31	63	7.1	27	4.7	1	4	0.7	3.9	0.83	2.3	0.3	2	0.31

4.6 Geochemistry of rhyolite

The seven representative volcanic rocks from southern part of Ulu Sokor gold deposit were analyzed for major and trace elements (Tables 4.5 and 4.6). These samples were characterized by range SiO_2 of 70.58-78.50 wt%, Al_2O_3 of 10.99-14.54 wt%, FeOt of 1.07-7.50 wt%, MgO of 0.20-0.53 wt%, CaO of 0.03-0.49 wt% except one sample SV4 is 2.94 wt%, Na_2O of 0.07-3.00 wt%, K_2O of 2.14-5.73 wt%, TiO_2 of 0.05-0.18 wt%, P_2O_5 of 0.01-0.05 wt% and Loss of Ignition (LOI) is 1.6-5.4 wt%. The major elements in the Hacker diagram for rhyolite from southern part of Ulu Sokor gold deposit are plotted (Figure 4.19). In general, the plots show good trends of decreasing FeOt, TiO_2 and MgO with increasing SiO_2. Meanwhile, Al_2O_3 shows a scattered trend.

According to Total Alkali Silica (TAS) diagram from Middlemost (1994), the samples studied are plotted on the rhyolite field (Figure 4.20). Based on binary plot of Ba/Sr versus Ba/Rb, rhyolite from this study area is controlled by barium and strontium magma fractionation (Figure 4.21). All rhyolites basically have high alkali content. The Th versus Co plot shows predominantly high-K calc alkaline and shoshonite characteristics (Hastie et al., 2007) (Figure 4.22). The $Al_2O_3/(CaO+Na_2O+K_2O)$ value is more than 1.0 ranging from 1.03 to 3.81 which shows peraluminous characteristics as well as S-type origin (Chappell & White, 1992) (Figure 4.23).

Ba, Sr and Rb are the suitable elements in order to determine the type and amount of major phase fractionation in felsic rocks because each element has its own behavior. For example, Ba is taken up by biotite and alkali feldspar, Sr by plagioclase and K-feldspar and Rb by biotite (Ghani & Singh, 2005). Based on log diagram Sr versus Ba (Figure 4.24), the trend is within plagioclase, alkali feldspar and biotite. According to this vector trend, it shows that the important fractionation in rhyolite is plagioclase, alkali feldspar and biotite. Selected trace element plots are given in Figure 4.25. Ba, Sr, U, Rb and Zr for rhyolite decrease with increasing SiO_2. However, Ba increases with increasing Sr. The decreasing Ba and Sr normally indicate that K-feldspar, biotite and plagioclase are being removed in differentiation sequence (Ghani & Singh, 2005).

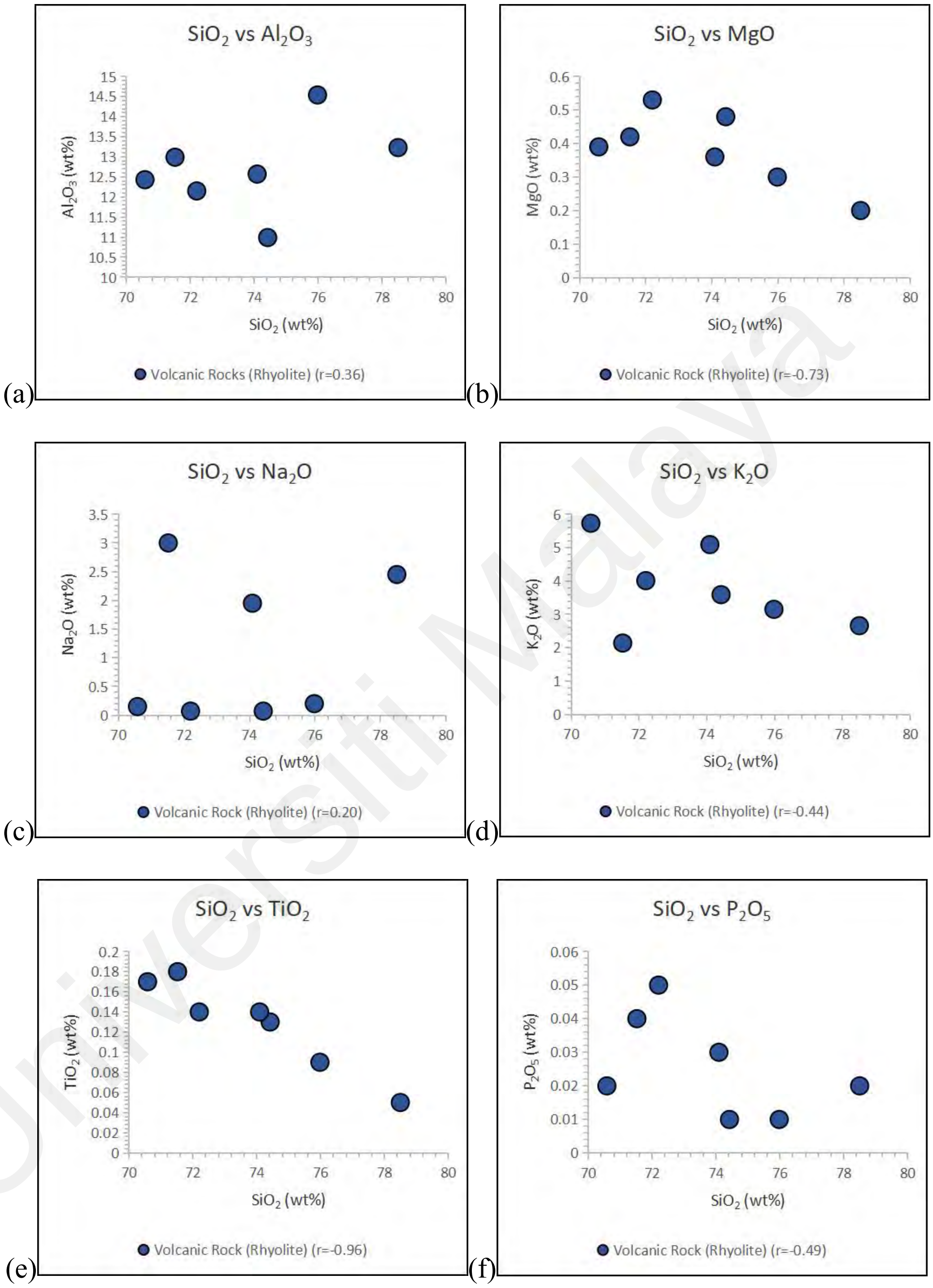

Figure 4.19: (a) to (f) Major element Harker variation diagram for rhyolite at southern part of Ulu Sokor gold deposit. Blue dots indicate sample of rhyolite.

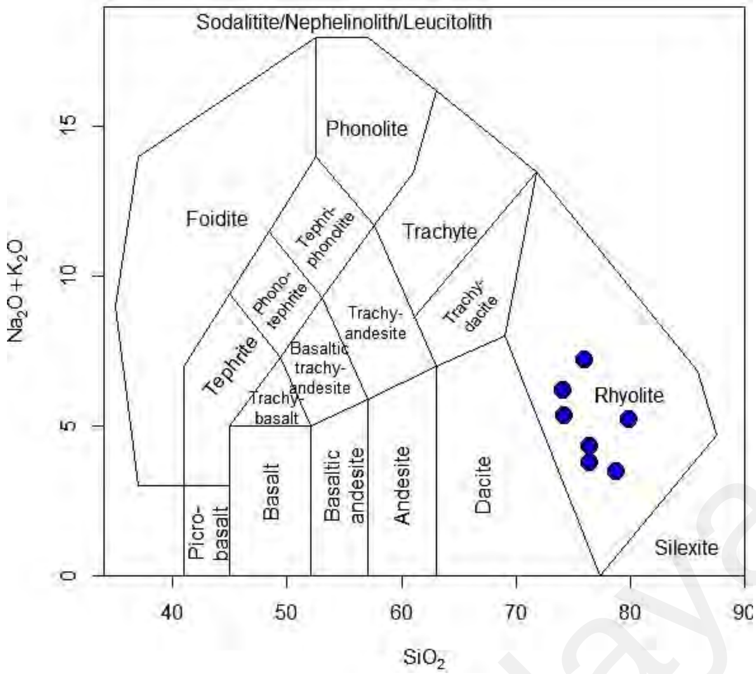

Figure 4.20: SiO_2 versus Na_2O+K_2O (TAS) diagram from (Middlemost, 1994). All the samples study are plotted on rhyolitic field. Blue dots indicate sample of rhyolite.

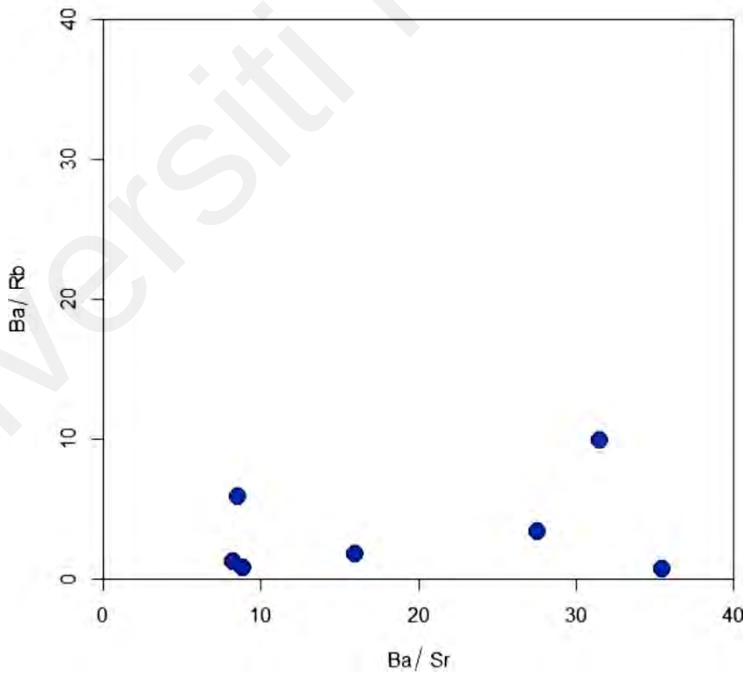

Figure 4.21: Diagram of Ba/Sr versus Ba/Rb. Most of the rhyolite are controlled by Barium and Strontium. Blue dots indicate sample of rhyolite.

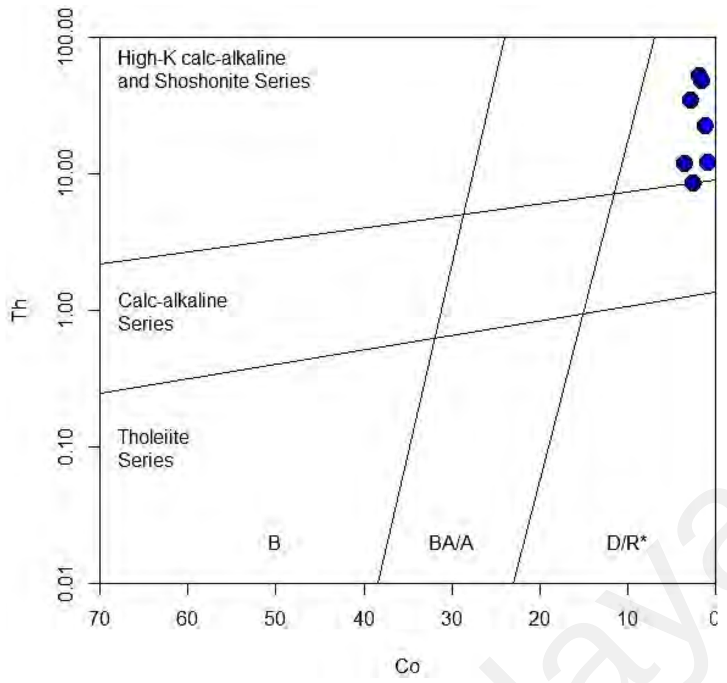

Figure 4.22: Discrimination variation diagram of Hasti et al. (2007). Most of the rhyolite plotted on High-K calc-alkaline and shoshonite series. Blue dots indicate sample of rhyolite.

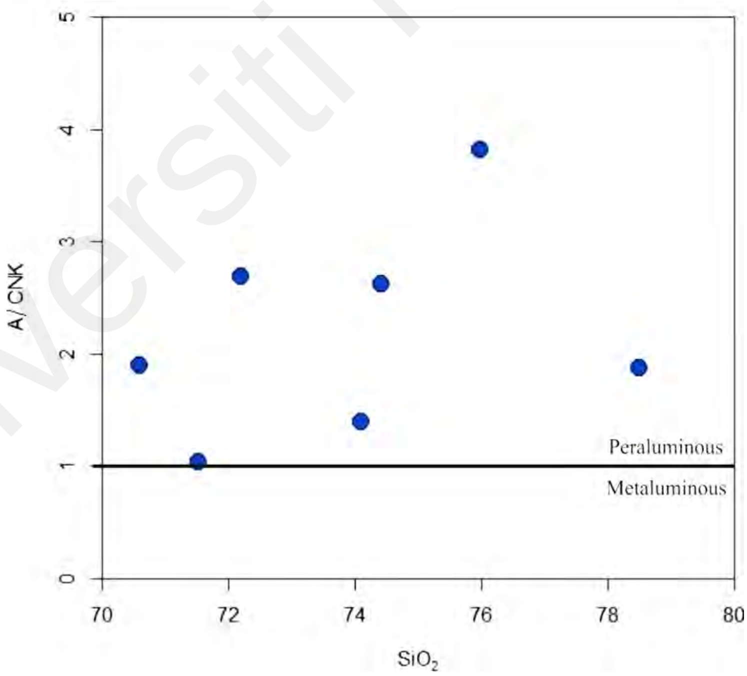

Figure 4.23: $Al_2O_3/(CaO+Na_2O+K_2O)$ versus SiO_2 diagram. A significant plot of the rhyolite on peraluminous field as well as S-type characteristic. Blue dots indicate sample of rhyolite.

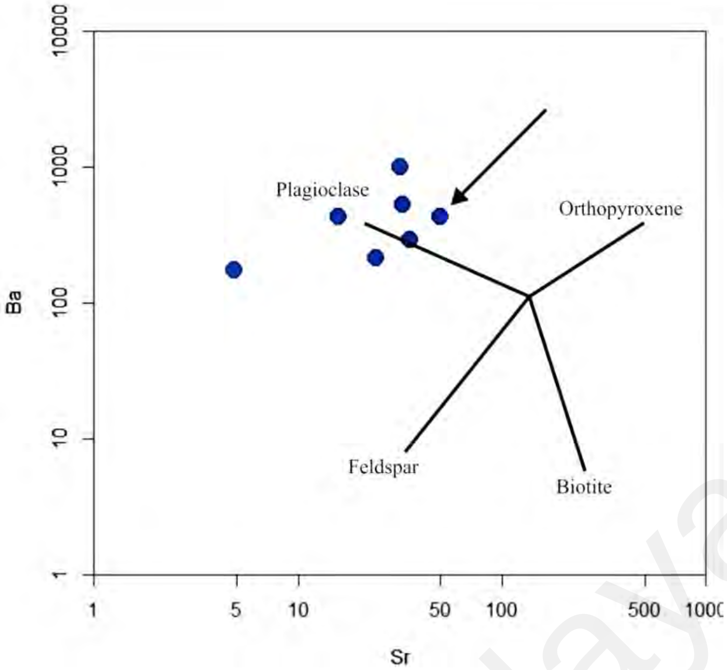

Figure 4.24: Mineral vector showing fractional crystallization trends of orthopyroxene, plagioclase, alkali-feldspar and biotite for rhyolitic liquids from Rollinson (1993) are used. The vector displayed for the rhyolite indicates that the fractionation of plagioclase, K-feldspar and biotite are the important role for the magmatic evolution. Blue dots indicate sample of rhyolite.

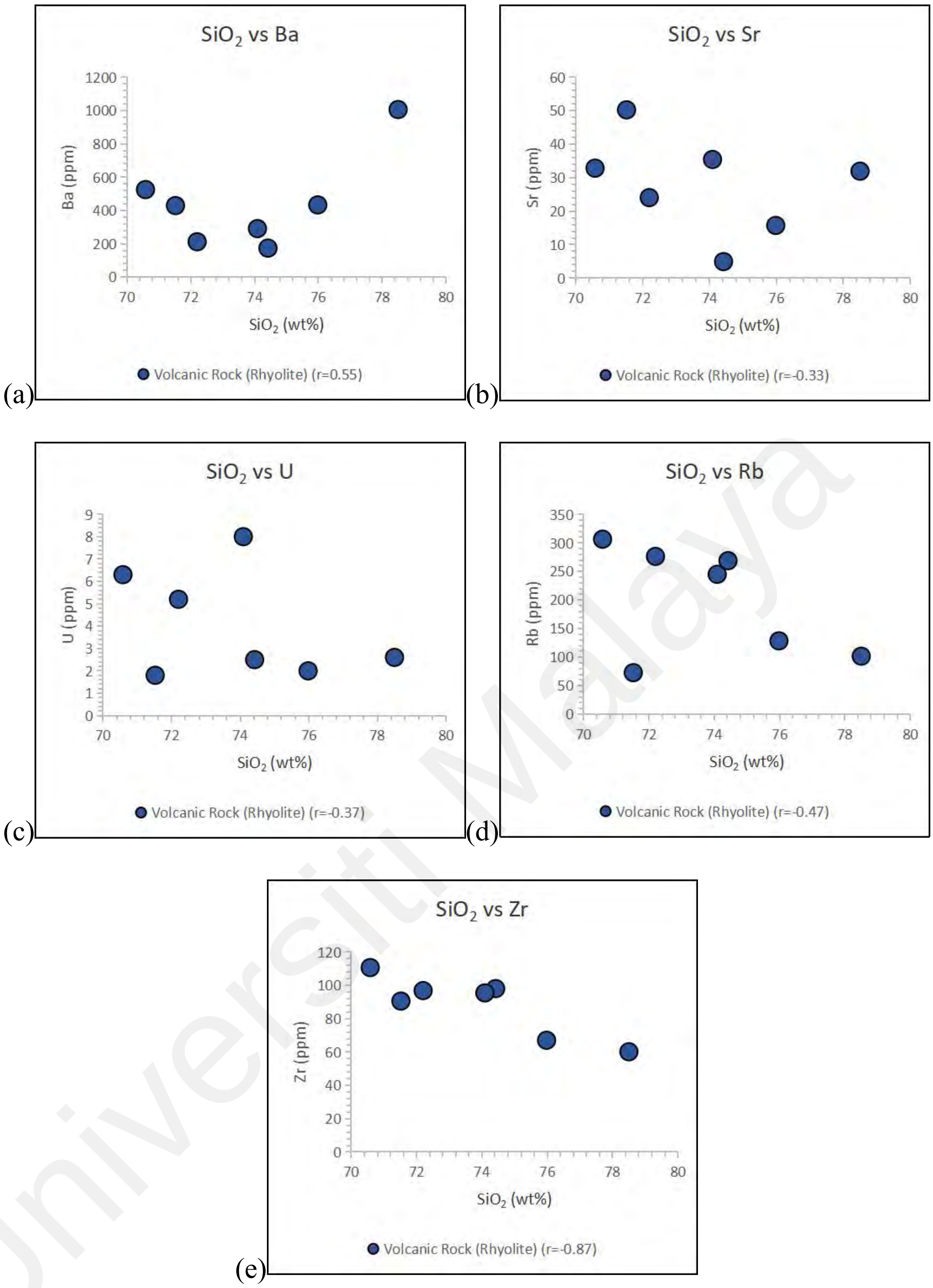

Figure 4.25: (a) to (e) Selected trace element variation diagram of the rhyolite at southern part of Ulu Sokor gold deposit. Blue dots indicate sample of rhyolite.

Based on normalized primitive mantle diagram (Sun & McDonough, 1989) (Figure 4.26), some elements show negative and positive anomalies which describe some fractionation and contamination respectively. Ba, Nb, Sr, P and Ti show the clearest and are most negative through plotting. The positive anomaly is presented by Pb element in this diagram. In general, these samples are slightly enriched in Large Ion Lithophile elements (LILEs) relative to High Field Strength Elements (HFSEs). In the chondrite normalized REEs diagram (Boynton, 1984) (Figure 4.27), these samples show enrichment in Light Rare Earth Elements (LREEs) compared to the Heavy Rare Earth Elements (HREEs). The average $(La/Yb)_N$ and $(Gd/Yb)_N$ ratios of the rhyolite are 23.06 and 14.68 respectively. The negative Eu anomaly is common in this diagram and the average value of Eu/Eu* ratio is 0.49. Based on the HREEs plot, two samples which are SV2 and SV3 from this study area show slight enrichment compared to others. Geotectonic study of discrimination diagrams is used in order to interpret the tectonic setting. Discrimination diagram of Ta/Yb versus Th/Yb from Pearce (1983) (Figure 4.28) is used in order to represent the tectonic setting of rhyolite and to identify possible subduction component.

The diagram is useful because the ratios are not strongly affected by partial melting and fractional crystallization. Th content is usually high in volcanic arcs and furthermore, the contamination of the crust results in an elevated Th/Yb ratio. The Ta/Yb ratio is a measure of the degree of mantle enrichment or depletion. As seen from the diagram, rhyolite is plotted above the Mid Oceanic Ridge Basalt (MORB)-array, indicating subduction enrichment. The rocks are also plotted on the continental arc side of the diagram. The Th/Yb ratio of the rocks increases linearly indicating either an increase in subduction component in the source region or greater crustal assimilation.

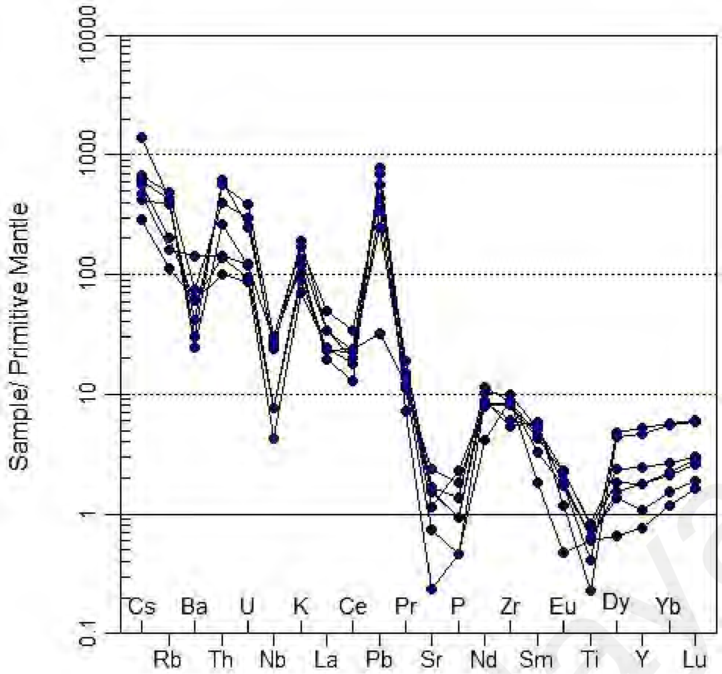

Figure 4.26: Primitive mantle-normalized multi-element spider diagram (Sun & McDonough, 1989) of the rhyolite at southern part of Ulu Sokor gold deposit. Blue dots indicate sample of rhyolite.

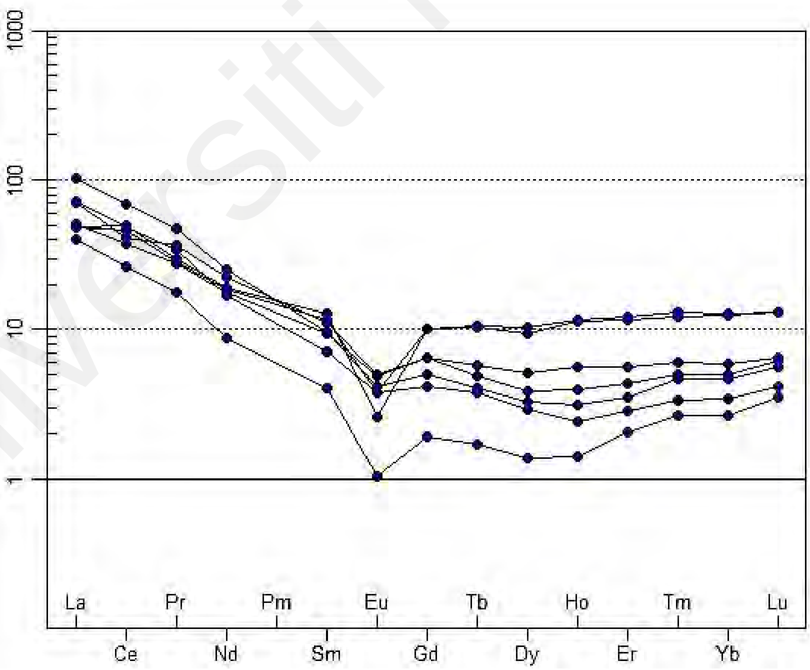

Figure 4.27: C1 chondrite normalized REEs diagram (Boynton, 1984) of the rhyolite at southern part of Ulu Sokor gold deposit. Blue dots indicate sample of rhyolite.

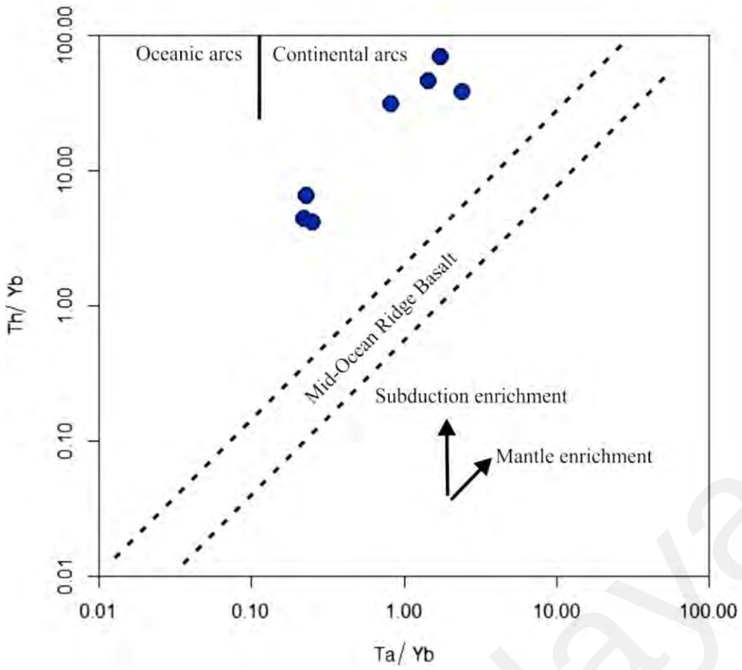

Figure 4.28: Ta/Yb versus Th/Yb diagram of the volcanic rocks (Pearce, 1983) of the rhyolite at southern part of Ulu Sokor gold deposit. Blue dots indicate sample of rhyolite.

Table 4.5: Major and trace elements concentration of rhyolite at southern part of Ulu Sokor gold deposit. Note that d.l. is detection limit.

Sample			SV1	SV2	SV3	SV4	SV5	SV6	SV7	Average
Element	**Unit**	**d.l**								
SiO_2	%	0.01	74.42	75.98	78.5	71.52	70.58	72.2	74.09	73.9
Al_2O_3	%	0.01	10.99	14.54	13.23	12.99	12.43	12.15	12.57	12.7
FeOt	%	0.04	7.5	2.11	1.07	3.13	5.68	5.24	3.05	3.97
MgO	%	0.01	0.48	0.3	0.2	0.42	0.39	0.53	0.36	0.38
CaO	%	0.01	0.1	0.04	0.08	2.94	0.05	0.03	0.19	0.49
Na_2O	%	0.01	0.07	0.2	2.45	3	0.15	0.07	1.95	1.13
K_2O	%	0.01	3.59	3.15	2.66	2.14	5.73	4.01	5.09	3.77
TiO_2	%	0.01	0.13	0.09	0.05	0.18	0.17	0.14	0.14	0.13
P_2O_5	%	0.01	0.01	0.01	0.02	0.04	0.02	0.05	0.03	0.03
LOI	%	0.1	2.6	3.4	1.6	3.5	4.5	5.4	2.4	3.34
Sum	%	0.01	99.91	99.96	99.96	99.95	99.82	99.89	99.91	99.91
Cs	ppm	0.1	4.9	4.5	3.7	2.3	5.3	10.9	3.3	4.99
Rb	ppm	0.1	268.8	128.4	101.6	72.7	306.4	276.3	244.9	199.87
Ba	ppm	1	174	433	1005	429	525	212	291	438.43
Th	ppm	0.2	22.2	11.7	12.1	8.5	34.2	52.3	47.6	26.94
U	ppm	0.1	2.5	2	2.6	1.8	6.3	5.2	8	4.06
Nb	ppm	0.1	20	5.5	5.5	3	17.3	18.5	21.3	13.01
La	ppm	0.1	13.4	16.2	16	16.7	23.4	23.7	33.7	20.44
Ce	ppm	0.1	22.8	40.1	42.9	32.1	35.8	41.7	60.2	39.37
Pb	ppm	0.1	55.5	17.7	2.3	24.2	49.3	40.3	31.2	31.5
Pr	ppm	0.02	1.97	3.19	3.36	3.1	4.12	3.82	5.27	3.55
Sr	ppm	0.5	4.9	15.7	31.9	50.2	32.8	24	35.4	27.84
Nd	ppm	0.3	5.6	11.8	11.9	11.3	14	10.7	15.7	11.57
Zr	ppm	0.1	98	67	60.1	90.5	110.6	96.8	95.4	88.34
Sm	ppm	0.05	0.82	2.37	2.59	1.92	2.26	1.46	1.98	1.91
Eu	ppm	0.02	0.08	0.29	0.2	0.38	0.39	0.29	0.32	0.28
Tl	ppm	0.1	0.2	0.2	<0.1	<0.1	0.2	0.1	<0.1	0.18
Dy	ppm	0.05	0.48	3.53	3.21	1.77	1.34	1	1.14	1.78
Y	ppm	0.1	3.5	23.6	21.4	11.2	8	4.9	8.1	11.53
Yb	ppm	0.05	0.58	2.83	2.75	1.3	1.1	0.75	1.04	1.48
Lu	ppm	0.01	0.12	0.45	0.44	0.22	0.21	0.14	0.19	0.25
Gd	ppm	0.05	0.53	2.79	2.77	1.77	1.78	1.15	1.39	1.74
Tb	ppm	0.01	0.08	0.5	0.49	0.27	0.23	0.18	0.19	0.28
Ho	ppm	0.02	0.1	0.82	0.79	0.39	0.28	0.17	0.22	0.4
Er	ppm	0.03	0.46	2.72	2.59	1.26	0.98	0.64	0.79	1.35
Tm	ppm	0.01	0.08	0.39	0.37	0.18	0.15	0.1	0.14	0.2
Ta	ppm	0.01	1.4	0.7	0.6	0.3	0.9	1.3	1.5	0.96

Table 4.6: Ratio some of major and trace elements of rhyolite at southern part of Ulu Sokor gold deposit.

Sample	SV1	SV2	SV3	SV4	SV5	SV6	SV7	Average
Element								
Na_2O+K_2O	3.66	3.35	5.11	5.14	5.88	4.08	7.04	4.89
A/CNK	2.92	4.29	2.55	1.61	2.1	2.96	1.74	2.59
La_N/ Yb_N	28.21	6.97	7.11	15.53	26	37.92	39.65	23.06
Gd_N/ Yb_N	10.79	11.58	11.88	15.88	19.08	17.76	15.79	14.68
Eu/ Eu*	0.37	0.34	0.23	0.63	0.59	0.68	0.59	0.49
Ta/ Yb	2.41	0.25	0.22	0.23	0.82	1.73	1.44	1.01
Th/ Yb	38.28	4.13	4.4	6.54	31.09	69.73	45.77	28.56

4.7 Geochemistry of ore rock

The 23 pulverized ore rock samples were performed on bulk ore geochemical analysis which is aimed to determine the pattern or style of gold (Au) with other selected metals (Table 4.7 and 4.8). The ore rocks were collected from two different pits namely, New Found and New Discovery. Based on the relationship of Au with other metals (log Au vs log metal) such as silver (Ag), bismuth (Bi), copper (Cu), lead (Pb), arsenic (As), zinc (Zn), antimony (Sb), tungsten (W) and tin (Sn), there are not much differences between these two pits (Figures 4.29, 4.30 and 4.31). The significant enrichment in these ore rocks is element Bi. However, some other metals can also be considered as significant in these ore rocks such as Pb, As, Cu and Zn.

As shown in the variation diagrams, the distribution refers to the categories in several patterns or style, such as positive, negative, flatted, and scattered trends. Some of the selected metals such as Ag, Bi, Cu, As and Sb have positive trends with increasing Au. The negative trends with increasing metal Au are Pb, Zn, W, vanadium (V), cobalt (Co) and thorium (Th). Variation diagrams which show flatted trends are metals tin (Sn), nickle (Ni), selenium (Se), molybdenum (Mo) and tantalum (Tl). While scattered trends are cadmium (Cd) and mercury (Hg). However, some of the samples show highly enriched such Pb (NF30 = 6551.1 ppm), W (NF36 = 278.2 ppm) and Sn (NF36 = 1054 ppm and ND12 = 1025 ppm). One interesting features in these ore is Bi which have extremely high value more than 2000 ppm in samples NF1 and NF30.

Log metal abundance versus log cumulative probability is plotted in order to determine the probability distribution pattern as shown in Figures 4.32, 4.33 and 4.34. In addition, the geometric mean value also used which can be calculated the average mean concentration within widely value data. The formula for the geometric mean is $n\sqrt{(a1 \times a2 \times ... \times an)}$. The geometric mean value of ore rock samples for Au is 1.8972 ppm with number samples are 23. The geometric mean value of other metals is shown in Table 4.9.

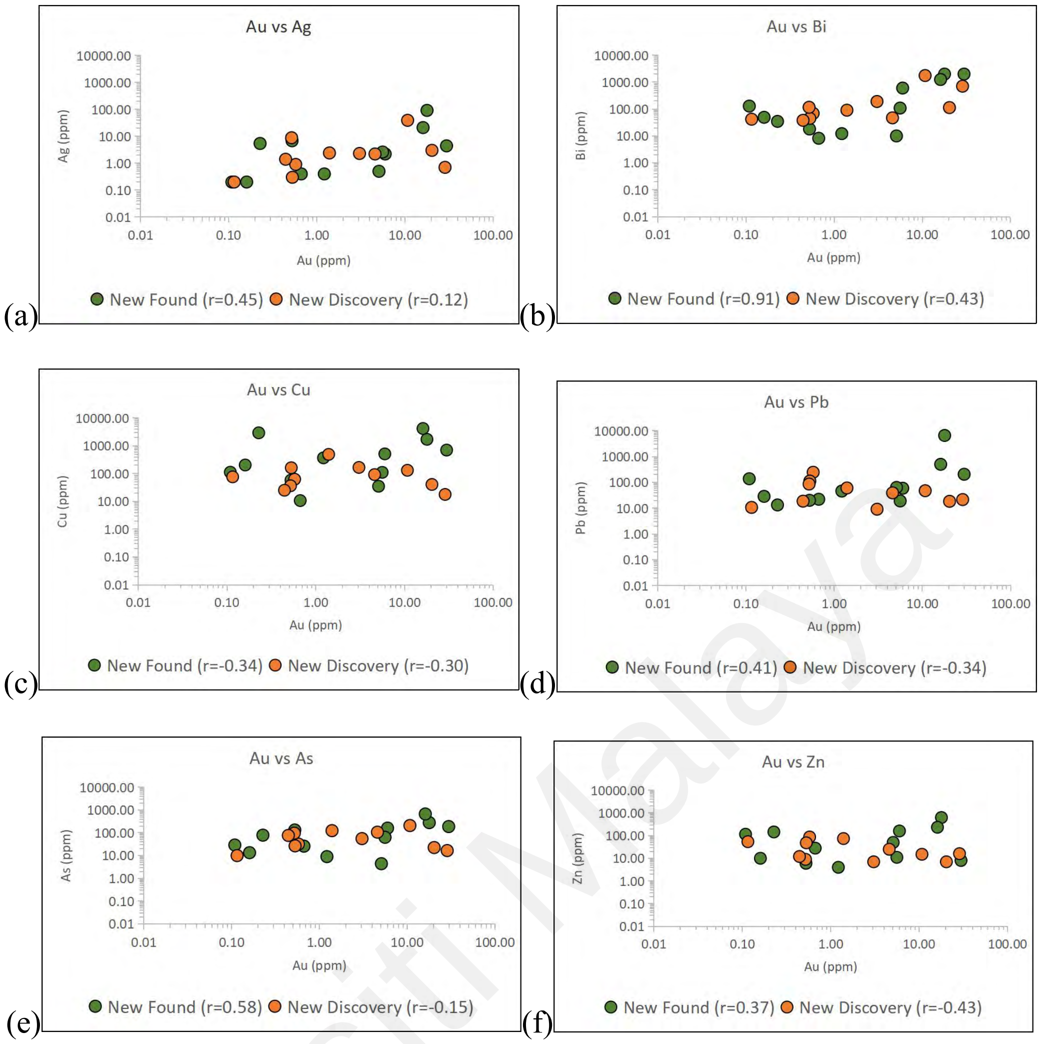

Figure 4.29: (a) to (f) Variation diagram of Au versus selected metal ore rocks at southern part of Ulu Sokor gold deposit. Unit: part per million (ppm).

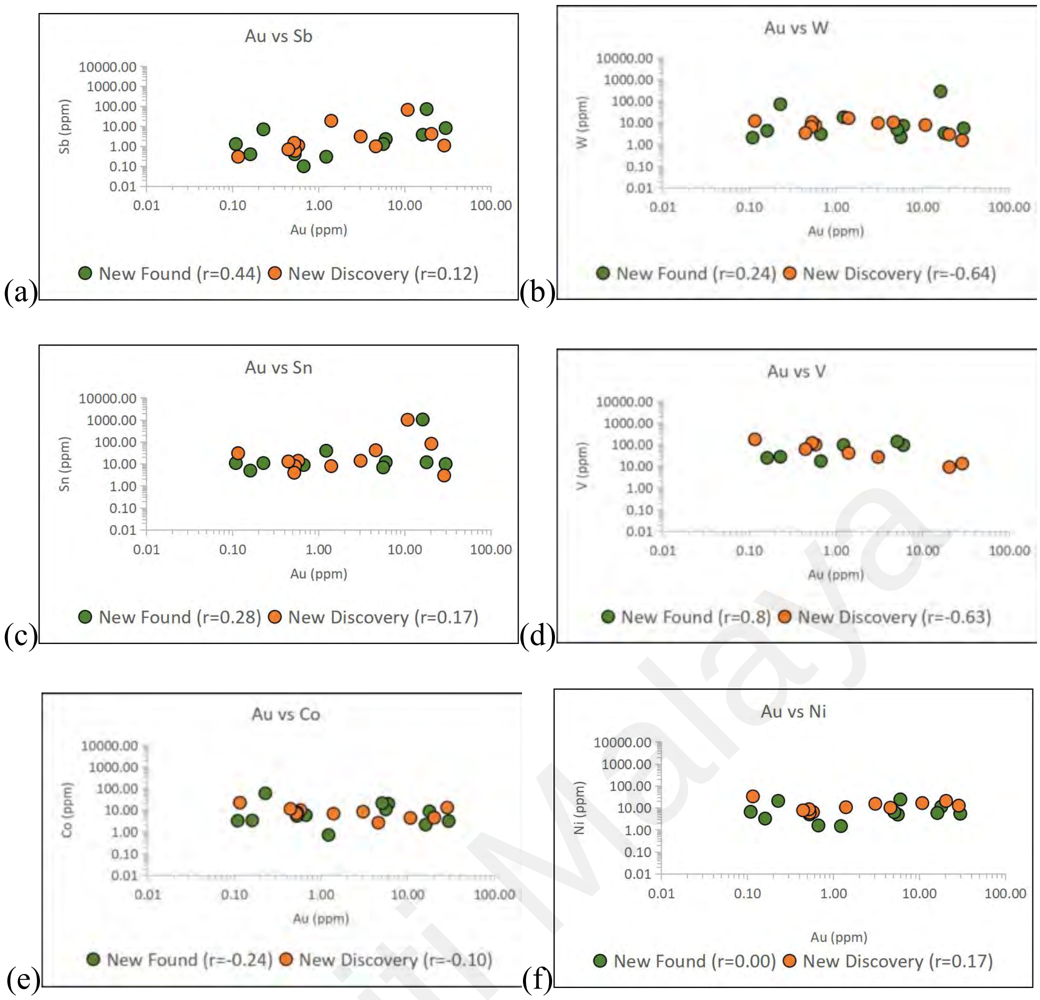

Figure 4.30: (a) to (f) Variation diagram of Au versus selected metal ore rocks at southern part of Ulu Sokor gold deposit. (continued 1) Unit: part per million (ppm).

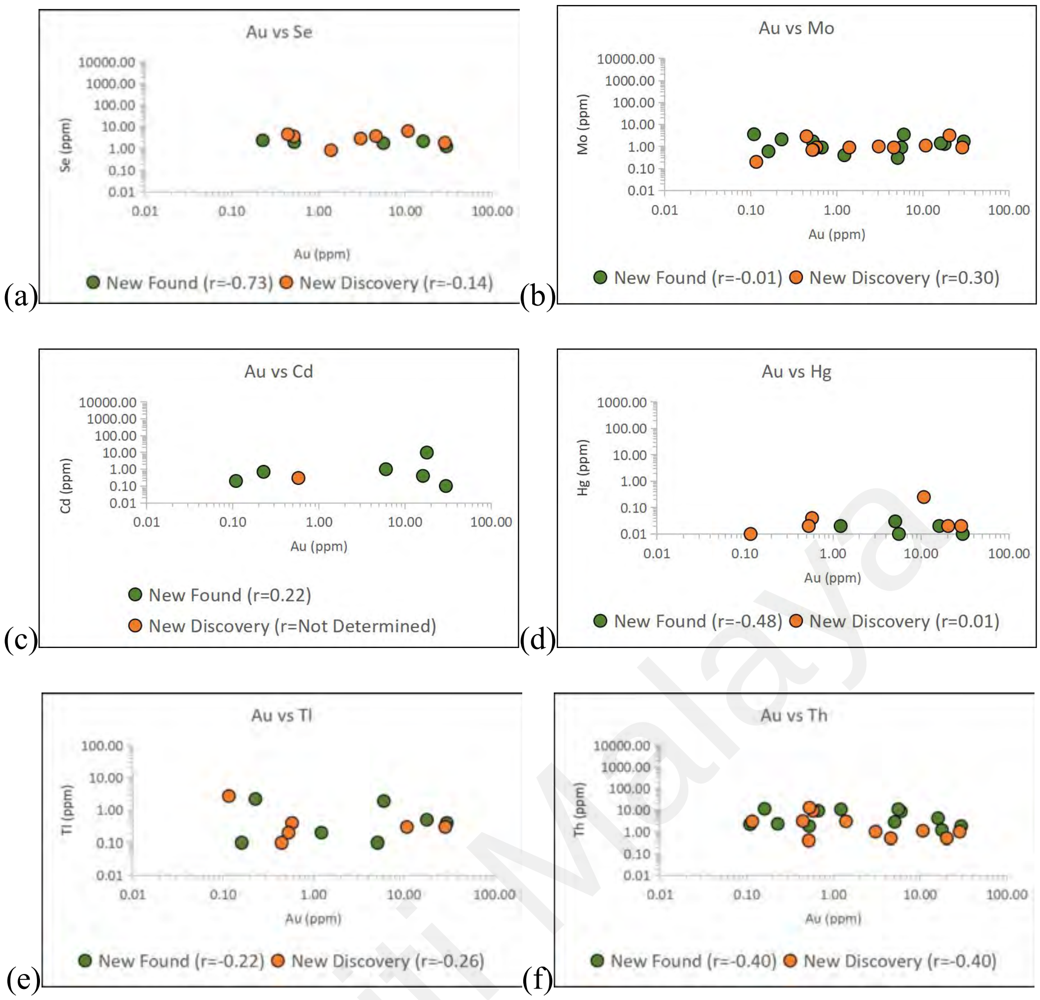

Figure 4.31: (a) to (f) Variation diagram of Au versus selected metal ore rocks at southern part of Ulu Sokor gold deposit. (continued 2) Unit: part per million (ppm).

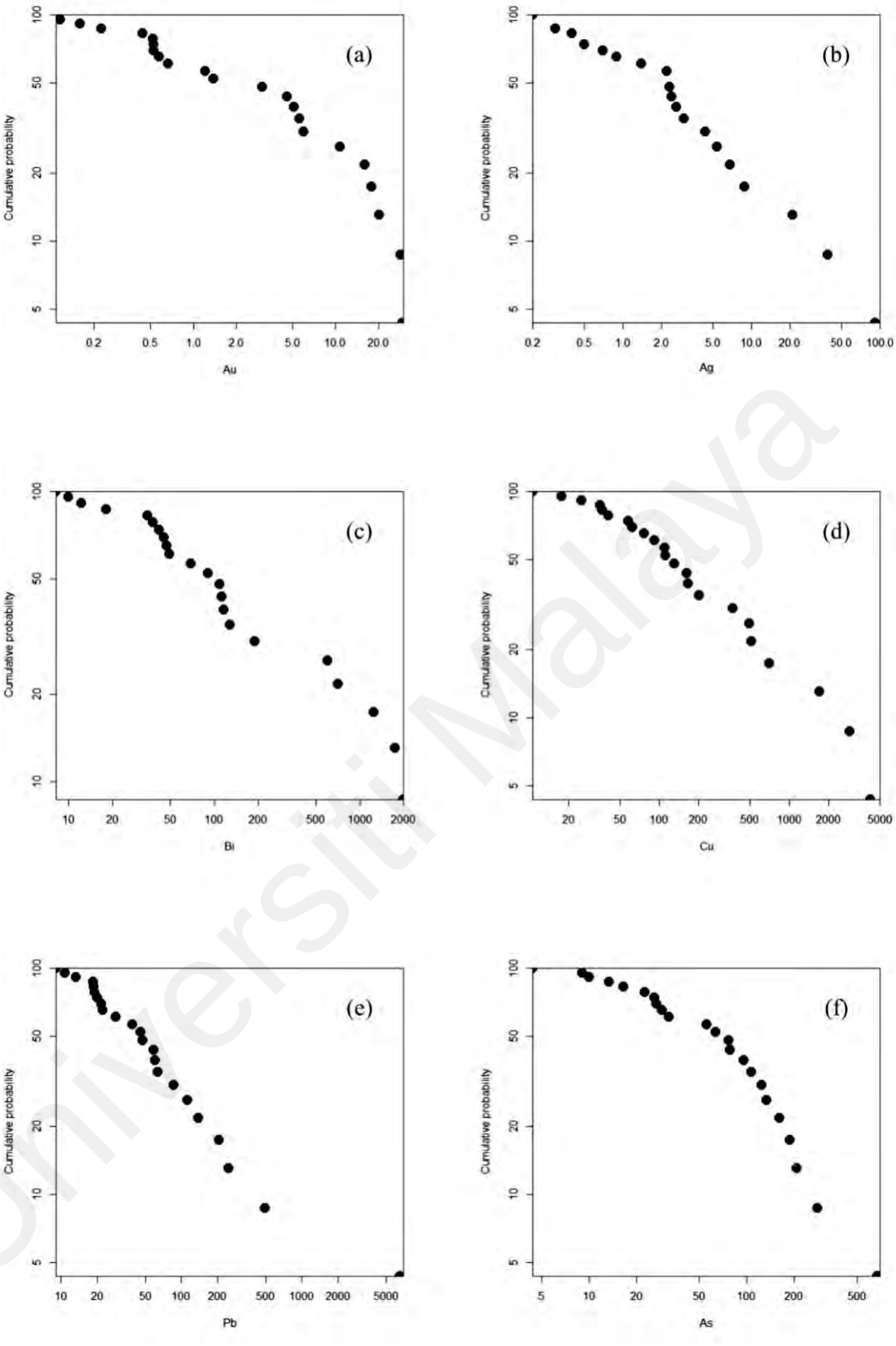

Figure 4.32: (a) to (f) Variation diagram of selected metal abundance versus cumulative probability ore rocks at southern part of Ulu Sokor gold deposit. Unit: part per million (ppm).

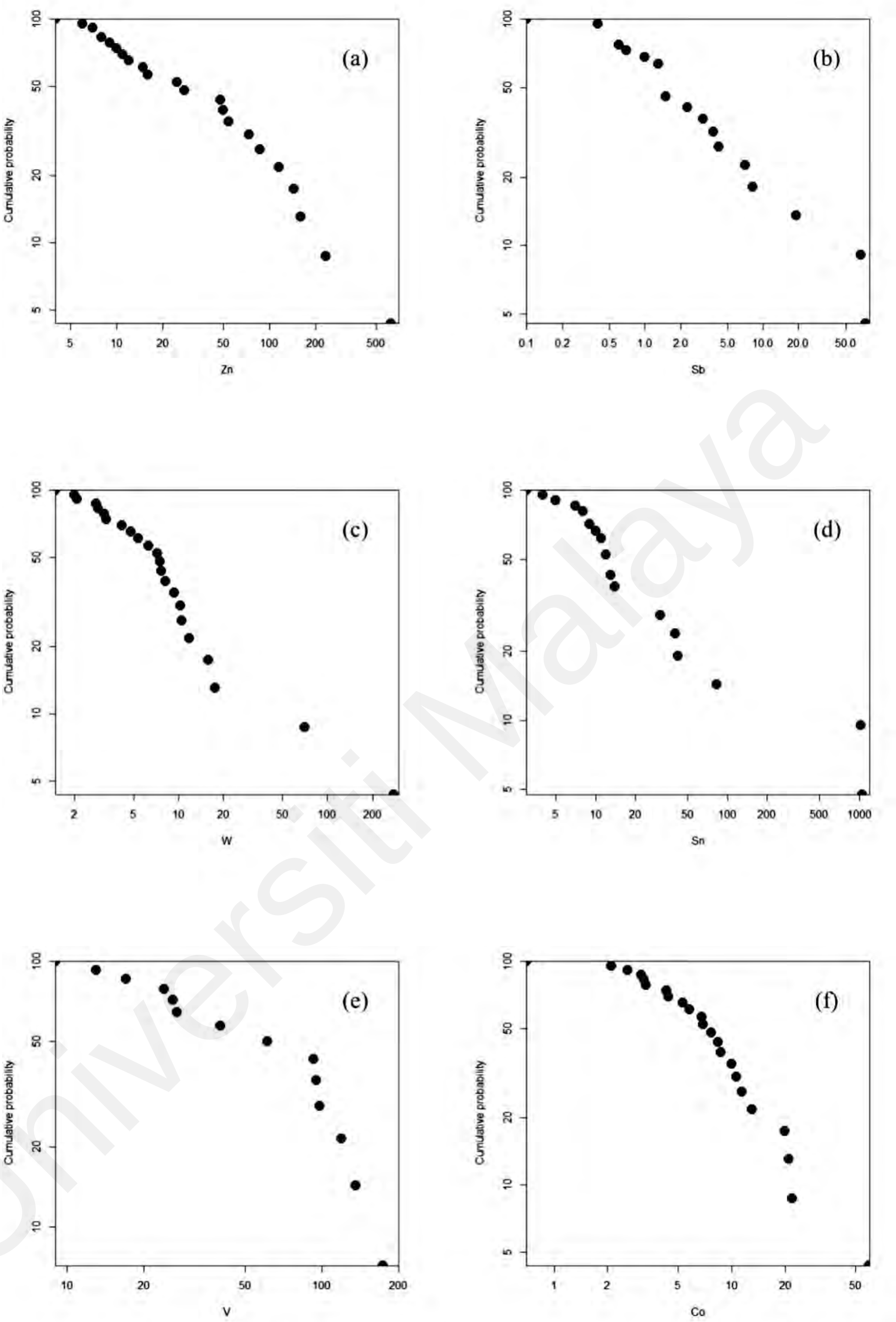

Figure 4.33: (a) to (f) Variation diagram of selected metal abundance versus cumulative probability ore rocks at southern part of Ulu Sokor gold deposit. (continued 1) Unit: part per million (ppm).

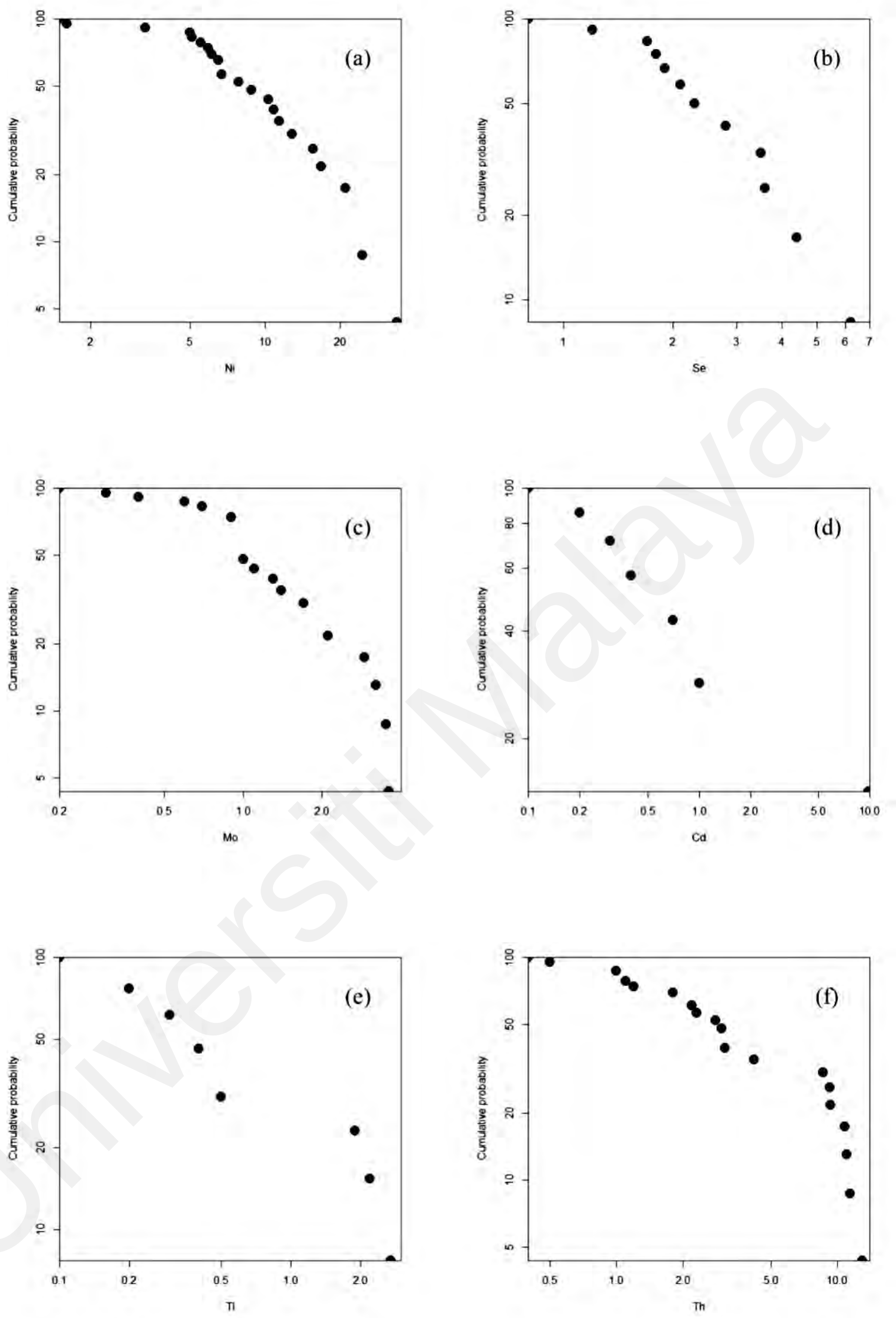

Figure 4.34: (a) to (f) Variation diagram of selected metal abundance versus cumulative probability ore rocks at southern part of Ulu Sokor gold deposit. (continued 2) Unit: part per million (ppm).

Table 4.7: Trace element composition ore rocks at southern part of Ulu Sokor gold deposit. Note that d.l. is detection limit.

Element	Au	Ag	Bi	Cu	Pb	As	Zn	Sb	W	Sn
Unit	ppm	ppm	ppm	ppm	ppm	ppm	ppm	ppm	ppm	ppm
d.l.	0.0005	0.1	0.1	0.1	0.1	0.5	1	0.1	0.5	1
Sample										
NF1	29.7662	4.4	>2000.0	701.9	205.6	187.7	8	8.2	5.4	10
NF30	17.8770	91.5	>2000.0	1709.3	6551.1	279.7	627	73.5	3.2	12
NF36	16.1187	21	1252.7	4189.2	498.6	669.8	233	3.8	278.2	1054
NF2	5.9893	2.2	603.1	512	59	160.9	160	2.3	7.2	12
NF31	5.6014	2.6	108.8	110.7	19	63.4	11	1.3	2.1	7
NF7	5.0909	0.5	10	35	63.5	4.4	50	<0.1	4.8	<1
NF5	1.2203	0.4	12.2	368.7	45.9	9	4	0.3	17.6	40
NF25	0.6679	0.4	8.2	10.7	22.1	25.9	28	0.1	2.9	9
NF14	0.5251	6.8	18.1	58.1	20.1	132.7	6	0.4	8.2	<1
NF3	0.2276	5.4	34.8	2927.7	13.3	78.7	145	7.1	70.6	11
NF15	0.1603	0.2	49.3	203.8	28.6	13.4	10	0.4	4.2	5
NF27	0.1089	0.2	129	112.2	137.8	29	115	1.3	2	11
ND25	28.6142	0.7	707.9	17.8	21.5	16.6	16	1.1	1.5	3
ND13	20.3347	3	113.3	40.7	18.4	22.5	7	4.2	2.8	83
ND12	10.7645	39.1	1759.8	131.5	47.4	207.6	15	67.6	7.7	1025
ND11	4.59	2.2	47.1	92.1	39.1	106.7	25	1	10.3	42

Table 4.7, continued.

Element	Au	Ag	Bi	Cu	Pb	As	Zn	Sb	W	Sn
Unit	ppm	ppm	ppm	ppm	ppm	ppm	ppm	ppm	ppm	ppm
d.l.	0.0005	0.1	0.1	0.1	0.1	0.5	1	0.1	0.5	1
Sample										
ND10	3.0621	2.3	191.1	166.7	9.1	55.6	7	3.1	9.4	14
ND9	1.3951	2.4	90.7	491.8	60.5	124.1	74	19	15.9	8
ND21	0.5777	0.9	68.9	62.7	245.8	32	87	1.1	7.5	14
ND22	0.5294	0.3	45.1	162.3	112.1	26.7	48	0.6	10.5	8
ND17	0.5191	8.8	116.6	36.5	85.8	96.1	9	1.5	6.3	4
ND14	0.4435	1.4	38.1	25.2	18.6	76.4	12	0.7	3.3	13
ND29	0.1157	0.2	41.9	76.4	10.7	10	54	0.3	11.8	31

Table 4.7, continued.

Element	V	Co	Ni	Se	Mo	Cd	Hg	Tl	Th
Unit	ppm	ppm	ppm	ppm	ppm	ppm	ppm	ppm	ppm
d.l.	8	0.2	0.1	0.5	0.1	0.1	0.01	0.1	0.2
Sample									
NF1	<8	3.1	5.5	1.2	1.7	0.1	0.01	0.4	1.8
NF30	<8	8.7	11.4	<0.5	1.3	9.8	<0.01	0.5	1.2
NF36	<8	2.1	5.9	2.1	1.4	0.4	0.02	<0.1	4.2
NF2	93	19.9	24.5	<0.5	3.5	1	<0.01	1.9	8.6
NF31	<8	10.6	5	1.7	0.9	<0.1	0.01	<0.1	11
NF7	136	21	6.5	<0.5	0.3	<0.1	0.03	0.1	2.8
NF5	95	0.7	1.5	<0.5	0.4	<0.1	0.02	0.2	10.8
NF25	17	5.8	1.6	<0.5	0.9	<0.1	<0.01	<0.1	9.3
NF14	<8	5.3	5.1	1.9	1.7	<0.1	<0.01	<0.1	1.8
NF3	27	59.6	21	2.3	2.1	0.7	<0.01	2.2	2.3
NF15	24	3.3	3.3	<0.5	0.6	<0.1	<0.01	0.1	11.4
NF27	<8	3.2	6.7	<0.5	3.6	0.2	<0.01	<0.1	2.2
ND25	13	13	12.8	1.8	0.9	<0.1	0.02	0.3	1
ND13	9	4.4	21	<0.5	3.2	<0.1	0.02	<0.1	0.5
ND12	<8	4.3	16.7	6.2	1.1	<0.1	0.25	0.3	1.1
ND11	<8	2.6	10.3	3.6	0.9	<0.1	<0.01	<0.1	0.5

Table 4.7, continued.

Element	V	Co	Ni	Se	Mo	Cd	Hg	Tl	Th
Unit	ppm	ppm	ppm	ppm	ppm	ppm	ppm	ppm	ppm
d.l.	8	0.2	0.1	0.5	0.1	0.1	0.01	0.1	0.2
Sample									
ND10	26	8.4	15.5	2.8	1	<0.1	<0.01	<0.1	1
ND9	40	6.8	10.8	0.8	0.9	<0.1	<0.01	<0.1	3
ND21	98	10	6.5	<0.5	0.9	0.3	0.04	0.4	9.2
ND22	119	7.7	6.1	<0.5	0.7	<0.1	0.02	0.2	12.9
ND17	<8	6.9	8.8	3.5	0.7	<0.1	<0.01	<0.1	0.4
ND14	61	11.4	7.8	4.4	2.9	<0.1	<0.01	0.1	3.1
ND29	173	22	33.6	<0.5	0.2	<0.1	0.01	2.7	3

Table 4.8: Rare earth elements (REEs) composition ore rocks at southern part of Ulu Sokor gold deposit. Note that d.l. is detection limit.

Element	La	Ce	Pr	Nd	Sm	Eu	Gd	Tb	Dy	Ho	Er	Tm	Yb	Lu
Unit	ppm	ppm	ppm	ppm	ppm	ppm	ppm	ppm	ppm	ppm	ppm	ppm	ppm	ppm
d.l.	0.1	0.1	0.02	0.3	0.05	0.02	0.05	0.01	0.05	0.02	0.03	0.01	0.05	0.01
Sample														
NF1	40.1	71.4	7.43	23.3	3.31	0.32	2.47	0.32	1.53	0.25	0.64	0.09	0.59	0.08
NF30	4.2	7.4	1.33	5.6	1.36	0.4	1.69	0.26	1.5	0.28	0.77	0.11	0.75	0.13
NF36	11.1	10.2	1.95	7.2	1.56	0.39	2.17	0.32	1.91	0.34	0.89	0.14	0.77	0.11
NF2	25.3	49.6	5.81	22.5	4.41	0.97	4.29	0.64	3.56	0.63	1.86	0.26	1.96	0.3
NF31	2.4	5.3	0.53	1.7	0.3	0.07	0.32	0.04	0.28	0.06	0.19	0.03	0.2	0.03
NF7	19.9	41.5	4.29	17.3	3.72	0.95	3.53	0.53	3.48	0.77	2.33	0.32	2.4	0.42
NF5	22.3	44	4.71	16.1	2.72	0.6	2.53	0.34	1.89	0.41	1.34	0.22	1.71	0.29
NF25	17.9	31.1	3.25	11.3	1.98	0.44	2.08	0.31	1.9	0.44	1.18	0.17	1.27	0.22
NF14	1	1.9	0.18	0.6	0.12	0.03	0.11	0.01	0.11	<0.02	0.07	0.01	<0.05	<0.01
NF3	12.6	24.6	2.68	10.9	2.23	0.45	2.35	0.36	1.88	0.36	0.97	0.1	0.73	0.1
NF15	30.6	33.4	6.65	26.5	5.28	1.22	3.94	0.47	2.99	0.62	2.04	0.32	2.09	0.37
NF27	9.1	16.8	1.85	6.9	1.56	0.32	1.64	0.25	1.74	0.32	1.08	0.15	1.07	0.18
ND25	4	6.6	0.9	3.7	0.81	0.13	0.79	0.14	0.89	0.2	0.6	0.1	0.54	0.08
ND13	3.8	5.4	0.76	3.3	0.43	0.13	0.63	0.09	0.62	0.11	0.35	0.05	0.3	0.04
ND12	41.9	80.3	10.45	39.1	7.47	1.51	5.69	0.69	3.46	0.52	1.52	0.17	1.14	0.16
ND11	1.9	2.4	0.34	1.1	0.23	0.06	0.33	0.05	0.36	0.09	0.19	0.04	0.16	0.03

Table 4.8, continued.

Element	La	Ce	Pr	Nd	Sm	Eu	Gd	Tb	Dy	Ho	Er	Tm	Yb	Lu
Unit	ppm	ppm	ppm	ppm	ppm	ppm	ppm	ppm	ppm	ppm	ppm	ppm	ppm	ppm
d.l.	0.1	0.1	0.02	0.3	0.05	0.02	0.05	0.01	0.05	0.02	0.03	0.01	0.05	0.01
Sample														
ND10	18.8	15.2	3.75	15.1	3.36	0.72	4.02	0.61	3.13	0.57	1.54	0.21	1.22	0.19
ND9	15.9	30.3	3.99	15.9	3.11	0.5	2.5	0.34	2.11	0.43	1.2	0.19	1.27	0.22
ND21	16.8	35.4	3.54	13.4	2.75	0.7	3.3	0.54	3.52	0.81	2.53	0.36	2.53	0.38
ND22	21.7	41.9	4.44	16.2	3.24	0.65	3.22	0.55	3.69	0.85	2.88	0.43	2.91	0.43
ND17	4.3	5.9	0.82	2.9	0.7	0.21	0.99	0.25	2.01	0.49	1.38	0.17	1.19	0.16
ND14	14.4	29.5	3.45	14.6	3.39	0.64	3.91	0.64	3.92	0.79	2.47	0.37	2.5	0.38
ND29	10.8	20.8	2.47	10	2.08	0.47	2.55	0.37	2.59	0.54	1.5	0.23	1.27	0.2

Table 4.9: Geometric mean value ore rocks at southern part of Ulu Sokor gold deposit.

Metal	Geometric mean (ppm)
Au	1.9 (n=23)
Ag	2.6 (n=19)
Bi	96 (n=22)
Cu	148 (n=23)
Pb	55 (n=23)
As	53 (n=23)
Zn	31 (n=22)
Sb	2 (n=18)
W	7 (n=23)
Sn	21 (n=17)
V	46 (n=14)
Co	7 (n=23)
Ni	8 (n=21)
Se	2 (n=12)
Mo	1 (n=16)
Cd	1 (n=7)
Tl	1 (n=8)
Th	3 (n=19)

4.8 Relationship between the gold mineralization and the host rock

The mineralization of a mineral cannot be separated from the host rock. This is because, the understanding of the host rock is the beginning of the initial picture of the existence of mineral. Based on the study conducted, the relationship between the gold mineralization and the host rock seems to have a correlation. Based on the location of Ulu Sokor gold deposit, it is located in Central Belt of Gold of Peninsular Malaysia.

The Central Belt of gold mineralization in Peninsular Malaysia is generally developed in the area of low grade metamorphic rock. It took place in the area of metasedimentary and volcanic rocks terrain which was formed during the collision of Sibumasu Block and East Malaya Block. This area was associated by the widespread of deformation system such as brittle, ductile, and shearing system zone (Ariffin, 2012). Consequences of the metamorphism and magmatic process in this area created a suitable environment for trap and source of gold mineralization (Ariffin, 2012).

Based on the findings of studies conducted on host rocks, which are phyllite and rhyolite, it seems to have a closed relationship with the findings of studies conducted by previous researchers. This statement refers to the geological conditions of a given area which created a suitable environment for trap and source of gold mineralization specifically in Ulu Sokor gold deposit.

Low grade metamorphism takes place at temperatures between about 200°C to 320°C, and relatively low pressure. The typical low grade metamorphic rock is phyllite, which covered most of the Ulu Sokor gold deposit. Based on the characteristic present in this study area, phyllite is form from shale at slightly higher degree of regional metamorphism from slate. The essential mineral ingredient of phyllite are microcrystalline quartz, chlorite and fine grained mica. Rhyolite in this study area seems to be subordinates with phyllite. As for understanding, host rock in Ulu Sokor gold deposit shows a similar characteristic for suitable environment for trap and source of gold mineralization in Central Belt of gold in Peninsular Malaysia.

CHAPTER 5: CONCLUSIONS

The objective of chemical analyses of host and gold mineralization using petrography and geochemical analyses is to derive general geology and gold prospecting in the southern part of Ulu Sokor gold deposit. The outcome of this analyses was used to establish the general geology of study area, the paragenetic sequence, and the significant element that contributed to the mineralization of gold within the various mineral assemblages.

5.1 Phyllite

Based on the petrological and geochemical data presented, phyllite at the southern part of Ulu Sokor gold deposits have been derived from shale and they are classified as pelitic and felsic source. The phyllite in this study area has undergone little heavy mineral fractionation and sediment recycling since these samples are slightly enriched with LREEs. Some of these samples studied have an elevated K_2O content, indicating K-metasomatism which reflects secondary addition of potassium. According to this CIA and ICV calculation, it shows that the phyllite are intensely weathered with the matured sources. The classifications of depositional conditions are plotted as continental island arc and oceanic island arc settings. Continental island arc and oceanic island arc are dominated by the development of the subduction process, which synchronous with the tectonic evolution of Bentong-Raub suture zone. They are representative of Sibumasu continental margin-slope deposits incorporated into the accretionary complex during subduction. (Metcalfe, 2013b) proposed the subduction occurred approximately during Early to Middle Permian (270 Ma) period. The geochemical characteristics of these studied samples support the tectonic setting of the depositional environment from the subduction field.

5.2 Rhyolite

The classification of the volcanic rocks is restricted based on rhyolite composition. According to geochemical studies, this area consists of typical type of volcanic arc environment which is based on the relationship between the collision of Sibumasu Block and East Malaya Block. The geochemical features include the enrichment in LILEs relative to HFSEs, and restricted calc-alkaline to shoshonitic rock formation, which indicate volcanic arc setting. The trace and major elements from the geochemistry of the volcanic rocks support the volcanic arc setting.

5.3 Gold mineralization

Gold mineralization is primarily hosted in structurally controlled quartz vein which occurs in various degrees of ductile-brittle environment. Based on the field relationships, ore microscopy and geochemical data analysis, the main gold mineralization type in the southern part of Ulu Sokor gold deposit is gold (Au)-bismuth (Bi). The brittle rock formation with the deformed quartz vein is the best host for gold and sulphide mineralization to occur in which they have features of open space development. In terms of mineral exploration and gold prospecting which is for the contribution on gold mining activity, the significant enrichment in this study area is Bi. Bi can be considered as a main element that need to be carefully looked to optimized the gold production. However, some other metals can also be considered as a significant value in this area such as Pb, As, Cu and Zn. From the bulk ore chemistry, the geometric mean values of Au and Bi are 1.8972 ppm Au (n=23) and 96.3 ppm Bi (n=22), respectively.

REFERENCES

Ariffifin, K.S. (2012). Mesothermal lode gold deposit Central Belt Peninsular Malaysia. In: Dar, I.A. (Ed.), Earth Sciences. *InTech, Croatia*, 313–342.

Bignell, J.D., & Snelling, N.J. (1977). K–Ar ages on some basic igneous rocks from peninsular Malaysia and Thailand. *Bulletin Geological Society Malaysia*, *8*, 89–93.

Boynton, W.V. (1984). Cosmochemistry of the rare earth elements; meteorite studies. In: Rare earth element geochemistry. Henderson, P. (Eds), Elsevier Sci. Publ. Co., Amsterdam, 63–114.

Chappell, B.W., & White, A.J.R. (1992). I- and S-Type Granites in the Lachlan Fold Belt. *Transactions of the Royal Society of Edinburgh: Earth and Environmental Science*, *83*, 1-26.

Bhat, M.I., & Ghosh, S.K. (2001). Geochemistry of the 2.51 Ga old Rampur Group pelites, western Himalayas: implications for their provenance and weathering. *Precambrian Research*,*108*, 1-16.

Bhatia, M.R., & Crook, K.A.W. (1986). Trace element characteristics of greywackes and tectonic setting discrimination of sedimentary basins. *Contributions to Mineralogy and Petrology*, *92*, 181-193.

Cox, R., & Lowe, D.R. (1995). A conceptual review of regional-scale controls on the composition of clastic sediment and the co-evolution of continental blocks and their sedimentary cover. J*ournal of Sedimentary Research*, *65*, 1-21.

Cullers, R.L., & Podkovyrov, V.N. (2000). Geochemistry of the Mesoproterozoic Lakhanda shales in southeastern Yakutia, Russia: implications for mineralogical and provenance control, and recycling. *Precambrian Research*, *104*, 77-93.

El-Bialy, M.Z. (2013). Geochemistry of the Neoproterozoic metasediments of Malhaq and Um Zariq formations, Kid metamorphic complex, Sinai, Egypt: Implications for source-area weathering, provenance, recycling, and depositional tectonic setting. *Lithos*, *175-176*, 68-85.

Clements, B., Burgess, P.M., Hall, R., & Cottam, M.A. (2011). Subsidence and uplift by slabrelated mantle dynamics: a driving mechanism for the Late Cretaceous and Cenozoic evolution of continental SE Asia? *Geol. Soc. Lond. Spec. Publ.*, *355*, 37–51.

Crawford, H.A. (1970). The Birth of the Duff Development Company in kelantan. *Plantation Agencies Penang, Persatuan Sejarah Malaysia*, 1-9.

Garcia, D., Fonteilles, M., & Moutte, J. (1994). Sedimentary fractionations between Al, Ti, and Zr and the genesis of strongly peraluminous granites. *Journal of Geology*, *102*, 411-422.

Ghani, A.A. (2009). Volcanism. In: Hutchison, C.S., Tan, D.N.K. (Eds.), Geology of Peninsular Malaysia. *Bulletin Geological Society Malaysia*, 198–210.

Ghani, A. A., & Singh, N. (2005). Petrology and geochemistry of the Sempah volcanic complex: Peninsular Malaysia. *Bulletin Geological Society Malaysia*, *51*, 103-121.

Goh, S.H., Teh, G.H., & Wan Hassan, W.F. (2006). Gold mineralization and zonation in the state of Kelantan. *Bulletin Geological Society Malaysia*, *52*, 129-135.

Gobbett, D.J., Hutchison, C.S., & Burton, C.K. (1973). Geology of the Malay Peninsula: West Malaysia and Singapore. *John Wiley-Interscience, New York*, 1–438.

Groves, D.I., Goldfarb, R.J., Gebre-Mariam, M., Hagemann, S.G., & Robert, F. (1998). Orogenic gold deposits-a proposed classification in the context of their crustal distribution and relationship to other gold deposit types. *Ore Geology Reviews*, *13*, 7-27.

Hastie, A. R., Kerr, A. C., Pearce, J. A., & Mitchell, S. F. (2007). Classification of Altered Volcanic Island Arc Rocks using Immobile Trace Elements: Development of the Th-Co Discrimination Diagram. *Journal of Petrology*, *48* (12), 2341-2358.

Herron, M.M. (1988). Geochemical classification of terrigenous sands and shales from core or log data. *Journal of Sedimentary Petrology*, *58*, 820-829.

Hutchison, C.S. (1977). Granite emplacement and their tectonic subdivision of Malay Peninsular, *Bulletin Geological Society Malaysia*, *9*, 187-207.

Hutchison, C.S.,Tan, D.N.K., & Malaya, U. (2009). Geology of Peninsular Malaysia. *Bulletin Geological Society Malaysia*, *Article*#479.

Leman, M.S. (1994). The significance of Upper Permian brachiopods from Merapoh area, northwest Pahang. *Bulletin Geological Society Malaysia*, *35*, 113-121.

Li, B., Jiang, S.Y., Zou, H.Y., Yang, M., & Lai, J.Q. (2015). Geology and fluid characteristics of the Ulu Sokor gold deposit, Kelantan, Malaysia: Implications for ore genesis and classification of the deposit. *Ore Geology Reviews*, *64*, 400-424.

Li, B., Zou, H.Y., & Yang, M. (2011). Ore-forming flfluid and stable isotope research of Ulu Sokor gold deposit, Malaysia. *Acta Minal. Sin*., *31*, 485–486 (in Chinese with English abstract).

Long, X., Sun, M., Yuan, C., Xiao, W., & Cai, K., (2008). Early Paleozoic sedimentary record of the Chinese Altai: Implications for its tectonic evolution. *Sedimentary Geology*, *208*, 88-100.

Mader, D., & Neubauer, F. (2004). Provenance of Palaeozoic sandstones from the Carnic Alps (Austria): petrographic and geochemical indicators. *International Journal of Earth Sciences*, *93*, 262-281.

MacDonald, S. (1967). The geology and mineral resources of north Kelantan and north Trengganu. Ipoh, West Malaysia. *Geology Survey Headquarters*, *10*, *Article*#202.

Makoundi, C., Zaw, K., Large, R.R., Meffre, S., Lai, C.K., & Hoe, T.G. (2014). Geology, geochemistry andmetallogenesis of the Selinsing gold deposit, central Malaysia. *Gondwana Resource*. *26*, 241–261.

McLennan, S.M. (1989). Rare earth elements in sedimentary rocks: influence of provenance and sedimentary processes. *Mineralogical Society of America Reviews in Mineralogy*, *21*, 169-200.

McLennan, S.M., Taylor, S.R., McCulloch, M.T., & Maynard, J.B. (1990). Geochemical and Nd–Sr isotopic composition of deep-sea turbidites: crustal evolution and plate tectonic associations. *Geochimica et Cosmochimica Acta*, *54*, 2015-2050.

McLennan, S.M., Hemming, S., McDaniel, D.K., & Hanson, G.N. (1993). Geochemical approaches to sedimentation, provenance and tectonics. In: Johnsson, M.J., Basu, A. (Eds.), Processes Controlling the Composition of Clastic Sediments. *Geological Society of America*, *284*, 21-40.

McLennan, S.M. (2001). Relationships between the trace element composition of sedimentary rocks and upper continental crust. *Geochemistry, Geophysics, Geosystems*, *2* ,*Article*#1021.

Metcalfe, I., Sivam, S.P., & Stauffer, P.H. (1982). Stratigraphy and sedimentology of Middle Triassic rocks exposed near Lanchang, Pahang, Peninsular Malaysia. *Bulletin Geological Society Malaysia*, *15*, 19–30.

Metcalfe, I. (2000). The Bentong–Raub suture zone. *Journal of Asian Earth Sciences*, *18*, 691–712.

Metcalfe, I. (2002). Permian tectonic framework and palaeogeography of SE Asia. *Journal of Asian Earth Sciences*, *20*, 551–566.

Metcalfe, I. (2013a). Gondwana dispersion and Asian accretion: tectonic and palaeogeographic evolution of eastern Tethys. *Journal of Asian Earth Sciences*, *66*, 1–33.

Metcalfe, I. (2013b). Tectonic evolution of the Malay Peninsula. *Journal of Asian Earth Sciences*, *76*, 195-213.

Metcalfe, I., & Chakraborty, K.R. (1996). A stratigraphic log of Semantan Formation along the Mentakab-Temerloh By-Pass, Pahang. *Geological Society of Malaysia Bulletin*, *35*, 37–46.

Middlemost, E. A. K. (1994). Naming materials in the magma/igneous rock system. *Earth Science Reviews*, *37* (3), 215-224.

Nakamura N. (1974). Determination of REE, Ba, Fe, Mg, Na and K in carbonaceous and ordinary chondrites. *Geochimica et Cosmochimica Acta*, *38*, 757-775.

Nesbitt, H.W., & Young, G.M. (1982). Early Proterozoic climates and plate motions inferred from major element chemistry of lutites. *Nature*, *299*, 715-717.

Pearce, J. (1983). Role of the sub-continental lithosphere in magma genesis at active continental margins. *Shiva Publishing Ltd., Cambridge, Mass.*, 230–249.

Rahman, M.N.A. (2019). Jurassic-Createaceous Stratigraphy of Malaysia. *Open Journal of Geology*, *9*, 668-670.

Richardson, J.A. (1939). The Geology andMineral Resources of the Neighbourhood of Raub, Pahang, Federated Malay States: With an Account of the Geology of the Raub Australian Gold Mine. *Printers, Ltd*.

Rishworth, D. (1974). The Upper Mesozoic terrigenous Gagau Group of Peninsular Malaysia. *Bulletin Geological Society Malaysia*, *1*, 1-78.

Roddaz, M., Christophoul, F., Burgos Zambrano, J.D., Soula, J.C., & Baby, P. (2012). Provenance of late Oligocene to quaternary sediments of the Ecuadorian Amazonian foreland basin as inferred from major and trace element geochemistry and Nd–Sr isotopic composition. *Journal of South American Earth Sciences*, *37*, 136-153.

Rollinson, H. (1993). Using geochemical data: evaluation, presentation, interpretation. *Longman*, *Article*#352.

Rudnick, R.L. & Gao, S. (2003). The composition of the crust. In: Rudnick, R.L. (Ed.), The Crust. *Treatise on Geochemistry*, *3*, 1-64.

Sawant, S.S., Vijaya Kumar, K., Balaram, V., Subba Rao, D.V., Rao, K.S., & Tiwari, K.S. (2017). Geochemistry and Genesis of Craton-derived Sediments from Active Continental Margins: Insights from the Mizoram Foreland Basin, NE India. *Chemical Geology*, *470*, 13-32.

Searle, M.P., Whitehouse, M.J., Robb, L.J., Ghani, A., Hutchison, C.S., Sone, M., ... Oliver, G.J.H. (2012). Tectonic evolution of the Sibumasu–Indochina terrane collision zone in Thailand and Malaysia: constraints from new U -Pb zircon chronology of SE Asian tin granitoids. *Journal of the Geological Society*, *169*, 489–500.

Shuib, M.K., & Ghani, A.A (2003). 'Mantle plume' type magmatism in the Central Belt Peninsular Malaysia and its tectonic implications. *Bulletin Geological Society Malaysia*, *46*, 365–371.

Sone, M., & Metcalfe, I. (2008). Parallel Tethyan Sutures in mainland SE Asia: new insights for Palaeo-Tethys closure. *Compte Rendus Geoscience*, *340*, 166–179.

Sun, S., & McDonough, W. F. (1989). Chemical and isotopic systematics of oceanic basalts: implications for mantle composition and processes. *Geological Society, London, Special Publications*, *42* (1), 313-345.

Tan, B.K. (1984). The tectonic framework and evaluation of the Central Belt and its margin, Peninsular Malaysia, *Bulletin Geological Society Malaysia*, *17*, 307-322.

Tate, R.B., Tan, D.N.K., & Ng, T.F. (2009). Geological Map of Peninsular Malaysia. In: Hutchison, C.S., Tan, D.N.K. (Eds.), Geology of Peninsular Malaysia. *Bulletin Geological Society Malaysia*.

Taylor, S.R., & McLennan, S.M. (1985). The Continental Crust: Its Composition and Evolution. *Blackwell Scientific Publishers, Oxford*.

Teoh, L.H., Lee, A.K., & Foo, K.Y. (1987). Gold Mineralization and Prospects in Kelantan, *Minerals and Geoscience Department Malaysia* (unpublished report).

Ueno, K., & Hisada, K. (1999). Closure of the Paleo-Tethys caused by the collision of Indochina and Sibumasu. *Chikyu Monthly*, *21*, 832–839 (in Japanese).

Wan Hassan, W.F., & Purwanto, H.S. (2002). Type deposits of primary gold mineralization in the Central Belt of Peninsular Malaysia, *Geological Society of Malaysia Annual Geological Conference 2002*, 26 - 27.

Xu, J., Xia, X., Huang, C., Cai, K., Yin, C., & Lai, C.K. (2019). Changes of provenance of Permian and Triassic sedimentary rocks from the Ailaoshan suture zone (SW China) with implications for the closure of the eastern Paleotethys. *Journal of Asian Earth Sciences*, *Journal of Asian Earth Sciences*, 234-248.

Yeap, E.B. (1993). Tin and gold mineralizations in Peninsular Malaysia and their relationships to the tectonic development. *Journal of Asian Earth Sciences*, *8*, 329–348.

Yong, B.T., Ghani, A.A., Khoo, T.T., & Shafari,M. (2004). Benom Complex: evidence of magmatic origin. *Bulletin Geological Society Malaysia*, *47*, 55–60.